Interaction of metallic nanoparticles with biomedical enzyme target: Neuronal nitric oxide synthase

A thesis submitted in fulfilment of the requirements for the degree of

Master of Science

In the

Department of Biochemistry, Microbiology and Biotechnology

Faculty of Science

Rhodes University

By

Nosiphiwe P Ngqwala

August, 2012

Supervisor: Prof C Whiteley

ABSTRACT

Alzheimer"s disease (AD) is the most common type of dementia characterized by intracellular appearance of neurofibrillary tangles, synaptic and neuronal loss; and extracellular accumulation of amyloid-β (Aβ) peptide in senile plaques. The initial causes leading to AD are unknown, and the available treatments are only effective at slowing the degeneration process. The accumulation of arginine in the brain of Alzheimer patients indicates a possible disruption of enzymes responsible for its metabolisim. One such enzyme is neuronal nitric oxide synthase (nNOS) and controlling its activity by interacting with nanoparticles may lead to a delay in the onset of the disease. Neuronal nitric oxide synthase was purified using DEAE-Sephacel ion exchange resulting in 10 % yield, 0.43 fold recovery and specific activity 0.09 U/mg. The enzyme was found to be a dimer with a molecular mass of 150 kDa. Characterisation of the nNOS showed an optimum temperature and pH of 50°C and 7.5 respectively, and it was relatively stable at the optimum conditions ($t_{½}$ = 100 min). The purity was analysed by SDS-PAGE followed by Western blot. Purified nNOS was challenged with 3-7 nm silver and 4-15 nm gold nanoparticles of between synthesized chemical using $AgNO_3$ and either sodium borohydride or sodium citrate. Results showed that gold nanoparticles are more effective at low concentration (5 μM) than silver nanoparticles due to their size difference. Incubation of different concentration of nanoparticles (5, 15, 25, 50 μM) with the purified nNOS showed an initial decrease of 5% in enzyme activity which over time was restored to 80%. This suggests that different nanoparticles are produced in different sizes and interaction over a given time may result in enzyme association–dissociation mechanism. Inhibition studies showed a strong binding of both nanoparticles with K_i values of 1.4 μM and 0.2 μM for silver and gold, respectively. Both nanoparticles inhibited the activity of nNOS extensively as they bound strongly to the inhibition site on the enzyme and were more in contact with fluorophores nanoparticles. This was confirmed by fluorimetry with binding constants of 0.0084 μM and 0.01092 μM for silver and gold, respectively. Results of this study suggest that silver and gold nanoparticles competitively inhibit nNOS.

DEDICATION

This thesis is dedicated to my son Likhona Ngqwala and the memory of my mother Thandeka Mahlaba.

ACKNOWLEDGEMENT

I sincerely wish to express my gratitude to the following persons without whom this dissertation would not be possible:

- Firstly, I would like to extend my sincerest gratitude to my supervisor Prof Chris Whiteley for your guidance, mentorship and endless patience and I say God bless you. I will always cherish all the memories I have of the „LAB 129 research group".
- I would like to thank Dr Jacqueline van Marwijk for your assistance and motivation during this project.
- I would like to extend my gratitude to the National Research Foundation (NRF) and Medical Research Council (MRC) for supporting this project.
- Women Academic Solidarity Association (WASA) I appreciate your company and I say thank you support.
- To my team mates of Lab 129 (2010/2011), thank you for sharing your ideas and suggestions with me. It has been a pleasure and an honour working with you
- I sincerely thank my friends: Nelson Odume, Lorraine Mutsvunguma and Fortunate Mokoena who painstakingly proof read my thesis and provided vital feed backs.
- Special thanks to my closest friends (Vuyo, Andiswa, Nelson, Mpho, Ntsiko, Ephraim, Jia, Vusi, Joe, Eden, Nico and Nokuyolo) for being there, in and out of the lab, for always encouraging me when times got tough and for letting me cry on your shoulders when I thought all was lost.
- I would like to thank my family for the love, support and encouragement I received throughout all.
- Finally, I would like to give praise to God for giving me the strength to accomplish this journey despite all odds.

DECLARATION

I, Nosiphiwe Patience Ngqwala, hereby declare that this MSc dissertation is my own unaided work completed in fulfillment of the requirements for the degree Masters of Science at Rhodes University.

Signature:…… Date:……

TABLE OF CONTENTS

LIST OF FIGURES

LIST OF TABLES

LIST OF ACRONYMS AND ABBREVIATIONS

γ-secretase	gamma-secretase
β-secretase	beta-secretase
<	less than
λ	wavelength
%	percentage
Δ F_{max}	maximum change in fluorescence
3-D	three-dimensional
µL	microliter
µM	micromolar
A_{max}	absorption maximum
Aβ	amyloid beta peptide
A	Absorbance
AD	alzheimer‟s disease
ADMA	asymmetric N^G, N^G –dimethyl-L-arginine
AFM	atomic force microscopy
Al	aluminium
APS	ammonium persulphate
ApoE	apoliprotein E
APP	amyloid precursor protein
AU	arbitrary units
BACE	beta-secretase or beta-site APP cleaving enzyme

BAEE	benzoyl-L-arginine ethyl ester hydrochloride
BBB	Blood brain barrier
BH_4	tetrahydro-L-biopterin dichloride
BSA	bovine serum albumin
C	concentration of amyloid peptide
CaM	calmodulin
(CaMK)PKC	calmodulin–dependent protein kinase
CNS	central nervous system
$CaCl_2$	calcium chloride
CdS	Cadmium sulphide
CSF	cerebrospinal fluid
Cu	Copper
ChE-I‟s	cholinesterase inhibitors
$C_6H_5Na_3O_7$	Trisodium citrate
D	donor
Da	dalton
DAF-2	4.5-diaminofluorescein
DAF-2 DA	4.5-diaminofluorescein diacetate
DAF-2T	Triazolofluorescein
DEAE	diethyl-amino ethylene
dH_2O	distilled water
DNA	deoxyribose nucleic acid

DTT	dithiothreitol
DMSO	dimethyl sulfoxide
EDTA	ethylenediametetraacetic acid
ESI	enzyme-substrate – inhibitor
eNOS	endothelial nitric oxide synthase
F	fluorescence intensity
FAD	flavin adenine dinucleotide
FDA	Food and Drug Administration
Fe	iron/heme
$FeCl_3$	ferric chloride hexahydrate
FMN	flavin mononucleotide
h	hour
$HAuCl_4$	tetrachloroauric acid
HCL	hydrochloric acid
8 OHG	8- hydroxyguanosine
HIV	Human immunodeficiency virus
CoA HMG-CoA-reductase	3-hydroxy-3-methyl-glutaryl-CoA reductase
iNOS	inducible nitric oxide synthase
k_{cat}	enzyme turn-over number
k_{cat}/K_m	catalytic efficiency
K_2CO_3	potassium carbonate
kDa	kilodalton

K_a	association constant
K_d	dissociation constant
K_i	inhibitor constant
K_m	Michaelis-Menten constant
K_{sv}	Stern Volmer constant
kV	kilovolts
L	ligand
L-NHA	N^G-hydroxy –L-arginine
M	molar
min	minutes
ml	milliliter
mM	millimolar
mtNOS	mitochondrial nitric oxide synthase
MCI	mild cognitive impairment
M_r	molecular weight
methHb	methemoglobin
nM	nanomolar
nm	nanometer
NaOH	sodium hydroxide
NADPH	nicotinamide adenine dinucleotide phosphate tetrasodium salt

NaCl	sodium chloride
NPs	Nanoparticles
NMDA	*N*-methyl-D-aspartate
NOS	nitric oxide synthase
nNOS	neuronal nitric oxide synthase
$NADP^+$	nicotinamide adenine dinucleotide phosphate
NO	nitric oxide
NH_4Cl	ammonium chloride
$(NH_4)_2\ SO_4$	ammonium sulphate
NFT	neurofibrillary tangle
NMMA	N^G-monomethyl-L-arginine
NSAIDs	Non-steroidal anti-inflammatory drugs
O_2	oxygen
O^{2-}	Superoxide
$ONOO^-$	peroxynitrate
PAGE	poly-acrylamide gel electrophoresis
PDB	protein data bank
PEG	poly(ethylene glycol)
PET	positron emission tomography
PKA	protein kinase-C
Phe	phenylalanine
PIN	Protein inhibitor of nNOS

PS 1	presenilin 1
PS 2	presenilin 2
PMSF	phenylmethylsulphonylfluoride
RES	reticuloendothelial system
ROS	reactive oxygen species
RNA	ribose nucleic acid
RFU	relative fluorescence units
RT	room temperature
S.E.M	standard error of mean
SDS	sodium dodecyl sulphate
SDS-PAGE	Sodium dodecyl sulphate-polyacrylamide Electrophoresis
s	second
$AgNO_3$	silver nitrate
TEMED	*N,N,N', N*-tetramethyl-ethylenediamine
ThT	thioflavin T
TRP	tryptophan
vs.	versus
v/v	volume per volume
w	tryptophan
w/v	weight per volumezinc
Zn	Zinc

LIST OF EQUATIONS

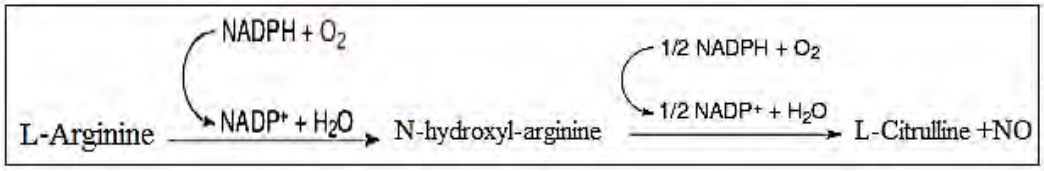

..Equation 1

$$\frac{[S]}{v} = \frac{[S]}{V_{max}} \quad \frac{K_m}{V_{max}}$$

……..Equation 2

$$k_{cat} = \frac{V_{max}}{[E_t]}$$

…….Equation 3

$$\text{Catalytic efficiency} = \frac{k_{cat}}{K_m}$$

..... Equation 4

$$\text{Activity} = \frac{(\Delta A \,.\, V_t).\, D_f}{(\varepsilon.\, t.\, V_e)} = \mu mol/ml/min$$

where

ΔA = change in absorbance

D_f = dilution factor

V_t = total volume

ε = extinction coefficient

t = time (min)

l = path length (cm)

V_e = volume of extract

……..Equation 5

$$AgNO_3 + NaBH_4 \rightarrow Ag + \frac{1}{2} H_2 + \frac{1}{2} B_2H_6 + NaNO_3$$ .....equation 6

$$A = E.\ c.\ l$$

Where
A = absorbance
E = molar extinction co efficient
c = concentration of the molar solution
l = length of the light path

.....Equation 7

$$K_i = \frac{np.\ V_{max}^{app}}{V_{max} - V_{max}^{app}}$$

np = concentration of nanoparticle

V_{max}^{app} = apparent maximum velocity in the presence of nanoparticle.

V_{max} =enzyme activity without nanoparticles

...equation 8

$$\frac{Fo}{\Delta F} = \frac{1}{\theta Ksv[q]} + \frac{1}{\theta}$$ .....equation 9

$$\frac{\log[(F-Fo)}{F} = \log Kd + n\log[q]$$

n = the concentration of binding site on the purified enzyme
Kd = dissociation constants

.....equation 10

LIST OF OUTPUTS

Local Conferences Proceedings:

- **Ngqwala N.P.,** van Marwijk, J. and Whiteley C.G. Interaction of metallic nanoparticles with biomedical enzyme targets: Neuronal nitric oxide synthase. *SASBMB 2012 Conference*, Winterton, Drakensberg Champagne Sport Resort 29 January -01 February.

Research Articles:

- Padayachee E., **Ngqwala N.P.** and Whiteley C.G. (2011). Association of β-amyloid peptide fragments with neuronal nitric oxide synthase: Implications in the etiology of Alzheimers disease. *Journal of Enzyme Inhibition and Medicinal Chemistry*, 1-9; **[DOI: 10.3109/14756366.2011.590805].**
- **Ngqwala N.P.**, Van Marwijk, J., and Whiteley C.G. (2012). Change in activity of neuronal nitric oxide synthase in the presence of silver nanoparticles (forthcoming).

CHAPTER 1: LITERATURE REVIEW

1.1. Introduction

Alzheimer‟s disease (AD) is an age related disease insidious at the onset and is characterised by impairment of memory and cognive disturbance. Although the exact cause of Alzheimer‟s disease is still unclear, evidence suggests that redox stress, inflammation, neurotransmitter dysfunction, atherosclerosis and impaired brain functions are associated with AD (Jing *et al*., 2009). At most 5 % of all cases of AD are associated with gene mutations. The genetic variations are found in small percentages and include chromosome 21 on the gene for the amyloid precursor protein, chromosome 14 on the gene for the presenilin 1 protein and chromosome 1 on the gene for presenilin 2. The mutations of chromosome 1, 14 and 21 tend to develop before age 65, but sometimes in individuals as young as 30 years. Alzheimer‟s disease developing at age 65 or older is sometimes caused by apolipoprotein E-e4 (ApoE-e4) a form of the ApoE gene, which provides the blueprint for a protein that carries cholesterol in the bloodstream (Perry *et al*., 2005; Scheuner *et al*., 1996). A clinical case of this disease was first described by Dr Alois Alzheimer in 1906 (Parihar and Hemnani, 2004). Although AD is not a psychological or mental illness, its victims often exhibit strange irrational and emotionally upset behaviour. The disease in itself is a medical condition involving neurodegenerative mechanisms in the brain, though its symptoms are psychologically and psychiatrically based (Jing *et al*., 2009).

Alzheimer‟s disease is characterised by intracellular appearance of neurofibrillary tangles, synaptic and neuronal loss as well as extracellular accumulation of amyloid-β (Aβ) peptide in senile plaques (Yaari and Corey-Bloom, 2007; Goeder and Spillanti, 2006; De Felice *et al*., 2004) (Figure 1.1 page 2 shows the differences between the normal brain and the Alzheimer‟s disease patients). Senile plaques are extracellular amyloid deposits found in the brain most prominently in Alzheimer disease but also in normal ageing (Cras *et al*., 1991). They are surrounded by astrocytes whose function is to store reserve arginine in the brain tissue (Haas *et al*., 2002). Genetic causes of AD are associated with protein abnormalities in the amyloid precursor protein (APP) (Haas *et al.,* 2002). In the brain of Alzhiemer patient, research claim that Aβ is generated by abnormal processing of APP in the neurons. The APP processing occurs in two pathways: a β- secretase based amyloidogenic and γ- secretase

based non-amyloidogenic pathway (Figure 1.2 page 3 shows the amyloidogenic and non-amyloidogenic pathway) (Reddy and Beal, 2008). In the α-secretase pathway, α-secretase cleaves in the middle of the amyloid-β region to release a large soluble APP-fragment, α-APPs. The carboxy (C)-terminal C83 peptide is metabolized to p3 by γ-secretase. However, in the amyloid-forming β-secretase pathway, β-secretase releases a large soluble fragment, β-APPs. The C-terminal C99 peptide is then cleaved by γ-secretase at several positions, leading to the formation of amyloid-β 40 (Aβ40) and the pathogenic amyloid-β 42 (Aβ42). γ-secretase cleavage also releases the APP intracellular domain, which could have a role in transcriptional regulation. The effects of β- and γ-secretase inhibitors can be distinguished in secondary assays: both inhibitor classes block the formation of pathogenic Aβ42, but β-secretase inhibitors also block the formation of β-APPs and C99, whereas γ-secretase inhibitors also block the formation of p3 and the APP C-terminal fragment, leading to accumulation of C99 and C83 (see Figure 1.2 in page 3) (Ehehalt *et al*., 2002).

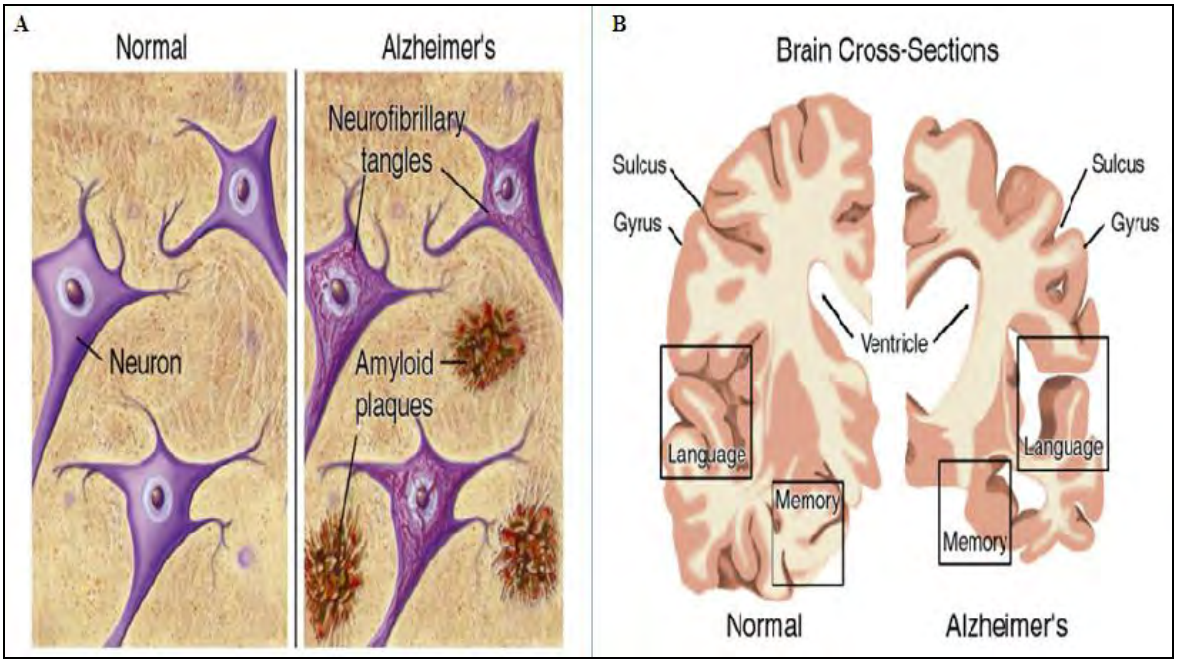

Figure 1.1: Normal brain and the presence of plaques and tangle in the brain of Alzheimer's patients and B: a cross section showing the difference between normal brain and Alzheimer's patient brain. Source: internet 1 (Appendix D)

In addition to this relationship and the accumulation of Aβ, an increase in the levels of arginine in brain of AD patients has been reported (Haas *et al.*, 2002). L-arginine (L-ARG) is

a semi-essential naturally occurring proteinogenic amino acid that is involved in two metabolic pathways, that is, the nitric oxide synthase (NOS) pathway where L-ARG is converted to nitric oxide (NO), and the L-citruline and arginase pathway (Jing *et al.,* 2009) where L-ARG is broken down into urea and Lornithine and genesis of polyamines including putrescine, spermidine, and spermine (Wu and Morris 1998). The first step gives an intermediate N-hydroxyl-arginine; oxidation produces L-Citrulline as main product and NO as the by-product in two steps (Iwanaga *et al*., 1999) (Figure 1.3 below shows the conversion of L-Arginine to L-Citrulline). Nitric oxide (NO) derived from L-ARG is the potential cause of redox stress that is cleared through reacting with superoxide (O_2^-) to generate peroxynitrite (ONOO-) (Jing *et al*., 2009).

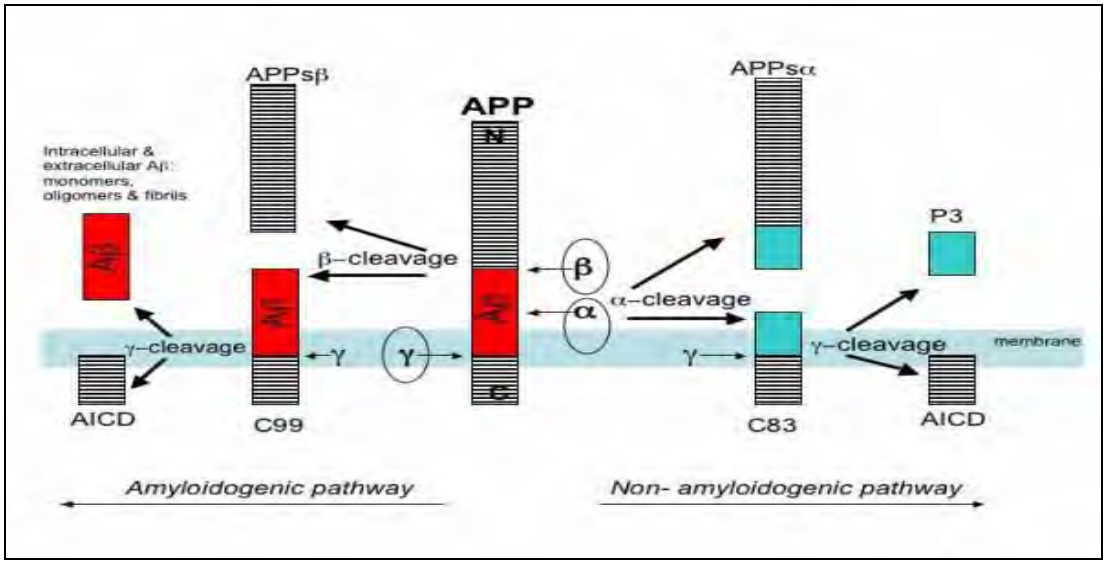

Figure 1.2: Schematic of cleavage of transmembrane glycoprotein amyloid precusor protein (adapted from Penelope and Mayer, 1999)

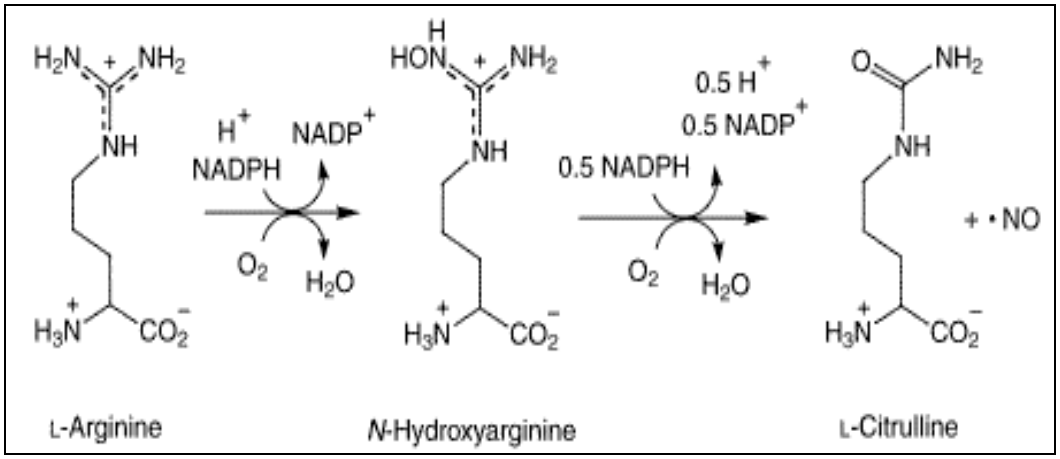

Figure 1.3: Catalytic mechanism of neuronal nitric oxide synthase (adapted from Penelope and Mayer, 1999)

1.2. Prevention and treatment of Alzheimer's diseases

Prevention of Alzheimer"s diseases could be primary, secondary, or tertiary (Figure 1.4 below shows the prevention stages of dementia).

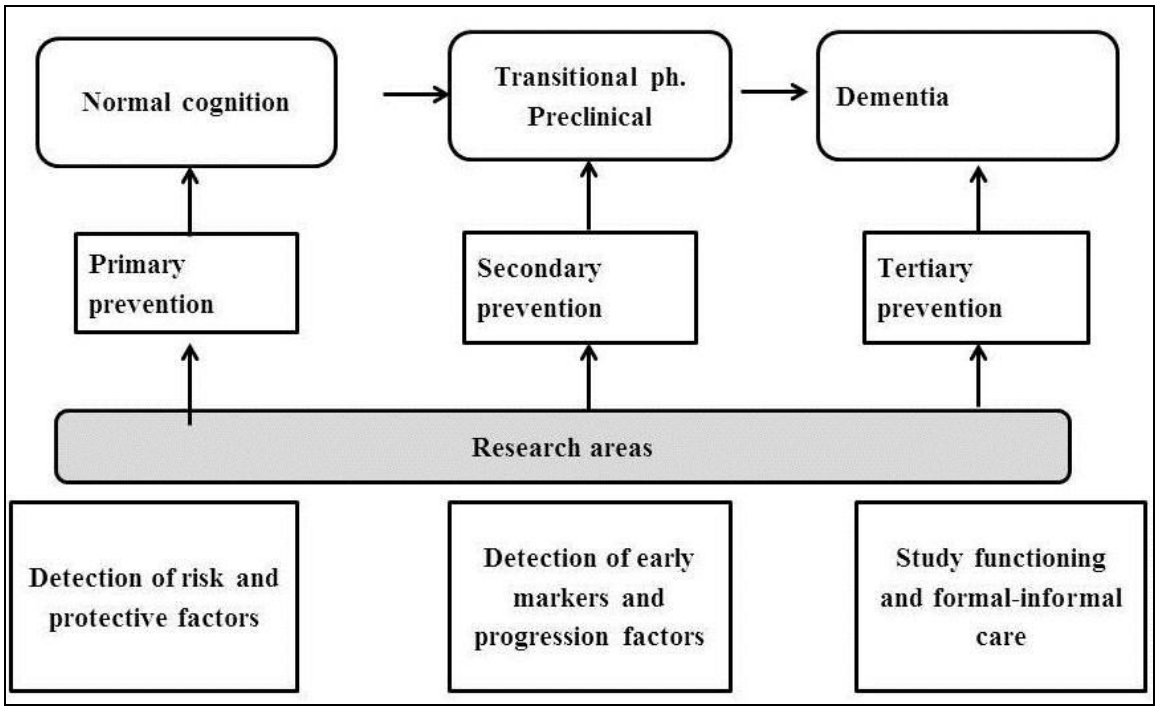

Figure 1.4: Potential preventive strategies for dementing disorders at different times of disease development (Adapted from Fratiglioni et al., 2007)

Primary prevention entails the reduction of the occurrence of the disease by decreasing or delaying the development of dementia. However, secondary prevention involves the reduction of the frequency of the disease by limiting its duration. On the other hand, tertiary preventive measures are tailored towards reducing complication and long term disability associated with AD (Brucki, 2009). This study focuses more on secondary prevention of Alzheimer"s diseases (AD).

Currently, there are five medications that are approved by the Food and Drug Administration (FDA) to treat AD. These are donepezil, galantamine, rivastigmine, tacrine, (they are referred to as acetyl cholinesterase inhibitors) and N-methyl-D-aspartate antagonist memantine (Neugroschl and Sano, 2010). Cholinergic drugs are non-steroidal anti-inflammatory drugs (NSAIDs) and they include cholinesterase inhibitors (ChE-Is) which improve cholinergic function in AD by inhibiting the destruction of intrasynaptic acetylcholine by acetylcholinesterase (Cummings, 2003; De Meyer *et al*., 2006). There is evidence that acetyl cholinesterase inhibitors act against free radicals and amyloid toxicity, thereby decreasing the release of cytokines from activated microglia in the brain and blood, and therefore play an anti-inflammatory role. In addition, NSAIDs down regulate pro-inflammatory signals as well as the autoimmune response from microglia cells which produces free radicals within amyloid plaques (Fawole, 2010; Parihar and Hemnani, 2004). Excessive free radical generation poses the risk of oxidative stress. Consequently, several epidemiological studies suggest that NSAIDs such as aspirin may provide some degree of protection from oxidative stress (Fawole, 2010; Citron, 2002). Drugs used for the treatment of AD fall into the following three broad categories.

1.2.1. Antioxidants

Antioxidants are substances that protect cells from damage caused by unstable molecules known as free radicals (Jomova *et al.*, 2010). Vitamin C and vitamin A are the best studied antioxidants. Plasma vitamin C is lower in Alzheimer"s diseases patients which results in cognitive impairment (Riviere *et al*., 1998). In a study conducted on 633 patients within the age of 65 years, it was reported that high dose of Vitamin C decreased the risk of AD (Morris *et al*., 1998). Owing to the beneficial effects of the α-tocopherol and ascorbic acid in reducing free radical load in the hippocampus and cortex, a considerable amount of research has gone into the investigation of the use of these vitamins for the treatment of AD (Giorgi *et al*., 2010). Both α-tocopherol and ascorbic acid have been shown to slow the progression of the

disease and reduce the risk of AD (Jomova *et al.*, 2010). Antioxidants such as vitamin A, vitamin D, lycopene, and beta-carotene have been reported to have positive effects in the prevention and treatment of AD (Foy *et al*., 1999).

1.2.2. Anti-excitotoxins

Excitotoxins are substances that bind with receptors in the neurons of the brain to allow a buildup of calcium within the cell that can damage or even kill the cell, gradually destroying the nervous system (Reisberg *et al*., 2003). Glutamate, the principal excitatory neurotransmitter in cortical and hippocampal neurons (Louzada *et al*., 2004) is oxidized in the brain of AD patients. Excessive activation of N-methyl-D-aspartate (NMDA) receptors by glutamate increases the vulnerability of the central nervous system (CNS) neurons leading to neuronal degeneration. However, an NMDA has been approved for only moderate to severe AD cases (Reisberg *et al*., 2003).

1.2.3. Statins

Statins are inhibitors of the cholesterol-synthesizing enzyme 3-hydroxy-3-methyl-glutaryl-CoA reductase (HMG-CoA-reductase) which has a proposed effect on Aβ production (Citron, 2002). In a study conducted by De Meyer *et al*., (2006), they found that a risk reduction of dementia by 60-70% in elderly patients treated with satin. However, it has not been confirmed which type of statin is effective in decreasing the occurrence of dementia based on their lipophilicity. Lipophilitic statins pass the brain barrier when compared to hydrophilic statins (Brucki, 2009). A study performed by Haag *et al.*(2009) on three different types of statin lowering drugs (i.e. lipophilic statins, hydrophilic statins and non-statin cholesterol) indicated that the permeability of the blood brain barrier is not the main protective mechanism. The use of non-statin cholesterol lowering drugs was associated with a reduced risk of they are lipophilic. Although statins may not be able to reverse neuronal degeneration once it has occurred, it can slow the progression of the neurodegenerative process (Castellani *et al*., 2008). Another relatively new strategy in preventing Alzheimer‟s disease is the potential of nitric oxide synthase enzyme inhibitors and the blocking of α- and β-secretase pathways (Citron, 2002). Figure 1.2 above and and Figure 1.5 below which show the treatment strategies applied in Alzheimers. Therefore, it is important to investigate the nature of the synthase enzyme and its relationship to AD as well as the enzyme inhibitory potential on AD.

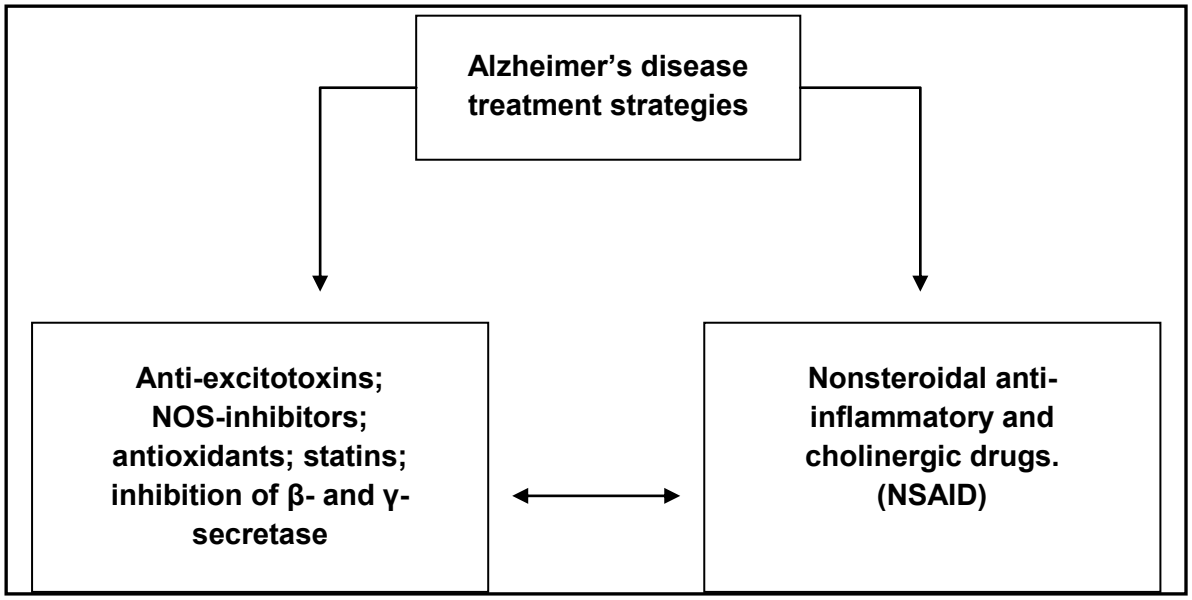

Figure 1.5: A few Alzheimer drug treatment strategies adapted from (adapted from Citron, 2002)

1.3. Nitric oxide synthases

Nitric oxide synthase is an enzyme that catalyses the breakdown of arginine into citrulline and nitric oxide (see Figure 1.3. above). It is a neurotransmitter that plays an important role in the physiological function of the central nervous system which is mainly expressed in neurons and astrocytes and neuronal stem cells (Bredt, 1999).

1.3.1. Biological importance of nitric oxide synthase

There are three isoforms of nitric oxide synthase namely nNOS that are found in neuronal tissues, inducible nitric oxide synthase (iNOS) whose synthesis is induced by proinflammatory cytokines or endotoxin, and endothelial nitric oxide synthase (eNOS) expressed in endothelial cells (Yi *et al*., 2009). The first step in the reaction is the N-hydroxylation of L-arginine, yielding NG-hydroxy –L-arginine as an intermediate. NG-hydroxy –L-arginine (L-NHA) is further oxidized to L-citrulline and NO in an NADPH–and O2-dependent step (Marletta *et al*., 1998) (see Figure.1.1 above). NG-hydroxy –L-arginine functions effectively as a substrate for nNOS and requires not only a guanidinium moiety but also an amino acid head group for catalysis to occur (Poulos *et al*., 2002). Moreover, NO synthesis requires a sequential transfer of the three electrons between the reductase and oxygenase domains to convert L-arginine to citrulline and NO (see Figure 1.1 above).

1.3.1.1. Inducible nitric oxide synthase

Inducible nitric oxide synthase (also known as iNOS, Type II, NOS-II and NOS-2) is the isoform which can be synthesized following induction by pro-inflammatory cytokines or endotoxin (Bredt, 1999). This enzyme was originally isolated from murine macrophages and is expressed in cells upon immunologic or inflammatory stimulus (Yi *et al*., 2009). The activity of iNOS is calcium independent as it is fully activated at basal intracellular calcium concentration (Calabrese, 2007). The enzyme is a 130 kDa cytosolic protein (Zhang and Snyder, 1995).

1.3.1.2. Endothelial nitric oxide synthase

Endothelial nitric oxide synthase, also known as (eNOS, Type III, NOS-III and NOS-3) is the isoform expressed in endothelial cells (Bredt, 1999). This enzyme is activated by an increase in intracellular calcium ion (Ca^{2+}), either from an influx of extracellular Ca^{2+} or intracellular stores (Andrew, 1999). Endothelial NOS was the third isoform to be identified. The enzyme is a 135 kDa protein and it is the only isoform that is membrane bound (Zhang and Snyder, 1995).

1.3.1.3. Neuronal nitric oxide synthase (nNOS)

Neuronal nitric oxide synthase is also known as nNOS, Type I, NOS-I, nNOS and eNOS are constitutively expressed and their activities are calcium-dependent (Calabrese, 2007). Neuronal nitric oxide synthase also performs a role in cell communication and is associated with plasma membranes (Bredt, 1999). The enzyme is a 150 kDa protein (Zhang and Snyder, 1995). Figure 1.6 below illustrates the secondary structure of nNOS.

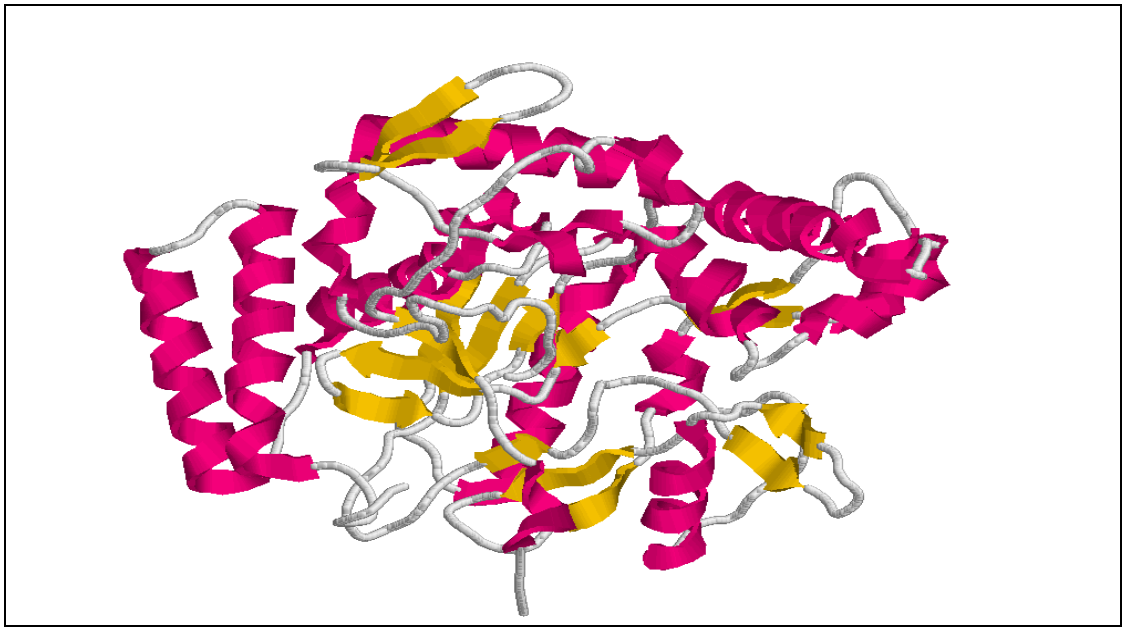

Figure 1.6: Secondary structure of homodimeric nNOS (PDB: 1zvi)

In all isoforms nNOS constitutes the predominant source of NO in synaptic spines neurons (Bredt, 1999). It is also present in skeletal muscle, cardiac muscle and smooth muscle where it controls blood flow and muscle contractility (Andrew, 1999).

1.3.1.4. Structure and properties of neuronal nitric oxide synthase

The neuronal NOS comprises of 1434 amino acids with a projected molecular weight of 160.8 kDa (Boissel *et al*., 1998). Neuronal nitric oxide synthase catalyses the oxidation of L-arginine to generate citrulline and nitric oxide as products in a wide range of tissues (Chun-Xia, 2011). Figure 1.7 below illustrates this point. The monomer of nNOS is an active dimer which requires tetrahydrobiopterin (BH_4), haem and an L-arginine binding site (Reif *et al*., 1999). It also exhibits a bidomain structure that consists of a oxygenase domain (N-terminal) and a reductase domain (C-terminal) which can be detached by a (CaM) binding motif (Sagami *et al*., 2001). The oxygenase domain which binds the substrate L-arginine contains a tetrahydrobiopterin binding site and a cytochrome P-450-type heme active site (Penelope and Mayer, 1999). Also, there is a binding site for zinc which facilitates nNOS dimerization. The reductase domain that binds the substrate nicotene adenine dinucleotide phosphate (NADPH) contains a binding site for flavin mononucleotide (FMN) and flavin-adenine dinucleotide (FAD) (Sagami *et al*., 2001). Flavin mononucleotide binding domain has an auto inhibitory loop that controls nNOS activity. Flavin mononucleotide and FAD are able to transfer

NADPH donated electron from the reductase domain to the oxygenase domain by a process called electron flow. This process enables the heme to be assisted by Ca^{2+}/CaM binding (Chun-Xia, 2011). Figure 1.7 below shows the metabolic pathway of nitric oxide.

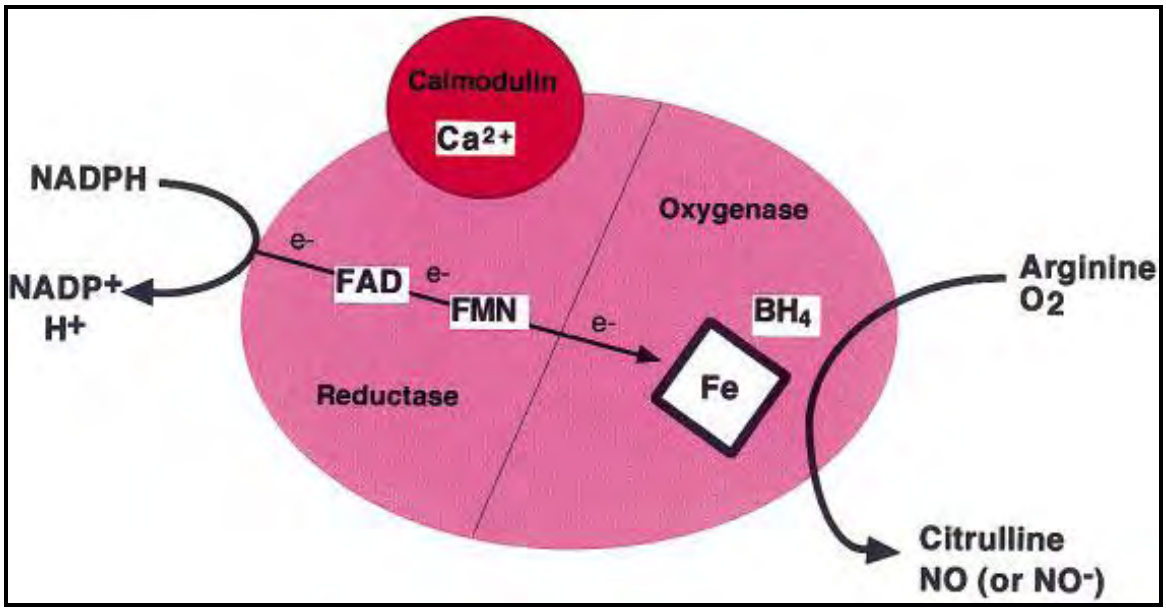

Figure 1.7: Schematic representation of nNOS structure and the metabolic pathway of nitric oxide formation (adapted from Chun-Xia 2011)

1.4. Nanotechnology in drug delivery

Nanotechnology is the use of engineered nanoparticles ranging between 1-100 nm in diameter. Their extremely small size enables them to interact with biological systems at the molecular level of life. They interact with the targeted cells or tissues to induce physiological responses while minimizing the side effects (Barbu *et al*., 2009).

Currently, drug delivery is a major concern for the treatment of Alzheimer"s diseases because the central nervous system (CNS) is surrounded by numerous protective barriers (Modi *et al*., 2010; Barbu *et al*., 2009; Singh *et al*., 2008). This caused developmental treatments for AD to become an active research area (Shanni *et al*., 2011; Nazem *et al*., 2010; Modi *et al*., 2009; Neuwelt *et al*., 2009; Pathan *et al*., 2009). The operating application of nanotechnology in neurology focused on neuroprotection, neurodegeneration and drug delivery beyond the blood brain barrier. It is also believed to improve the treatment of AD (Modi *et al*., 2010). Figure 1.8 above shows the application of nanotechnology treatment in Alzheimers disease.

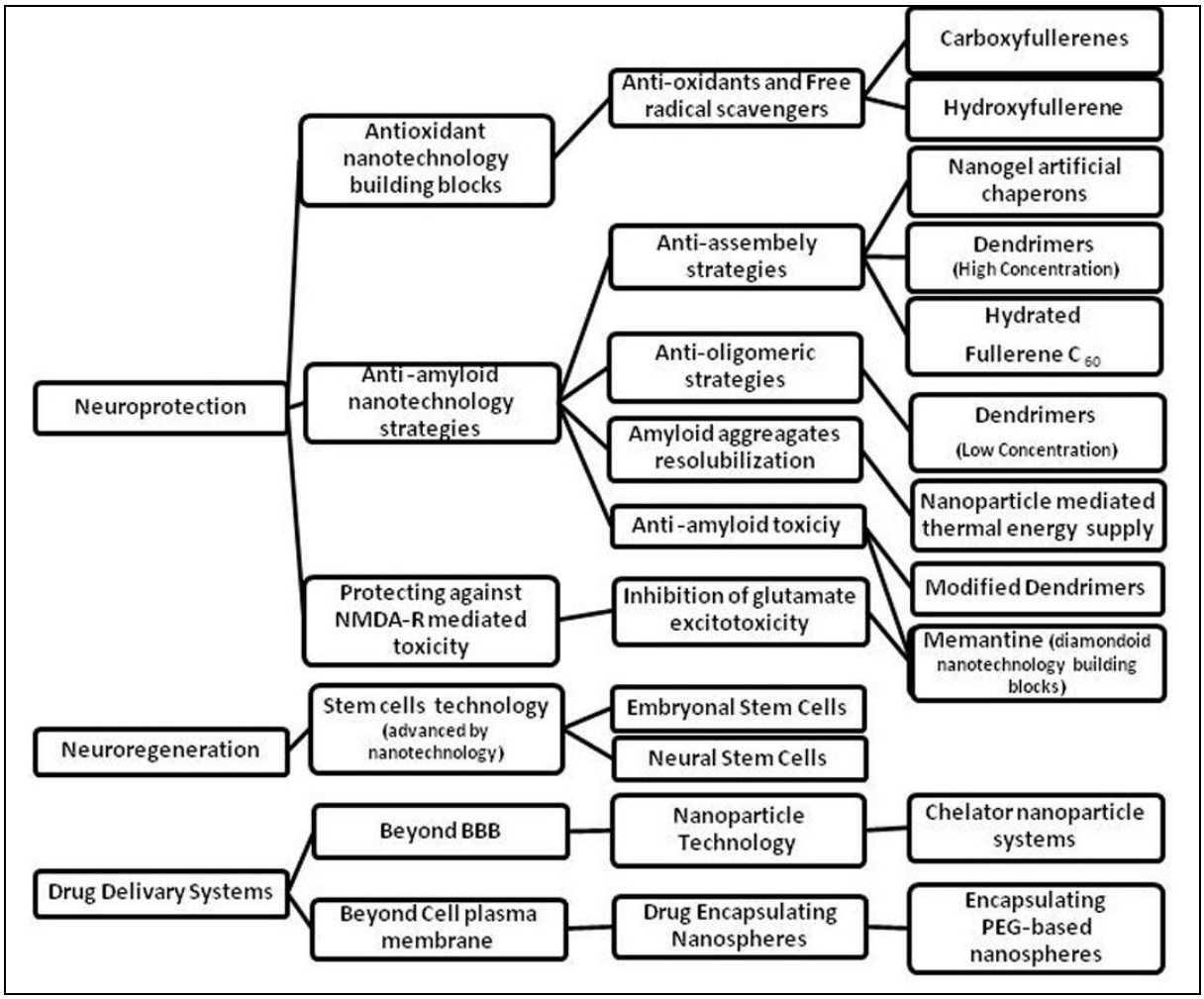

Figure 1.8: Summary of applications of nanotechnology in the treatment of Alzheimer's disease (Adapted from Nazem et al., 2010)

- **Neuroprotection**

The design of therapeutic agents that protect neurons against neurotoxicity is currently an area of intense research (Fazil *et al*., 2011; Nazem *et al*., 2008; Pardridge, 2007; Takada-Takatori *et al*., 2006; Wang *et al*., 2006). Antioxidants and anti-amyloid therapeutics are used against amyloid toxicity and oxidative stress while fuerfullerenols are used for neuroprotection against amyloid β 42(50) (Nazem *et al*., 2008). A study performed by Dungan *et al.* (1997) in cultured cortical neurons revealed that caboxyfullerness induced oxidative stress and neurotoxicity in β 42.

- **Neurodegeneration**

Neuroprotection measures are not yet confirmed to completely cure Alzheimer's disease because it is believed that no neuroprotection measure can offer complete protection of neurons form neurodegeneration (Iriti *et al.*, 2010). Stem cell technology has some success in the treatment of AD. Neural progenitor cells are neural stem cells or multipotent neural precursors that comprise of a relatively undifferentiated population of cells that are capable of giving rise to the broad array of specialized neurons and glia of the central nervous system. Recent evidence showed that some specific regions of the CNS (dentate gyrus, subventricular zone stratum and substantia nigra) have a high concentration of neural progenitor cells (Nazem *et al*., 2008).

- **Drug delivery**

Penetration of drugs into the brain is restricted. Only 2% of small drug molecules penetrate through the blood brain barrier (Nazem *et al*., 2008). Nanotechnology decreases drug release and peripheral toxicity in the brain by using metal chelating therapy which reduces oxidative stress based on the effects of homeostasis of metallic ions (Modi *et al*., 2010). Shea *et al*. (2005) designed a special poly ethylene glycol (PEG) nanosphere for vitamin E delivery to human neuroblastoma cultured cells which were exposed to Aβ. They reported an improvement in vitamin E efficacy against Aβ induced oxidative stress. Several nanostructures such as silver and gold were employed for the development of nano enabled drug delivery systems in the treatment of neurodegenerative disorders (Ochekpe *et al*., 2009).

1.4.1. Polymeric nanoparticles

Polymeric nanoparticles are nanoparticles which are prepared from polymers. Polymeric nanoparticles are commonly used as drug carriers in neurodegenerative disease (NDs) and are highly stable. Lipophilic may inherently increase their penetration through the blood brain barrier (Behan *et al*., 2001). As a result of their properties, polymeric nanoparticles can be manipulated into the macrophages of the reticuloendothelial system (RES), and have consequently been used in drugs such as doxorubicin (Behan *et al*., 2001; Calvo *et al*., 2001).

1.4.2. Polymeric nanospheres and nanosuspensions

Nanospheres are dense polymeric matrices in which a drug is diffused and prepared by a process called micro-emulsion polymerisation (Hyuk *et al*., 2005). Nanosuspensions contain a high drug loading capacity and can be used for numerous drugs in the central nervous system. Most polymeric nanospheres and nanosuspensions exhibit excellent pharmacokinetic

control, and are suitable for the entrapment and delivery of a wide range of drugs and other molecules with varying physicochemical properties compared to conventional nanoparticles (Friedrich *et al*., 2005).

1.4.3. Polymeric nanogels

Polymeric nanogels are composed of networks of crosslinked polymers that often combine ionic and non-ionic polymeric chains that are prepared using an emulsification solvent evaporation approach (Bronich *et al*., 2006). They are able to incorporate molecules such as oligonucleotide ribose nucleic acid (RNA), deoxyribose nucleic acid (DNA), proteins and low molecular drugs. They are the most promising carriers of central nervous system because of their ability to decrease the degradation of biomolecules during their transport. Vinogradov *et al*. (2005) have encapsulated oligonucleotides within a crosslinked nanogel for delivery across the blood brain barrier. This study showed that nanogels with reducible bonds provided a faster intracellular drug release over a short time period, and enhanced therapeutic effect compared with conventional biodegradable carriers, which have drug release kinetics measuring of several weeks. (Modi *et al*., 2009).

1.4.4. Carbon nanotubes and nanofibres

Carbon nanotubes are allotropes of carbon with a cylindrical nanostructure that are currently used to improve chronic central nervous system electrical stimulation (Kabanov and Gendelman, 2007). Electrospinning is a process by which polymer nanofibers can be produced using an electrostatically driven jet of polymer solution. The electrospun nanofibers can even be aligned to construct unique functional nanostructures such as nanotubes and nanowires (Yarin *et al.*, 2001). They have not been extensively applied in drug delivery research because of their high toxicity that may cause cellular death via an oxidative-stress pathway. Electrospun nanofibres represent nanostructures in two dimensions and macroscopic structures in another dimension. Though nanofibres are safer to synthesize than carbon nanotubes, they pose less risk to air pollution. Electrospun nanofibres of drug-loaded biodegradable polymers may also be used to design neural prosthetics, an application that may not be feasible with other forms of nanostructures (Modi *et al*., 2009).

1.4.5. Polymeric nano-micelles

Polymeric nano-micelles have core shell architecture with a hydrophobic core which can incorporate up to 20–30% (w/w) of hydrophobic drugs that prevent the release of premature

drugs and degradation (Ochekpe *et al*., 2009). The shell is designed to stabilize the nano-micelles and prevent the drug from interacting with serum proteins and untargeted cells. When the target cells are reached, the drug is released by diffusion. Nano micelles can use different solutes with different structures because of their various morphologies. They are more versatile than other nanostructures because they are able to release drugs and other molecules based on their environmental conditions (Oishi *et al*., 2007).

1.4.6. Polymeric nano-liposomes

Nano-liposomes are vesicular structures composed of uni or multi-lamellar lipid bi-layers surrounding internal aqueous compartments (Kabanov and Gendelman, 2007). They have been studied to target central nervous system drug delivery for various applications such as, attaching polymers to poly methacrylic acid-co-stearyl methacrylate or polyethylene glycol units to improve the circulation time of liposomes in the blood, and by conjugation to antibodies or ligands such as lectins for target specific drug delivery and stability (Mora *et al*., 2002; Schmidt *et al*., 2003; Chekhonin *et al*., 2005). Thus, nano-liposomes short half-life always have to be modified (e.g. sulfatide, ganglioside monosialoganglioside galactose [GM1], mannose, Tween-80) or lipids derived from poly ethylene glycol or PEG derivatives that are inserted into the lipid bilayer (Modi *et al*., 2009).

1.5. Synthesis of nanoparticles

Currently, the synthesis of nanoparticles has been the subject of intense research because of their commercial importance and applications (Zhang *et al*., 2009). Nanoparticles can be broadly grouped into three subfamilies, namely: organic nanoparticles (i.e. carbon nanoparticles fullerenes), inorganic nanoparticles (i.e. noble metal nanoparticles such as gold and silver) (Singh *et al.,* 2010), and semiconductor nanoparticles (i.e. titanium dioxide and Zinc oxide) (Xu *et al*., 2006). Because of their characteristics (i.e shape and size) and their wide range of applications, various methods are being developed for their synthesis (Kanan, 2010; Ochekpe *et al*., 2009; Sonneville-Aubrun *et al*., 2004). There are two main approaches for nanoparticle synthesis namely the “top down” approach and the “bottom up” approach. The top down approach involves the formulation of nanoparticles using larger particles to direct their assembly while the bottom up approach involves processes that build towards larger and more complex systems by starting at the molecular level and maintaining precise control of molecular structure (Ochekpe *et al*., 2009). Typically, nanoparticles can be

synthesized by physical, chemical and biological methods. Some of these methods are very expensive and can involve hazardous chemicals (Kanan, 2010).

1.5.1. Biological processes

- **Bacteria based synthesis of nanoparticles:** This involves the use of bacterial strain for biomanufacturing processes e.g. Lactobacillus strains (Bazylinski and Frankel 2004).

- **Fungi based synthesis of nanoparticles:** This involves the use of fungi and is mostly used for large scale synthesis, for example, Fungus *Verticillium* sp. produces the metallic nanoparticles when exposed to gold and silver ions (Mukherjee *et al* 2001).

- **Yeast based synthesis of nanoparticles by yeast:** This process is usually employed for the industrial synthesis of quantum semiconductors, for example, *Candida glabrata* for Cadmium sulphide (CdS) quantum nanocrystals (Kowshik *et al*., 2003).

- **Biological synthesis of nanoparticles by virus:** This method has received great attention because of its relative ease of manipulation and extended intact towards biological particles (viruses). Cowpea chlorotic mottle virus and cowpea mosaic virus have been used as nucleation cages for the mineralization of inorganic materials (Kannan *et al*., 2010).

- **Biological synthesis of nanoparticles by plant source.** This process involves relatively rapid reduction of metallic materials, for example, *Pelargoniumgraveolens* (the extract of geranium leaves) for the reduction of Ag^{+} ions to Ag nanoparticles (Shankar *et al*., 2003).

- **Biogenesis of nanoparticles by algae:** This is a "bottom up" approach where the main reaction that occurs involves reduction/oxidation or the synthesis of gold nanoparticles by the reduction of aqueous $AuCl_4$ by using *Sargassum wightii* (Kanan, 2011).

1.5.2. Physiochemical processes

- **Sol-gel technique** is a type of wet chemical technique that is used in fabrication of metal oxides from a solution which acts as a precursor for integrated network (gel) of discrete particles or polymers (Mackenzie and Bescher, 2007).

- **Solvothermal synthesis** is a versatile low temperature route in which polar solvents are being used under high pressure and high temperatures to facilitate the interaction of precursors during synthesis (Zhang, 2003).

- **Chemical reduction** is the reduction of an ionic salt using reducing agents to synthesize nanoparticles, for example sodium borohydride, hydrazine hydrate and sodium citrate (Guzmán *et al*., 2008).

- **Laser ablation** is the process of removing material from a solid surface by irradiating with a laser beam e.g. carbon nanotubes (Yang, 2007).

- **Inert gas condensation** is the process where different metals are evaporated in separate crucibles inside an ultra-high vacuum chamber filled with helium or argon gas, for example gold nanoparticles from gold wires (Werner *et al*., 2011).

1.5.3. Metal nanoparticles

Silver and gold nanoparticles are the most commonly utilized nanoparticles due to their anti-microbial and their attractive physicochemical properties (Medina *et al*., 2007). Silver nanoparticles are ideal candidates for molecular labelling because of their surface Plasmon Resonance effect and their large effective scattering cross section (Elechiguerra *et al*., 2005). Nanoparticles contain large specific surface areas for biological interactions and they can easily penetrate biological cells. There has been a considerable progress in the synthesis of NPs with well controlled dimensions and geometry. (Wu et *al*., 2009; Cheon and Horace, 2009). Nanoparticles can also be applied in fluorescent labelling because of their tuneable emission spectra. The diameter of a nanoparticle determines the wavelengths of light absorbed (Figure 1.9 below shows Rayleigh light scattering of nanocrystals).

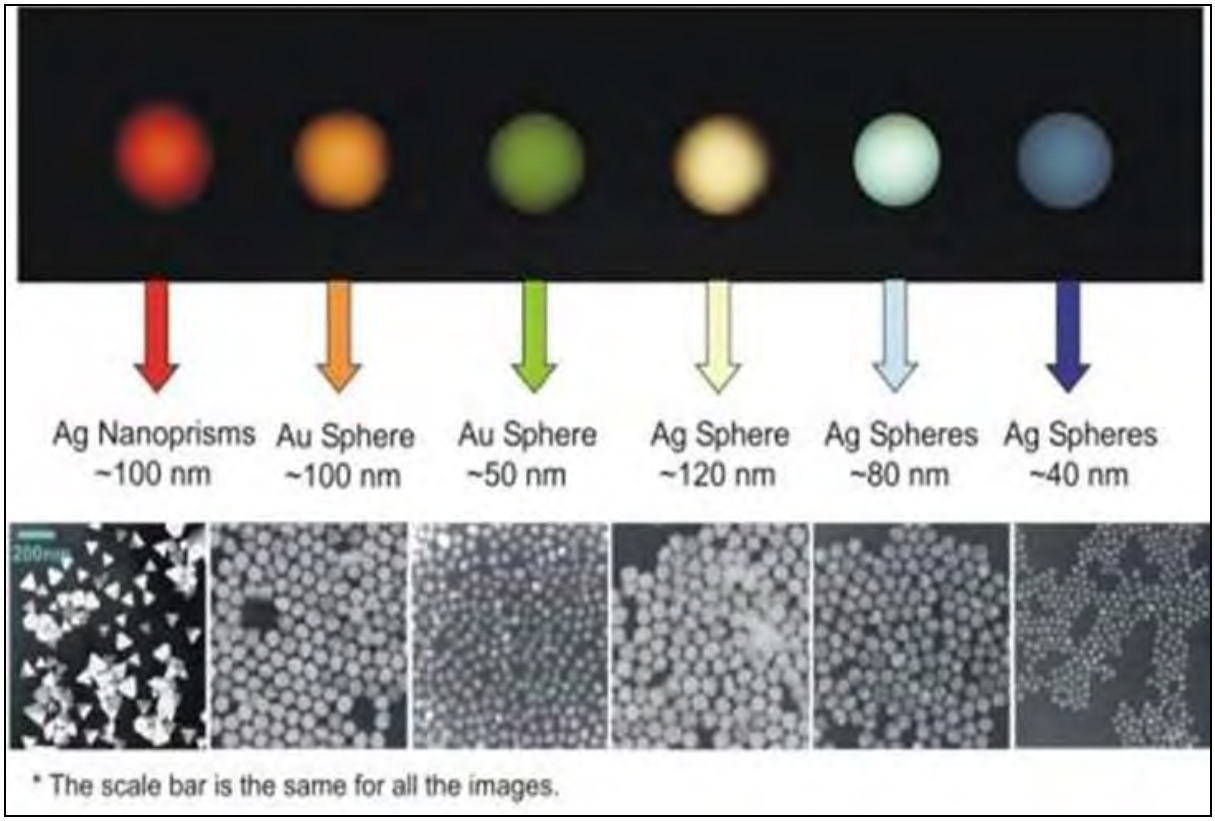

Figure 1.9: Rayleigh light scattering of nanocrystals: shape, size and composition matter (Adapted from Whiteley et al., 2011)

1.5.3.1. Gold nanoparticles

Gold nanoparticles are known as nano gold if they are less than 100 nm with an intense red colour but larger particles are dirty yellowish in colour in the suspension. This may be due to surface plasmon absorbance (Ghosh *et al.,* 2008). Gold nanoparticles have been used for the treatment of arthritis in rats and dogs where these particles were implanted in the knees of these animals and timing of drug release and uptake can thus be controlled. Gold nanoparticles have been used to bind antibodies which are attached to the cancer cell receptors. Also, they detect toxins whereby the nanoparticle binds to the toxin the whole solution changes colour to indicate the presence of the toxin. A study that was conducted on the combination of colloidal gold by microwave radiation to treat Alzheimer‟s disease showed that colloidal gold can destroy the beta-amyloid fibrils and plaque (Zhang *et al.,* 2009; Brambilla *et al.,* 2011).

1.5.3.2. Silver nanoparticles

Silver nanoparticles are ultra-fine particles of silver which have different colours due to plasmon absorbance (see Figure 1.9 above) (Singh *et al*., 2009). Silver has anti-bacterial properties, which results in a chemical change of the bacteria structure causing the cells to rupture, resulting to cell death (Singh *et al*., 2008). The ability to bind to spikes of Human immunodeficiency virus (HIV) virus and prevent it from latching on to the cell ensures that the HIV virus does not bind to host cells and therefore the infection can be suppressed (Singh *et al*., 2009). Silver has also been used in surgical instruments or to mask in wound healing (Bondy, 2011; Humberto *et al*., 2010).

1.6. Biomedical targets

Biomarkers are the key to advancing the understanding of pathophysiology of AD which may have important implications for patient‟s diagnosis and treatment. Biomarkers are instrumental not only in the diagnosis of AD, but in the monitoring of also aids in following of disease progression and in response to treatment. It is unlikely that a single biomarker will meet the needs for clinical diagnosis. Biomarkers may offer an appropriate sensitivity and specificity for the disease (Craig-Schapiro *et al*., 2009). The identification of enzyme biomarkers and their concentration level requirements is important for an effective biomarker design. Interestingly, nNOS could be a good biomarker which mechanistically influences the production of NO and clearance in the brain. It maybe hypothesized as being catalytic for oxidative stress.

1.6.1. Neuronal nitric oxide synthase (nNOS) and its role as a potential biomarker of Alzheimer's diseases (AD)

The understanding of nNOS as an enzymatic biomarker for Alzheimer‟s diseases could be enhanced by elucidating its role in the amyloidogenic pathway. Elevated levels of arginine are found in the cerebrospinal fluid of Alzheimer‟s patients. nNOS is an enzyme that is crucial in the metabolism of arginine to citrulline and nitric oxide (Andrew, 1999). The fact that there is a low level of citrulline and a high level of arginine in the cerebrospinal fluid of AD patients could mean that there is a metabolic abnormality with an enzyme that metabolizes this amino acid and, thus reflects the possible use of nNOS as a biomarker in AD (Plasman *et al*., 2007). Figure 1.10 below illustrates the role of nNOS as a potential biomarker in amyloidogenic pathway. But the question remains whether these nanoparticles,

especially gold and silver, in general would inhibit nNOS? On the other hand, when arginine levels are low and nNOS catalytic activity is high, there is excess production of NO and formation of superoxide radicals which generates reactive oxygen species (ROS) and peroxynitrite (ONOO-) that are far more neurotoxic than NO. See Figure 1.10 below:

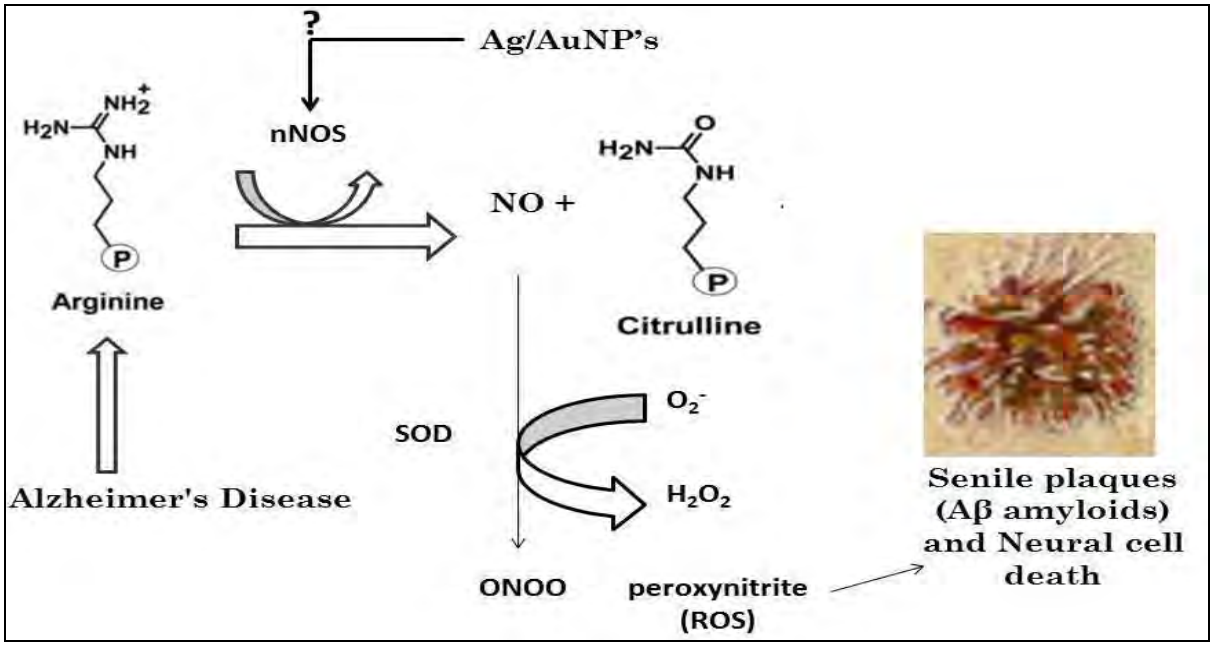

Figure 1.10: Schematic diagram describing the role of neuronal nitric oxide synthase nNOS in the amyloidogenic pathway, adapted from (Adapted from Penelope and Mayer, 1999). Nitric oxide (NO) and superoxide dismutase (SOD)

1.7. Potential inhibitors of neuronal nitric oxide synthase (nNOS)

It is clear that there is a great need to control and regulate the neuronal isoform of NOS in particular, since it is this isoform that is related to AD. This is due to its location in the brain and that it metabolises arginine as substrate. Research has thus been expanded to discover inhibitors and regulators of nNOS activity in order to find ways to inhibit this enzyme and prevent the production of excess nitric oxide.

1.7.1. Heat shock protein 90 (HSP90)/HSP70

Heat shock protein 70 (HSP70) and heat shock protein 90 (HSP90) are chaperones of nNOS with opposite actions on Alzheimer‟s diseases (AD) ubiquitination. HSP70 stimules action of nNOS while HSP90 inhibits it (Martinez-Ruiz *et al*., 2005). HSP90 is important for nNOS-α stabilization and regulation if nNOS dimerization through the facilitation of heme insertion in

the monomer (Figure 1.11 illustrates HSP70/HSP90 stabilization or degradation of nNOS) (Billecke *et al*., 2004; Martinez-Ruiz *et al*., 2005).

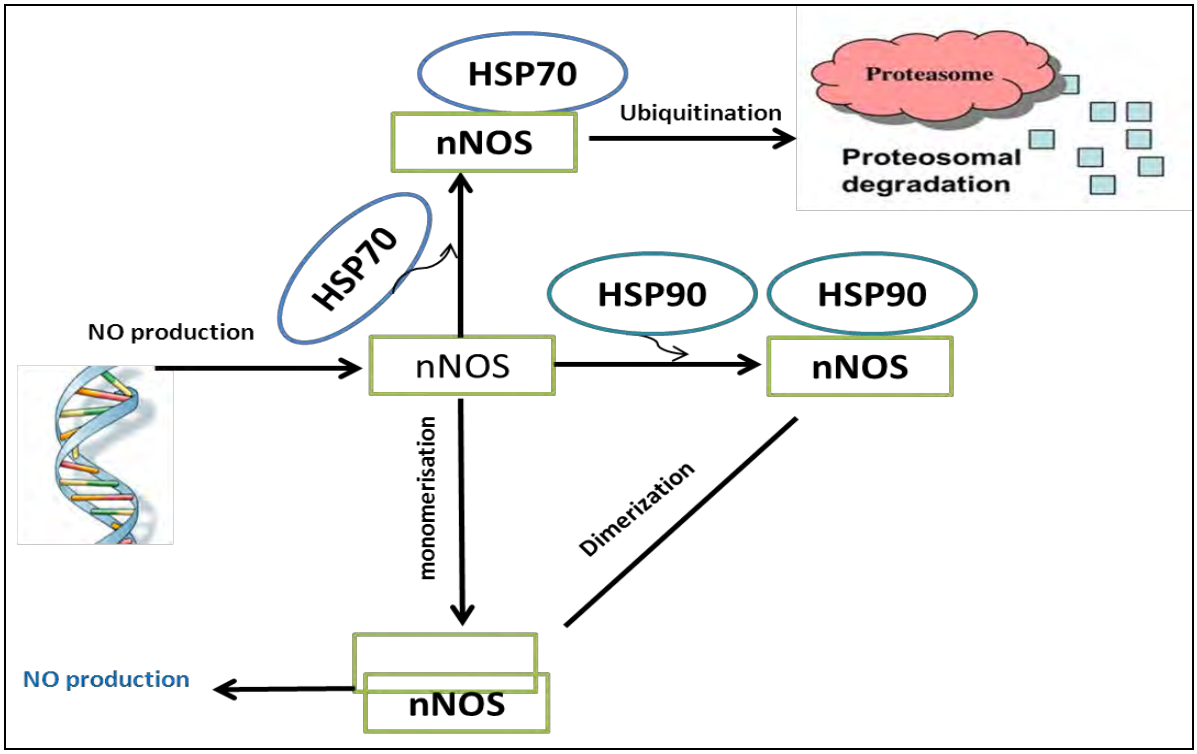

Figure 1.11: A schematic representation of the HSP70/HSP90 machinery that makes the quality control decision for stabilization or degradation of nNOS. Adapted from Luo and Zhu (2011)

1.7.2. Calmodulin-dependent protein kinase (CaM)

Calmodulin-dependent protein kinase (CaM**)** functions as an allosteric activator of nNOS and Alzheimer"s diseases. In the absence of CaM and Ca^{2+}, electron flow from flavin adenine dinucleotide to flavin mononucleotide will slow down (Song *et al*., 2004). The binding of CaM to nNOS facilitates electron flow from NADPH to the reductase domain flavin from where it flows to the heme centre. Neuronal nitric oxide synthase is inactive at the basal level of intracellular Ca^{2+}. In contrast, when intracellular Ca^{2+} concentration decreases to the basal level, CaM dissociates from nNOS and nNOS returns to the inactive state (Zhou *et al*., 2009; Poulos, 2005).

1.7.3. Phosphorylation

Phosphorylation of nNOS has an effect on its activity and is controlled by kinases and phosphatases (AMP–dependent protein kinase (PKA), Ca^{2+} calmodulin–dependent protein kinase (CaMK), protein kinase-C (PKC), and phosphatase (Zhou *et al*., 2009). Calmodulin–dependent protein kinase (CaMK II) phosphorylates nNOS at Ser847, which reduces nNOS activity by inhibiting Ca^{2+}-CaM binding. By contrast, protein phosphatase 1 decreases the level of nNOS phosphorylation at Ser847, resulting to an increase in nNOS activity. Phosphorilation of Ser412 increases nNOS activity, whereas dephosphorylation by phosphatases decrease nNOS activity (Song *et al.*, 2004).

1.7.4. Protein inhibitor of nNOS Alzheimer's diseases

Protein inhibitors are enzyme inhibitors that interacts in some way with the protein to prevent it from working in the normal manner. Neuronal nitric oxide synthase is not inhibited or monomerised by protein inhibitor of nNOS (PIN). The N-terminal extension of nNOS also contains a binding site for the 89-amino acid protein PIN. PIN can be co-immunoprecipitated with nNOS but not with eNOS or iNOS (Zhou *et al*., 2009).

1.7.5. Adapter proteins of nNOS

There are nine primary interacting proteins involved with neuronal nitric oxide synthase. These include post-synaptic density protein 95 (PSD95), clathrin assembly lymphoid leukemia (CALM), Ca^{2+} calmodulin–dependent protein kinaseIIA (CaMKIIA), Disks large homolog 4 (DLG4), DLG2, 6- phosphofructokinase (PFK), muscle type (PFK-M), carboxy-terminal PDZ ligand of nNOS (CAPON) protein, syntrophin and dynein light chain (LC) (Luo and Zhu *et al*., 2011); Xia *at al*., 2011; Jaffrey *et al*., 1998). Post-synaptic density-95 (PSD-95) and PFK-M are important adapter proteins of nNOS in neurons, and are critical signalling proteins (Che *et al*., 2000). The interaction among N-methyl-D-aspartate type-glutamate receptors (NMDARs), PSD95 and nNOS are critical for nNOS activation and NO generation, which could lead to neuron and astrocyte apoptosis (Mungrue and Bredt, 2004). Dexras 1 might participate in CNS neuronal cell death through regulating NO signalling by binding to nNOS and CAPON (Eugenin *et al*., 2007). Overexpression of CAPON leads to an increase in dendritic protrusion, which depends on the Phosphotyrosine-binding domain of CAPON, suggesting an important role of CAPON in mammalian synapses (Richier *et al*., 2010). The interaction of nNOS with PFK might have a neuroprotective effect because of the product of PFK activity, fructose-1, 6-bisphosphate (Firestein and Bredt, 1999).

CHAPTER 2: INTRODUCTION TO THE PRESENT STUDY

Neurodegenerative diseases are heterogeneous group of disorders characterised by a gradually progressive, selective loss of anatomically or physiologically related neuronal systems (Jhala and Hazell**,** 2011; Zündorf and Reiser 2011). The most common neurodegenerative disease include Alzheimer‟s, amyotrophic lateral sclerosis and Parkinson‟s diseases; trauma and aging itself are associated with excessive oxidative stress. High oxidative stress results when organs in the body such as the brain or the central nervous system (CNS) become sites for free radical production (Singh *et al*., 2007). Globally, among the common neurodegenerative diseases, Alzheimer‟s disease (AD) accounts for over 65 000 deaths per year in individuals over the age of 65 and it is estimated that the number of people older than 65 years will approach 370 million by the year 2050 in the U.S.A. alone (De Felice *et al*., 2002). In South Africa, over 140 000 people suffer from dementia and it has been estimated that about 37.9 million people will be over the age of 65 by the year 2025 (Cummings, 2003). As a result, of the estimated growing population of individuals over the age of 65, the number of people that will be affected by AD will also grow and may have adverse negative social and economic impacts on the families of such individuals. AD is a chronic disease with a great risk on advanced age. It is estimated that there are older women than men who have dementia because of the fact that women live longer on average than men (Plasman *et al*., 2007).

Alzheimer‟s disease is characterised by an intracellular appearance of neurofibrilary tangles, and synaptic and neuronal loss as well as extracellular accumulation of amyloid-β (Aβ) peptide in senile plaques (De Felice *et al*., 2004). Senile plaques are surrounded by astrocytes, which also store reserve arginine in brain tissue (Cras *et al*., 1991). Five percent of all reported cases of AD are associated with gene mutations whereas majority of AD cases are sporadic (Perry *et al*., 2005). Genetic mutation, which causes AD are usually associated with protein abnormalities in the amyloid precursor protein (APP). The third secretase plays a partial role in the process (De Felice *et al*., 2004). Nitric oxide synthases (NOS‟s) are a class of enzymes found in mammals and other species that utilize L-arginine to generate nitric oxide (NO). Nitric Oxide is an important signalling molecule in the brain (Poulos *et al*., 2002). These enzymes function as active dimers comprised of three isoforms of NOS namely, neuronal NOS (nNOS); endothelial NOS (eNOS) and inducible NOS

(iNOS). Neuronal nitric oxide synthase (nNOS) is found in neuronal tissue of both the central and peripheral nervous system, and is involved in cell communication (Zhang and Snyder, 1995).

The initiating causes that lead to AD are unknown, and the available treatments are only effective at slowing the degeneration process (De Felice *et al*., 2004). Currently, there are only five medications approved for the treatment of AD by the U.S.A. Food and Drug Administration (FDA) and these include donepezil, galantamine, rivastigmine, tacrine (collectively referred to as acetyl cholinesterase inhibitors), and N-methyl-d-aspartate antagonist memantine (Neugroschl and Sano, 2010). Because available treatments are only effective at slowing down the degenerative processes, alternative methods are being investigated (Fros *et al*., 2010). Nanotechnology has potential for the development of more effective treatment for the AD.

Nanotechnology is currently employed for the treatment, diagnosis, monitoring and control of various kinds of diseases (Menezes *et al*., 2010; Singh *et al*., 2008). Nanotechnology offered novel tools for the early detection of AD (Singh *et al*., 2008). The operating application of nanotechnology in neurology focused on neuroprotection, neurodegeneration and drug delivery, beyond the blood brain barrier (BBB) are believed to improve treatment of AD (Modi *et al*., 2009). Nanotechnology uses nanoparticles for the treatment, detection and monitoring of diseases as well as acting as markers. Although several nanoparticles exist, silver (Au) and gold (Au) nanoparticles are among the most commonly used nanoparticles due to their anti-microbial properties and attractive physicochemical properties. Silver is a transition metal with high electrical and thermal conductivity. The surface plasmon resonance and large effective scattering cross section of individual silver nanoparticles make them ideal candidates for molecular labelling (Elechiguerra *et al*., 2005). Silver nanoparticles (NPs) contain large specific surface areas for biological interactions which enable them to easily penetrate biological cells (Singh *et al*., 2008). Gold has high optical and chemical properties at nanoscale for biomedical imaging and therapeutic applications (Medina *et al*., 2007). Neuronal nitric oxide synthase has cysteine residues at the interface between the two subunits, which form a disulphide bridge between the monomers. As a result of the Ag/Au nanoparticles having a strong affinity for sulphur, and consequently the binding Ag/Au nanoparticles with nNOS can be a useful diagnostic tool for treatment of AD.

The development of any effective diagnostic tools, treatment regimens, drugs and/or metabolites which can indicate early outset or inhibit the progression of Alzheimer‟s disease requirers an enhanced understanding of the molecular causes and mechanisms underlying the neurodegenerative processes (De Felice *et al*., 2004). Due to unavailability of effective drugs for the treatment of AD, there is need to investigate and develop both novel biomarkers as well as therapeutic agents for the detection and treatment of AD. The overall aim of this study therefore is to examine the interaction of Ag/Au nanoparticles on the activity of neural nitric oxide synthase, with a view to elucidating a possible mechanism of the outset of neurodegenerative diseases (Alzheimer‟s disease). The specific objectives of the study are:

- To extract, purify and characterise neural nitric oxide synthase from bovine brain.
- To synthesise and characterise silver and gold nanoparticles.
- To interact silver and gold nanoparticles with the purified neural nitric oxide synthase
- To monitor the interaction of these particles with nNOS by using both kinetic and fluorimetric techniques.

CHAPTER 3: ENZYME ISOLATION AND PURIFICATION

3.1. Introduction

Neuronal nitric oxide synthase (nNOS) is the enzyme that catalyses the oxidation of L-arginine to form L-citrulline and nitric oxide, depending on the catalytic mechanism and levels of arginine in the brain. Neuronal nitric oxide synthase may be an important diagnostic marker in the onset of Alzheimer‟s disease (AD) (Packer, 1994). Enzymes are often isolated under controlled conditions such as pH, temperature and ionic strength because they are unstable molecules with a definite physico-chemical organization. They are proteins and their standard extraction and purification procedures are similar to those used for other proteins except that the activity of the enzyme is assayed at each steps of extraction and purification. In most cases, more than one purification step is necessary to reach the desired purity (Reymond and Sicard, 2006) and numerous assays have been used to quantify the enzymatic reaction of nNOS (Packer, 1994). In this chapter, different methods are employed for the isolation, purification and characterisation of neuronal nNOS. Results obtained are presented critically discussed. The objectives of this chapter are:

- To run assays for the enzyme (citrulline) and protein assay (Bradford reagent)
- To purify nNOS from bovine brain, employing methods of poly (ethylene) glycol precipitation, ammonium sulphate precipitation and ion exchange chromatography;
- To determine the molecular weight of nNOS using the technique of gel electrophoresis;
- To determine kinetic parameters of nNOS and its physiological optimum pH, temperature and thermal stability.

Despite numerous previous reports on the successful purification and characterisation of nNOS from rat cerebella (Padayachee *et al*., 2011; Zweier and Giraldez, 1998), it was imperative to conduct similar purification and characterisation steps in order to monitor the degree of purity and to establish the appropriate kinetic parameters for enzyme efficiency. Bovine brain was used as a model for research into AD due to the relationship between prion proteins and amyloid peptides and their similar mechanistic approach in relation to nNOS (Kajava *et al*., 2006).

3.2. Principles of techniques applied for enzyme isolation and purification

3.2.1. nNOS assay

This assay is a chromogenic, discontinuous assay that relies on colour visibility of the citrulline product. The reaction is terminated by using concentrated acid, for example, hypochloric acid. Arginine is used as a substrate. The reaction requires equimolar amounts of NADPH and O_2, as well as, flavin-adenine dinucleotide (FAD) or flavin mononucleotide (FMN), protoporphyrin IX heme iron, (6R)-tetrahydro-L-biopterin (BH_4) and Ca^{2+}/calmodulin. During the reaction electrons donated by the conversion of reduced nicotinamide adenine dinucleotide phosphate (NADPH) to Nicotinamide adenine dinucleotide phosphate (NADP) act as the cofactors heme and BH_4, which catalyze the reaction between oxygen (O_2) and L-arginine, as shown in the reaction in equation 1. The reaction also requires bound calmodulin for electron flow. BH_4 functions exclusively as one of the electron donor during reductive activation of the oxyferrous complex of hemedioxy enzymes. Arginine is added to the enzyme extract, incubated for several minutes, and then the reaction stopped by the addition of an EDTA-containing buffer which chelates the calcium ions required by nNOS, and consequently inactivates the enzyme (Li and Poulos, 2005).

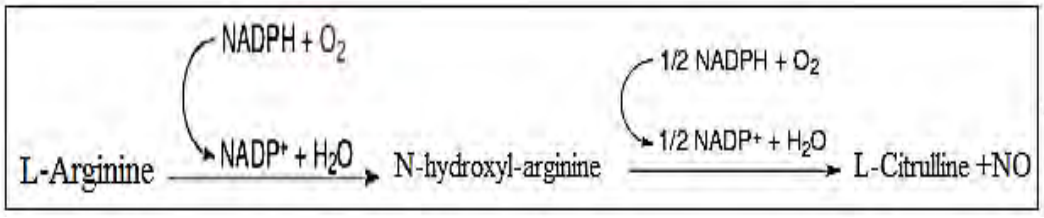

..Equation 1

3.2.2. Bradford Assay

Bradford assay is based on an immediate absorbance shift from 470 nm to 595 nm that occurs when sulphonic acid groups of the dye, Comassie Brilliant blue, binds to the protein in acidic solution. The mechanism of dye binding can be explained by the dye existence of its three absorbing species, a red cationic species A_{470}; a green neutral species at A_{650}; and a blue anionic species at A_{595} and the colour changes are due to successive loss of charge. Prior to protein binding, the dye molecules exist in a doubly protonated red cationic form. Upon binding to the protein, the blue anionic form is stabilized and detected at 595 nm. The advantage of this process is that the colour development is relatively rapid and the assay can be performed within 10 minutes. However, interfering substances such as strong bases can

form a complex with the dye, which results in an absorbance shift above the equilibrium (Hafiz, 2005). The protein concentration can also be determined by measuring absorbance at 280 nm (A_{280}). This assay is fast and convenient, since it does not require additional reagents or incubations, no protein standard needs to be prepared. However factors such as pH, ionic strength, secondary, tertiary, and quaternary structure are reported to alter the absorbance spectrum (Layne, 1957; Stoscheck, 1990).

3.2.3. Ammonium sulphate precipitation

Enzymes and other proteins are highly charged molecules, which are precipitated with appropriately charged neutralizing chemicals. Many cytosolic proteins are water soluble and their solubility is a function of the ionic strength and pH of the solution. Because of its high solubility even at lower temperatures, ammonium sulphate is the most commonly used salt for precipitating proteins (Chamow and Ashkenazi, 1999, Harlow and Lane, 1998). It stabilizes most proteins in solution and also helps reduce the lipid content of the sample. Proteins in aqueous solutions are heavily hydrated and, with the addition of salt, the water molecules become more attracted to the salt than to the protein due to the higher charges. This competition for hydration is usually more favourable towards the salt, which leads to interaction between the proteins, resulting in aggregation and finally precipitation (Chamow and Ashkenazi, 1999). The precipitate can then be collected by centrifugation and the protein pellet is re-dissolved in a low salt buffer. Since different proteins have distinct characteristics, it is often the case that they precipitate at a particular concentration of salt (Harlow and Lane, 1998).

3.2.4. Dialysis

Dialysis is a technique that is used to remove low molecular weight solutes and buffer exchange. This method is based on the properties of a semi permeable membrane that separates the protein solution from the dialysis buffer. It allows for free passage of molecules below certain molecular weight, the so-called „molecular weight cut-off", and retains macromolecules unable to penetrate the membrane pores. The process of dialysis is driven by the difference in concentration of the solutes on the two sides of the membrane (Figure 3.1 below illustrates the dialysis process) (Deutscher, 1990).

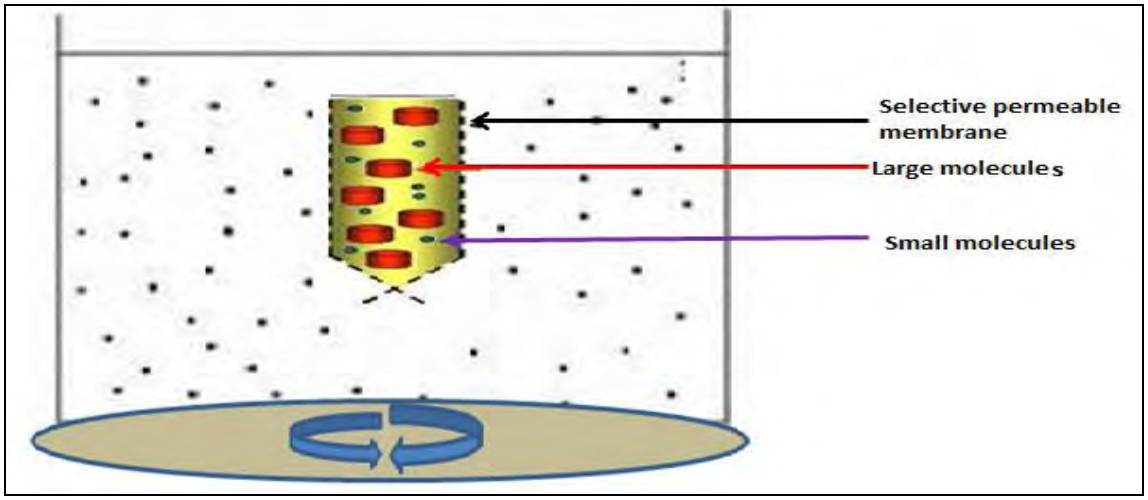

Figure 3.1: Schematic diagram showing dialysis (adapted from internet 2: Appendix D)

3.2.5. Poly (ethylene) glycol (PEG)

Poly ethylene glycol (PEG) is a water-soluble, inert polymer of cross-linked dextrins that is used for fractional precipitation of proteins and other macromolecules (Thrash *et al*., 1991). When mixed with protein samples, PEG increases the viscosity of the solution and reduces the solubility of proteins, which enables it to precipitate the protein based on sizes (Plourde *et al*., 1991). PEG is not influenced by the buffer conditions of the sample and, unlike other organic precipitating agents such as acetone and ethanol it does not easily denature or interact with proteins, even at high concentrations and increased temperatures (Deutscher, 1990). The protein samples are mixed with buffered solutions containing 5-40 % (w/v) PEG and incubated at optimal temperature for 30-60 minutes (Thrash *et al*., 1991). The samples are centrifuged and the remaining protein in the supernatant is assayed. This provides an estimate of the maximum concentration of PEG that can be added without losing the protein of interest, and also the minimum concentration of PEG required in bringing the protein out of solution (Deutscher, 1990). PEG is usually removed from the sample by ultrafiltration or in subsequent chromatographic steps. It is important to note that osmotic effects of PEG can alter the performance of the chromatography column (Deutscher, 1990).

3.2.6. Ion exchange chromatography

An ion exchange chromatography is the most common type of chromatographic technique used for the separation and purification of proteins on the basis of their charges (Bonnerjera *et al*., 1986). There are two different types of ion exchange groups namely, the anion exchanger, such as diethylaminoethyl (DEAE) and a cation exchanger, such as CM

(Carboxymethyl) (Cummins *et al*., 20110). Figure 3.2(a) below illustrates different ion exchangers:

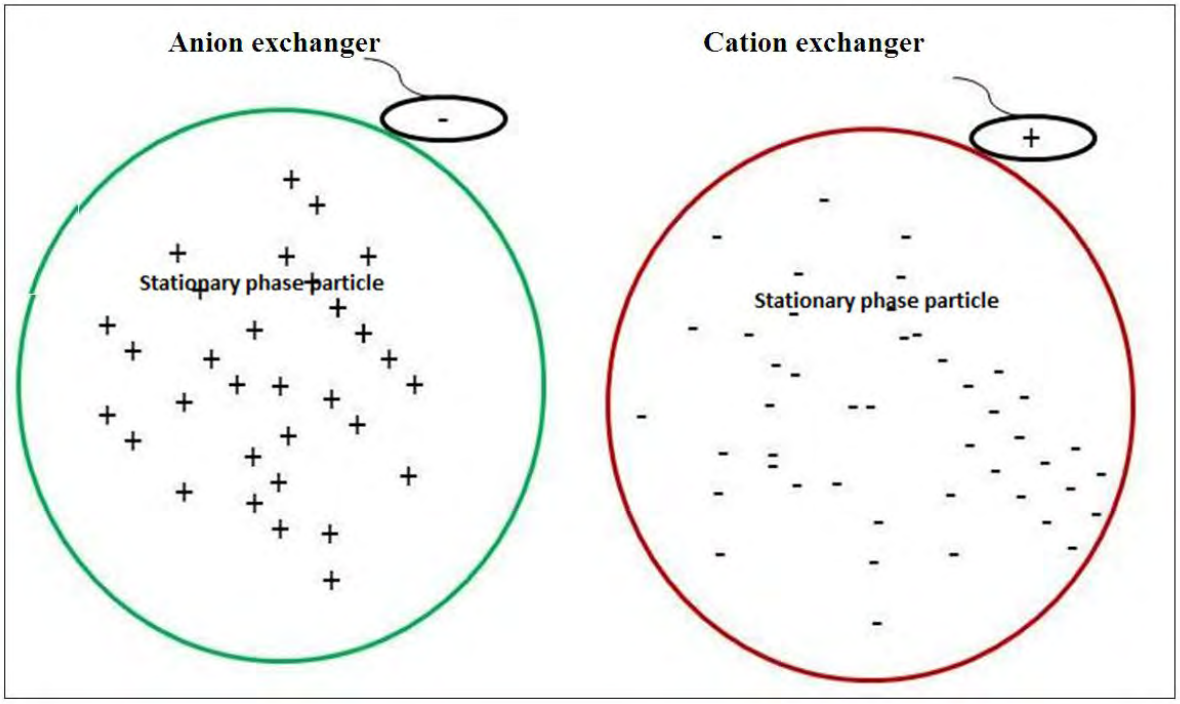

Figure 3.2(a): Schematic diagram showing anion and cation exchanger groups adapted from internet 3: Appendix D)

Ion exchange chromatography differs from other types of liquid chromatography in that, the stationary phase carries ionisable functional groups, fixed by chemical bonding (Deutscher, 1990). This method depends on the surface residues on the protein, buffer conditions, and the proteins net a positive or negative charge. An ideal buffer should be in the physiological pH range of 6 to 8. At this pH range, most proteins have been observed to be negatively charged and would bind to positively charged molecules of the resin. Change in the buffer pH condition could make the protein relatively positive, thereby allowing it to bind to a negatively charged resin material. The protein is loaded onto this packed column and is allowed to bind. Thereafter, the column is washed. The bound proteins are eluted - depending on their tightness of binding by subjecting them to either increasing concentrations of salt or changes in pH and proteins with low charge (Swiatek and Ward, 2009). Figure 3.2(b) below illustrates ion exchange process:

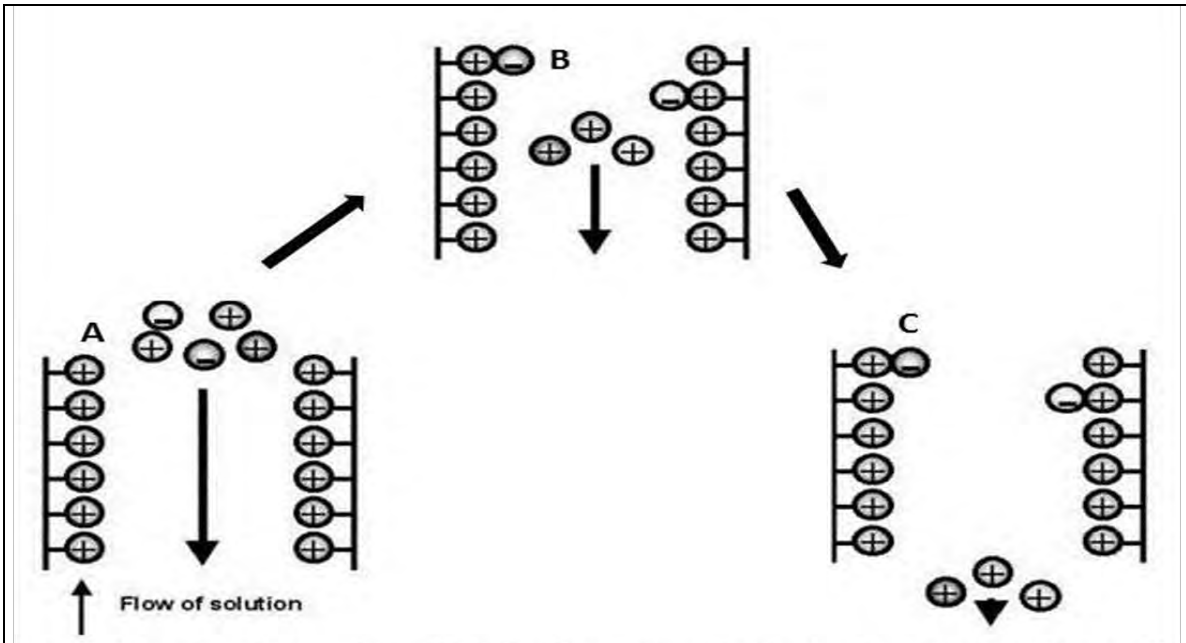

Figure 3.2(b): Schematic diagram of an ion exchange process (adapted from internet 4: Appendix D)

3.2.7. Gel filtration chromatography

Size-exclusion chromatography is generally used to separate biological molecules, determine molecular weights and molecular weight distributions of polymers. Protein size depends on the number of its amino acids that can be used in protein purification. The column material (see Figure 3.3 below that illustrates size-exclusion chromatography in a column) consists of a porous matrix for proteins to diffuse into the smaller sized proteins are entangled inside the porous material restricting their mobility, while larger sized proteins pass through freely. The larger molecules would be the first ones to elute, while the smallest ones would be last to elute (Bonifacino *et al*., 2004).

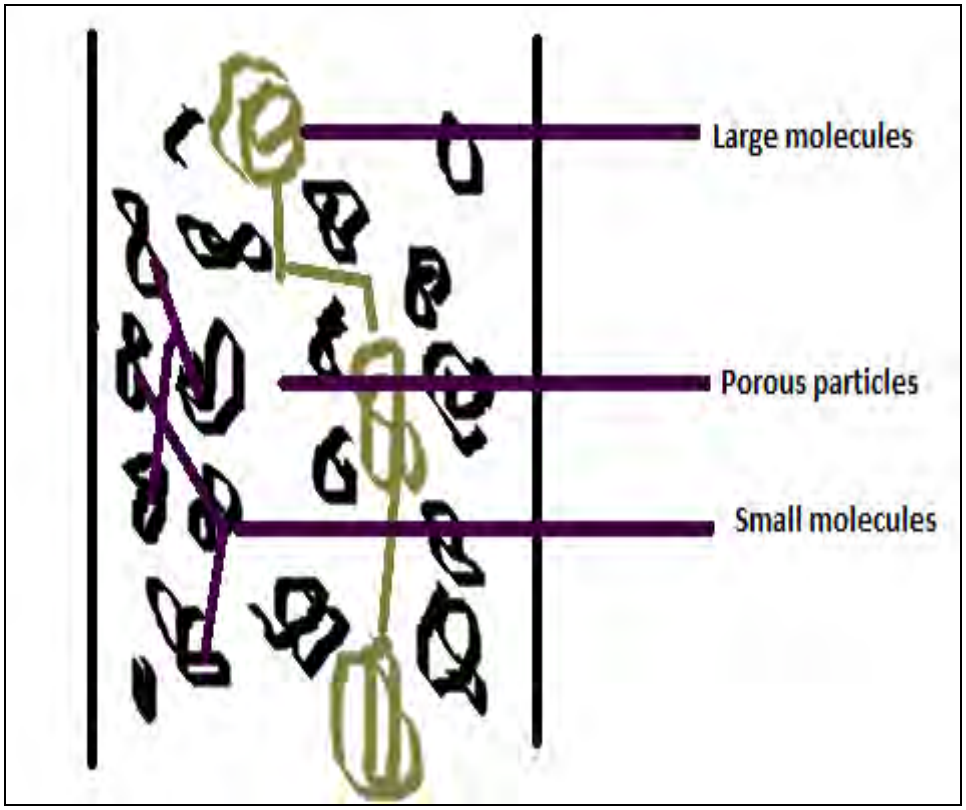

Figure 3.3: Schematic of a size-exclusion chromatography column (adapted from internet 5: Appendix D)

Molecules smaller than the pore size have a longer path and transit time than larger molecules (Bonifacino *et al.,* 2004). Different molecules therefore have different total transit times through the column. This type of a chromatogram is called the selective permeation region. Molecules that are smaller than the pore size can enter all pores, and have the longest residence time on the column and elute together as the last peak in the chromatogram (Denis *et al.* 2008).

3.2.8. Freeze drying

Freeze-drying is a technique by which a protein is frozen, and then dehydrated by sublimation, with complete retention of its original form. Sublimation is a process by which a frozen liquid (solid) goes directly into the gaseous state without passing through the liquid phase (Carpenter *et al*., 1993). This method is accomplished by freezing the solution first and the frozen solution placed in a vacuum chamber where the freeze-drying process occurs. The time needed to completely dry proteins varies according to its volume and the degree of saturation. Although freeze drying is often the process of choice for production of therapeutic proteins, protein degradation may occur in-process and/or during storage (*Id*).

3.2.9. Sodium dodecyl sulphate-polyacrylamide gel electrophoresis (SDS-PAGE)

Sodium dodecyl sulfate-polyacrylamide gel electrophoresis (SDS-PAGE) is among the commonest techniques used for the separation of proteins and nucleic acids (Wittig and Schägger, 2005). Electrophoresis is the migration of charged molecules in a media upon application of an electric field. The rate of migration depends on the charge on the molecule, its molecular mass, size and the strength of the electric field. The most commonly used matrix is agarose or polyacrylamide. A porous support and the size of the pores can be varied by changing its concentration and sodium dodecyl sulphate (SDS) which is an anionic detergent which denatures proteins by binding to the polypeptide backbone. The charge on a protein is determined by the pH of the medium and the amino acid composition of the protein. Each protein has an isoelectric point which is the pH at which the protein has no net charge and an electrophoretic separation of nucleic acid. In order to remove the disulphide bridges in proteins before they adopt the random-coil configuration necessary for separation by size, 2-mercaptoethanol or dithiothreitol is added as a reducing agent. In denaturing SDS-PAGE, separation migration is determined not by intrinsic electrical charge of the polypeptide, but by molecular weight (Laemmli, 1970)**.** "Native" or "non-denaturing" poly acrylamide gel electrophoresis that is run in the absence of SDS and the mobility depends on both the protein's charge and its hydrodynamic size. The electric charge driving the electrophoresis depends on the intrinsic charge in the protein at the pH of the running buffer while the amino acid composition of the protein also depends on the post-translational modifications such as addition of sialic acids. Native gels are excellent tools for detecting changes in charges, unfolded oligomers and aggregates binding events such as protein-protein or protein-ligand, because of their sensitivity to any process that alters either the charge or the conformation of a protein (Wittig and Schägger, 2005; Schägger, 2003).

3.2.10. Western blot

Western blotting is used to determine the presence of a specific protein in a sample after separation on SDS-PAGE. The proteins are separated by SDS-PAGE and then transferred to a nitrocellulose membrane or Polyvinyldifluoride (PVDF) (Burnette, 1981). The membrane is incubated with a source of non-specific protein (such as milk proteins) to bind to any remaining sticky places on the membrane. A primary antibody is then added to the solution to bind to its specific target protein, followed by washes and incubation in a solution of secondary antibody. The secondary antibody recognizes the primary antibody and binds at locations on the blot, together with the primary antibody. The secondary antibody is further

conjugated with an enzyme or marked with a nucleotide, to allow for its detection (Banerjee and Ghosh, 2004). Figure 3.4 below illustrates the Western blot process:

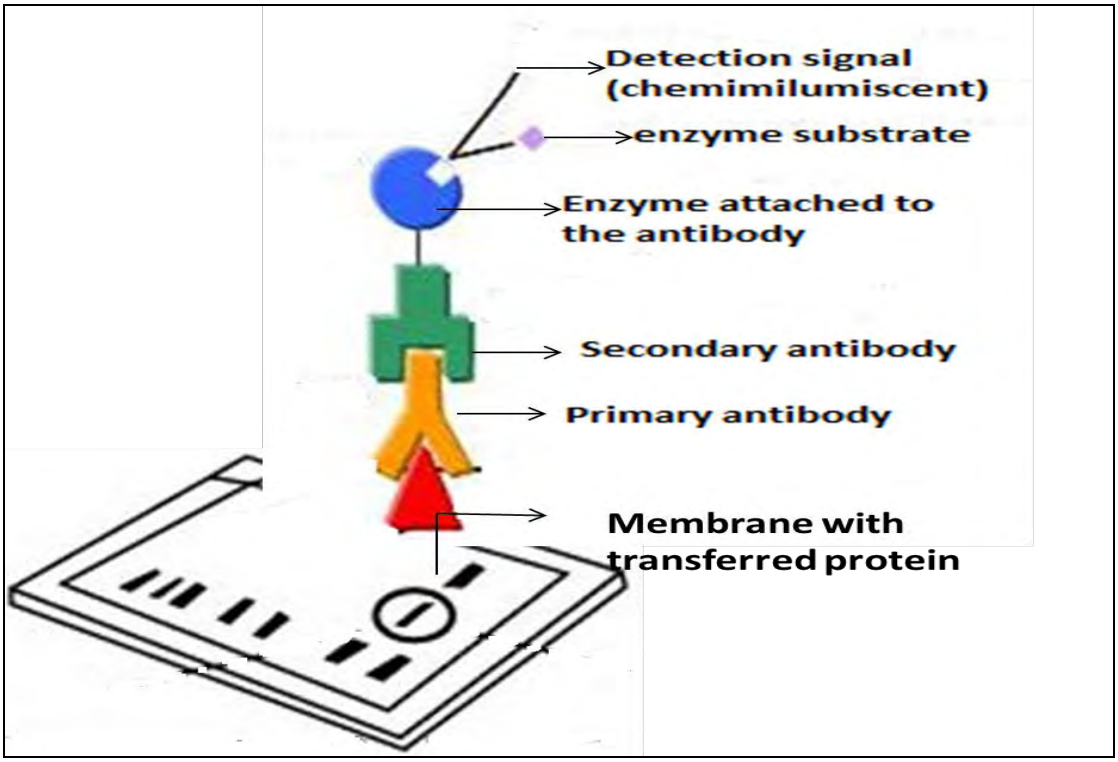

Figure 3.4: Schematic of a Western blot process (adapted from internet 6: Appendix D)

3.2.11. Enzyme kinetics

The mechanism of enzyme catalyzed reactions is often studied by undertaking kinetic measurements on enzyme-substrate reaction systems. Enzyme kinetics is principally concerned with the measurement and the mathematical description of enzyme-substrate complexes, the reaction rate and its associated constants (Kemp *et al*., 1980). This includes measuring rates of the enzyme-catalyzed reactions at different substrate and the enzyme concentrations. In the following sections, a simple model for the catalytic behaviour of an enzyme and the kinetic model that arises from its reaction by determining K_m and V_{max} experimentally and $k_{cat,}$ temperature effects, pH and temperature stability on nNOS activity are presented (Somero, 1978**)**.

The Hanes-Woolf plot is another rearrangement of the Michaelis-Menten function that yields a straight line (equation 2). Hanes–Woolf plot, the ratio of the initial substrate concentration [S] to the reaction velocity v is plotted against [S] (equation 2) where Km is the Michaelis–Menten constant and V_{max} is the maximum reaction velocity. Enzyme kinetics are important

for determination of enzyme purity (equation 3), to evaluate enzyme concentrations in complex extracts. Equation 4 is used to measure substrate specificity (Cornish-Bowden, 2004).

$$\frac{[S]}{v} = \frac{[S]}{V_{max}} + \frac{K_m}{V_{max}}$$

……..Equation 2

$$k_{cat} = \frac{V_{max}}{[E_t]}$$

…….Equation 3

$$\text{Catalytic efficiency} = \frac{K_{cat}}{K_m}$$

…….Equation 4

3.3. Reagents and materials

Bovine brain (approximately 370 g) obtained from Grahamstown Connocks butchery was used for this study. Electrophoresis reagents such as acrylamide; bis-acrylamide; bromophenol blue; N, N, N‟, N‟- tetramethyl-ethylenediamine (TEMED); ammonium persulphate; β-mercaptoethanol; Enzyme assay reagents such as Nα- benzoyl-L-arginine ethyl ester hydrochloride (BAEE); DL-citrulline; calcium chloride; tetrahydro-L-biopterin dichloride; β-nicotinamide adenine dinucleotide phosphate reduced tetrasodium salt; thiosemicarbazide; 2,3 butanedione monoxime; ammonium sulphate; poly [ethylene glycol] (PEG 20 000); bovine serum albumin; Bradford reagent; ethylenediametetraacetic acid (EDTA); 4-(2-hydroxyethyl) piperazine-N‟- [2-ethane-sulphonic acid monosodium salt] (Hepes); Sephacryl S300HRcolumn; and DEAE-Sephaceland Coomassie Brilliant Blue R-250 stain were purchased from Sigma-Aldrich. Commercial neuronal nitric oxide synthase (rat brain) was obtained from rat brain, Dithiothreitol (DTT); sodium dodecyl sulphate

(SDS); glycerol (50%); Tris (hydroxymethyl) aminomethane; phenyl methylsulphonylfluoride (PMSF); ferric chloride hexahydrate ($FeCl_3$); sodium chloride (NaCl); perchloric acid; sulphuric acid; ortho-phosphoric acid; glacial acetic acid and hydrochloric acid, primary antibody (rabbit anti-nNOS antibody (1:5,000) and mouse/ rabbit secondary antibody (1:12 000); bench-top centrifuges (Epperndorf 5810R and Eppendorf MiniSpin®); heating blot and pH meter (Ionolab pH level 1); and snake skin dialysis tubing obtained from Pierce, Rockford (Illinois, USA) were obtained from Merck Chemicals South Africa. Prestained molecular weight marker peq GOLD 10-150 kDa was obtained from Inqaba biotec. All the experiments, reagents were dissolved in milli-Q water and all the experimental conditions throughout the purification were performed at 0-4 °C, unless stated otherwise.

All the chromatographic columns, PowerPac Basic electrophoresis kit (model 300) and the fraction collector (model 2110) were purchased from Bio-Rad, South Africa. UV analyses that were performed on a PowerWaveXTM microplate reader were purchased from Bio-Tek Instruments (Vermont, USA).

3.4. Methods

3.4.1. Isolation of neuronal nitric oxide synthase

Fresh bovine brain (374 g) was homogenized in Hepes buffer (50 mM, pH 7.6, 600 ml) containing EDTA (1.0 mM), NADPH (1.0 mM), DTT (0.5 mM) and PMSF (0.43 mM) and 20 ml was sonicated (10W, 30 s intervals, 4 min), followed by centrifugation (10 000 x g, 4 °C, 30 min). The cell free supernatant extract assayed for nNOS activity, protein and stored as 20 ml aliquots at - 70 ºC until required.

3.4.2. Bradford assay

Protein quantification for all experiments was routinely determined according to the method of Bradford (1976), using bovine serum albumin (BSA) as a standard. The assay was performed in a 96-well microtiterplate in triplicates. Enzyme extract (5 µl) was added to a single well, followed by 245 µl Bradford reagent. The mixture was incubated at room temperature for 5 minutes. Absorbance of the solution was measured at 595 nm and the concentration of the unknown samples was determined using the slope of the straight line of a BSA standard curve (see Appendix A1).

3.4.3. nNOS assay

The nNOS assay was conducted according to the protocol described by Boyde and Rahmatullah (1980) with slight modifications. The assay reaction was started by the addition of 10 µl of brain extract in assay buffers 80µl and allowed to incubate at 50 ºC for 2 minutes before being stopped with perchloric acid (5 M, 10 µl) (Appendix A2). The mixture was treated with 150 µl of chromogenic reagent and cooled to 22 ºC for 2 minutes. The reduction of benzoyl-L-arginine ethyl ester was then determined spectrophotometrically at 530 nm. The citrulline extinction coefficient (ε_{530}) was 27.3 ml.µmol^{-1} (Skakibara and Yanagisawa, 2003), and activity of nNOS was determined (equation 5). According to the equation 5, one unit of an activity was defined as the amount of nNOS that produced 1 µmol of citrulline per min per ml reaction mixture min per ml reaction mixture (see Appendix A3).

$$\text{Activity} = \frac{(\Delta A \,.\, V_t).\, D_f}{(\varepsilon.\, t.\, V_e)} = \mu\text{mol/ml/min} \qquad \text{.....Equation 5}$$

where

ΔA = change in absorbance

D_f = dilution factor

V_t = total volume

ε = extinction coefficient

t = time (min)

l = path length (cm)

V_e = volume of extract

3.4.4. Ammonium sulphate precipitation

A cell free supernatant extract (5 ml) was precipitated using 20–50 % ammonium sulphate at (4°C, 50) while stirring and then centrifuged at (4 000 x *g*, 4 °C, 50 minutes) to yield a supernatant (S1) and a pellet (P1). P1 was collected and redissolved in Tris-HCl (50 mM, pH 7.5, and 5 ml) and dialyzed (4 °C for 24 h) against the same buffer to remove excess salt. The enzyme assay and Bradford assay were performed on both P and S as described previously in subsections 3.4.2 and 3.4.3(see Appendix A2).

3.4.5. Dialysis

The protein samples were dialyzed using a snake skin dialysis tubing (10 000 Da cut-off) for the removal of unwanted small molecules. Prior to dialysis, the membrane was soaked in

Tris-HCl (10 mM, pH 7.5) for 5 minutes. A tubing clamp was used to close one end of the dialysis tubing and the protein sample was pipetted into the tubing. The tubing was closed off with another clamp and placed into a large beaker with Tris-HCl buffer (10 mM, pH 7.5, 4 °C) which was stirred slowly (4 °C, 24 h). Thereafter, the dialyzed solution was removed from the tubing. The enzyme and Bradford assay were subsequently performed and concentrated as described in subsections 3.4.2 and 3.4.3 above (also see Appendix A4).

3.4.6. Poly (ethylene glycol) 20 000 precipitation

The protein was concentrated using Poly (ethylene glycol) 20 000 precipitation. A 25 g dry matrix of poly (ethylene glycol) was added to different 5 ml aliquot of a dialyzed enzyme extract and was left to stand (24 hours, 4 °C). The concentrated sample was reconstituted in Tris-HCl buffer (10 mM, pH 7.5, 5 ml) and then assayed for activity using the enzyme and Bradford assay as previously described 3.4.2 and 3.4.3 above (see also Appendix A4). Size and ion exchange chromatography techniques were carried out for further purification of the enzyme based on charges and sizes.

3.4.7. Anion- exchange on DEAE-Sephacel®

Anion- exchange (DEAE-Sephacel®) was used to separate protein charge. The concentrated sample (2ml) obtained after Poly (ethylene glycol) 20 000 precipitation was applied on to a glass Econo-Column® (0.81 x 44 cm) packed with DEAE- Sephacel® anion-exchanger resin, with a bed volume (200 ml). First, the column was equilibrated with Tris-HCl buffer (50 mM, pH 7.6), then washed with the same buffer until A_{280} nm was at the baseline. Next, the adsorbed proteins were eluted with NaCl (0-1 M) in the same buffer at a flow rate of 2 ml/min (6 ml per tube). A total of 33 fractions (6 ml) were collected and dialysed against Tris-HCl buffer (10 mM, pH 7.6), freeze dried and reconstituted in the same buffer (5 ml). These were assayed for protein A_{280} and enzyme as previously described 3.4.2 and 3.4.3 above (see also Appendix A5a and A5b).

3.4.8. Size-exclusion chromatography

The final purification step was size-exclusion chromatography. The active fractions obtained from the DEAE- Sephacel® column were pooled, dialysed against 50mM Tris HCl buffer at pH 7.4 and concentrated to 3 ml using freeze dry. The sample was then loaded onto the Sephacryl S300HR column (1 x44 cm) at a flow rate of 2 ml/min (6 ml per tube). A total of 33 fractions (6 ml) were collected. Protein concentration was estimated by measuring absorbance at 280 nm and the enzyme activity was determined as previously described in

3.4.2 and 3.4.3 above. The active sample was concentrated and subjected to SDS-PAGE analysis (see Appendix A5).

3.4.9. Freeze drying

A dried powder of the pooled samples from inon exchange and gel filtration chromatography was obtained by freeze-drying. To carry out all purification methods, the sampled powder in the freeze-drying bottle was resuspended in 5ml deionised water.

3.4.10. SDS and native PAGE analyses

The separation of proteins by SDS-PAGE was performed with a few modifications from the method of Laemmli (1970). The apparatus was assembled according to the manufacturer‟s instructions. The 5% stacking gel and 12% separating gel were run at a constant voltage of 120 V for 1 h 30 minutes. After the electrophoresis run was complete, the gel was stained with Coomassie Brilliant Blue R-250. The procedure for native PAGE was performed with 5 % stacking gel and 8 % separating gel at a constant voltage of 100 V. After electrophoresis, the gels were stained with Coomassie Brilliant Blue R-250, then destained in methanol, acetic acid, and water (1:1:8 v/v/v). Staining was carried out overnight and destaining the following day with both Destain I solution (for two periods of 20 minutes each) and Destain II solution (for one period of 20 minutes) (see Appendix A1 (a), A1 (b), and A5c).

3.4.11. Western blot analysis

The SDS gel analysis was carried out according to the method described in subsection 3.4.9 above. Proteins were transferred onto nitrocellulose membrane (Bio-Rad Laboratories, Hercules, USA) for 2 hrs at 250 mA in cold transfer buffer (25 mM Tris-HCl pH 7.4, 192 mM glycine, 10 % methanol). Ponceau stain (0.1 % Ponceau stain in 1 % acetic acid) was also used to verify protein transfer. The stain was then removed by rinsing the membrane in water and thereafter in Tris buffered saline (TBS) [150 mM NaCl, 50 mM Tris-HCl (pH 7.6)]. Subsequently, the membrane was incubated in blocking solution (TBS containing 5 % fat-free powdered milk) for 1 hr, followed by an overnight incubation with primary rabbit anti nNOS antibody (1: 5,000) prepared in blocking solution. The membrane was washed three times for 15 mins in TBS-Tween (TBS containing 2 % Tween-20). For secondary antibody incubation, the membrane was incubated with mouse/rabbit secondary antibody (1:12 000) provided by the BM Chemiluminescence Western Blotting Kit (Mouse/Rabbit) (Roche, Mannhein, Germany) for an additional 45 mins, followed by three 15 mins washes

with TBS-Tween. The reaction was detected by the VersaDoc TM Model 4000 imaging system (Bio-Rad Laboratories, Hercules, USA) (Appendix A6).

3.4.12. Enzyme characterisation

3.4.12.1. Kinetics

The kinetic properties namely, the Michealis Menten constant (K_m) and the maximal enzyme velocity (V_{max}) were determined by varying the substrate (benzoyl-L-arginine ethyl ester) between 5-20 mM and calculated from the Hanes-Woolf plot (see equation 2: and Appendix A3).

3.4.12.2. Effect of temperature on nNOS activity

The effect of temperature on nNOS activity was determined from 20 °C–100 °C under the standard enzyme assay conditions as described in 3.4.2 above.

3.4.12.3. Determination of temperature stability

The stability of nNOS was determined at optimum pH and various temperatures (i.e. 25 °C, 37 °C, and 50 °C). Aliquots were analyzed for nNOS activity for a maximum period of 180 minutes, and nNOS activity at time zero was considered to be 100 % residual activity (0.08U/ml).

3.4.12.4. Effect of pH on nNOS activity

To determine the pH optimum, the enzyme activity was assayed at different pH values [sodium acetate (pH 3–5.5, 50 mM); Hepes (pH 6-7, 50 mM); Tris-HCl buffer (pH 7.5-9, 50 mM)] under the standard enzyme assay at optimum temperature, conditions described in 3.4.3 above.

3.5. Results and discussion

Fresh bovine brain was homogenized in Hepes buffer, centrifuged and the cell free supernatant extract assayed for nNOS activity and protein before being used for further analyses. The time dependant enzyme production of citrulline was determined in order to establish a standard time parameter for subsequent enzyme activity assays. The results for the production of citrulline are shown in Figure 3.4 below, and the enzymatic production of citrulline was based on the fearon reaction, in which citrulline formed a rose pink colour with 2, 3 butanedione monoxime in acid solution (Archibald, 1944). The formation of the coloured

product was apparently favoured by the presence of thiosemicarbazide and ferric chloride which accelerated the carbamido-diacetyl reaction catalytically (Archibald, 1944).

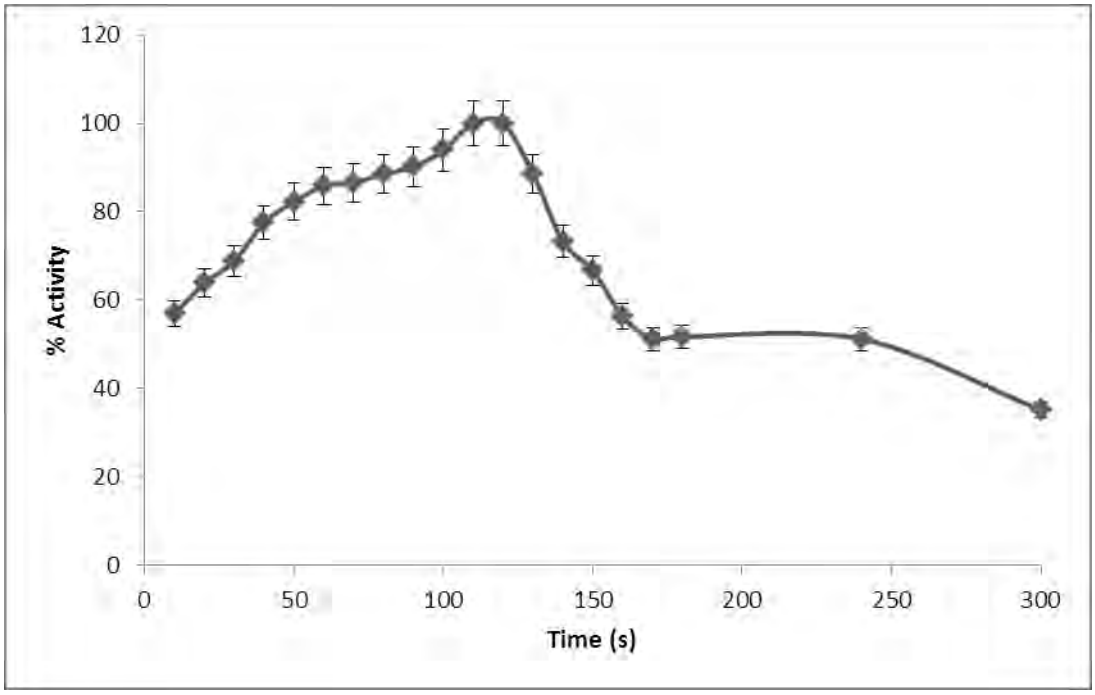

Figure 3.5: Enzymatic progress curve representing the amount of citrulline product per unit time, 0.08 U/ml= 100%

The results revealed that the amount of citrulline produced minute was relatively high and was inclusive of both residual brain citrulline and nNOS citrulline production expressed as a percentage (see Figure. 3.5 above). A presentation of results in Figure 3.5 above shows that 100% citrulline production occurred within 2 minutes and this time frame was used in subsequent activity assays. The total activity of nNOS was spectrophotometrically determined as 0.08 U/ml. The amount of nNOS total enzyme extract was determined as 39 mg/ml using Bradford assay at 595 nm (see Table 3.1 below).

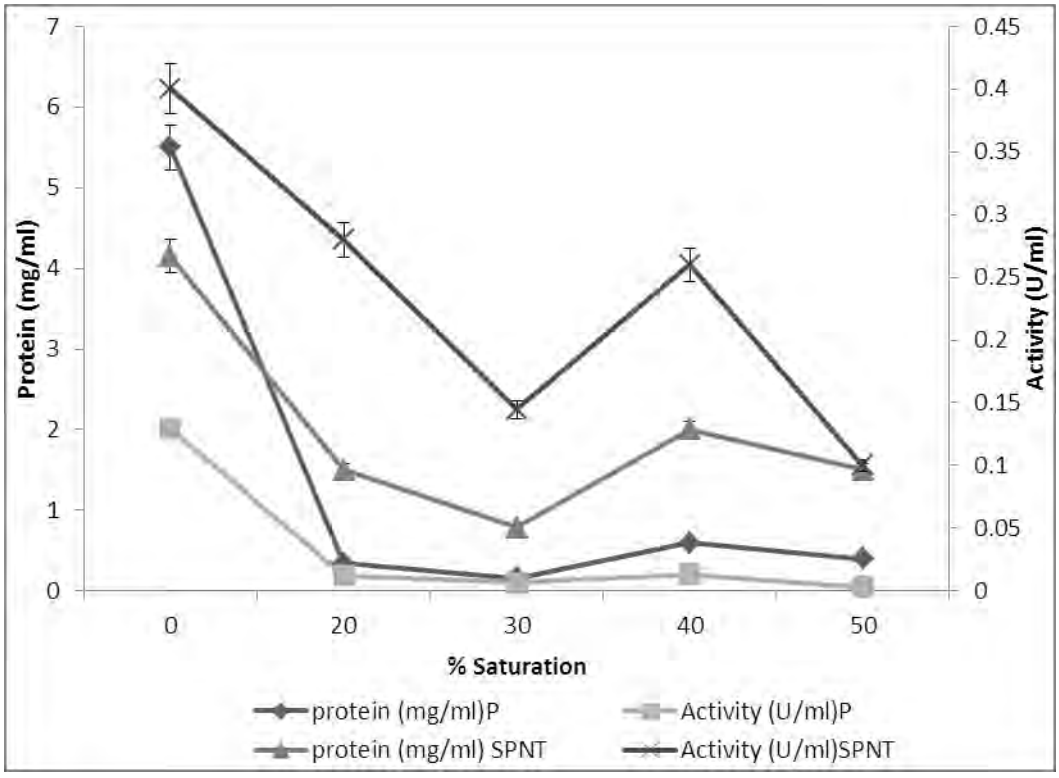

Figure 3.6: Protein concentrations and activity of supernatant and the pellet from bovine brain extract using $(NH_4)_2SO_4$ precipitation; values represent the mean (± S.E.M) of three trials

$(NH_4)_2SO_4$ precipitation was the first concentration step performed after sonication and centrifugation of the crude (15 ml) extract to yield supernatant (S) and pellet (P). Protein concentration and enzyme activity assays were conducted for both the S and P in order to determine the best $(NH_4)_2SO_4$ cut required to precipitate the enzyme and extraneous protein (see Figure 3.6 above).The results in Figure 3.6 above show that a low concentration of S protein (0.79 mg/ml) with an enzyme activity (0.144 U/ml) was precipitated at 30% $(NH_4)_2SO_4$. At 50 % $(NH_4)_2SO_4$ precipitation, S shows a higher protein concentration (0.144 mg/ml) with a similar enzyme activity (0.79 U/ml). However, the highest concentration of protein (2 mg/ml) and the highest enzyme activity (0.26 U/ml) were precipitated at 40 % $(NH_4)_2SO_4$ for the S (see Figure 3.6 above). The results revealed that the highest amount of nNOS in S was precipitated at 40% NH_4 $(SO_4)_2$.

Table 3.1: Partial purification table of the nNOS sourced from bovine brain.

Fraction	Protein (mg/ml)	Volume (ml)	Total Protein (mg)	Activity (U/ml)	Total Activity (U)	Specific Activity (U/mg)	Fold Purification	Yield %
Crude	2.6	15	39	0.54	8.01	0.21	1	100
$NH_4(SO)_2$	2.02	17	34	0.24	4.08	0.12	0.6	51
PEG	1.72	12	20.6	0.27	3.24	0.16	0.8	40
DEAE-Sephacel	0.91	10	9.1	0.08	0.8	0.09	0.43	10
DEAE-Sephacryl SHR-300	0.014	10	0.141	0.02	0.2	1.4	6.6	3

Nevertheless, $NH_4(SO_4)_2$ precipitation showed a less specific activity (0.12 U/mg) to that of 17 ml crude extract (0.21 U/mg) which produced a 51% yield with a one fold purification, indicating failure in concentrating nNOS (see Table 3.1 above). Similarly, the second purification step involving PEG 20 000 that was performed, also proved unsuccessful in concentrating nNOS. Although a fairly high specific activity (0.16 U/mg) was obtained compared to NH_4 $(SO_4)_2$, PEG 20 000 produced a similar yield of 40% and a similar purification fold increase (see Table 3.1 above). Thus, these two techniques produced no fold purification and were abandoned in favour of ion exchange chromatography by DEAE-Sephacel. Due to the fact that fractions obtained by use of ammonium sulphate and subsequent concentration with PEG did not exhibit the expected activity, the crude enzyme was subjected to a single ion exchange chromatographic technique and fractions. Forty-five (6 ml/fraction) were collected after elution with 1M NaCl (see Figure 3.7 below). These undialysed fractions were assayed using the enzyme and Bradford assay as described in 3.4.2 and 3.4.3 above. The fractions with highest peak 1(i.e. fraction 11-13); peak 2 (i.e. fraction17-19); peak 3 (i.e. fraction 23-24) were pooled, dialysed, reconstituted in Tris-HCl buffer (10 mM, pH 7.5, 5 ml) and protein concentration and enzyme activity were determined. The specific activity of the dialyzed sample was very low (0.09 U/mg) and thus,

produced a very low yield (10%) and a fold of 0.43 (Table 3.1 above). This indicated an unsuccessful attempt at purifying nNOS. However, it was eluted at 260 mM NaCl, similar to what has been reported (Swiatek and Ward, 2009). The eluted samples were used for further purification.

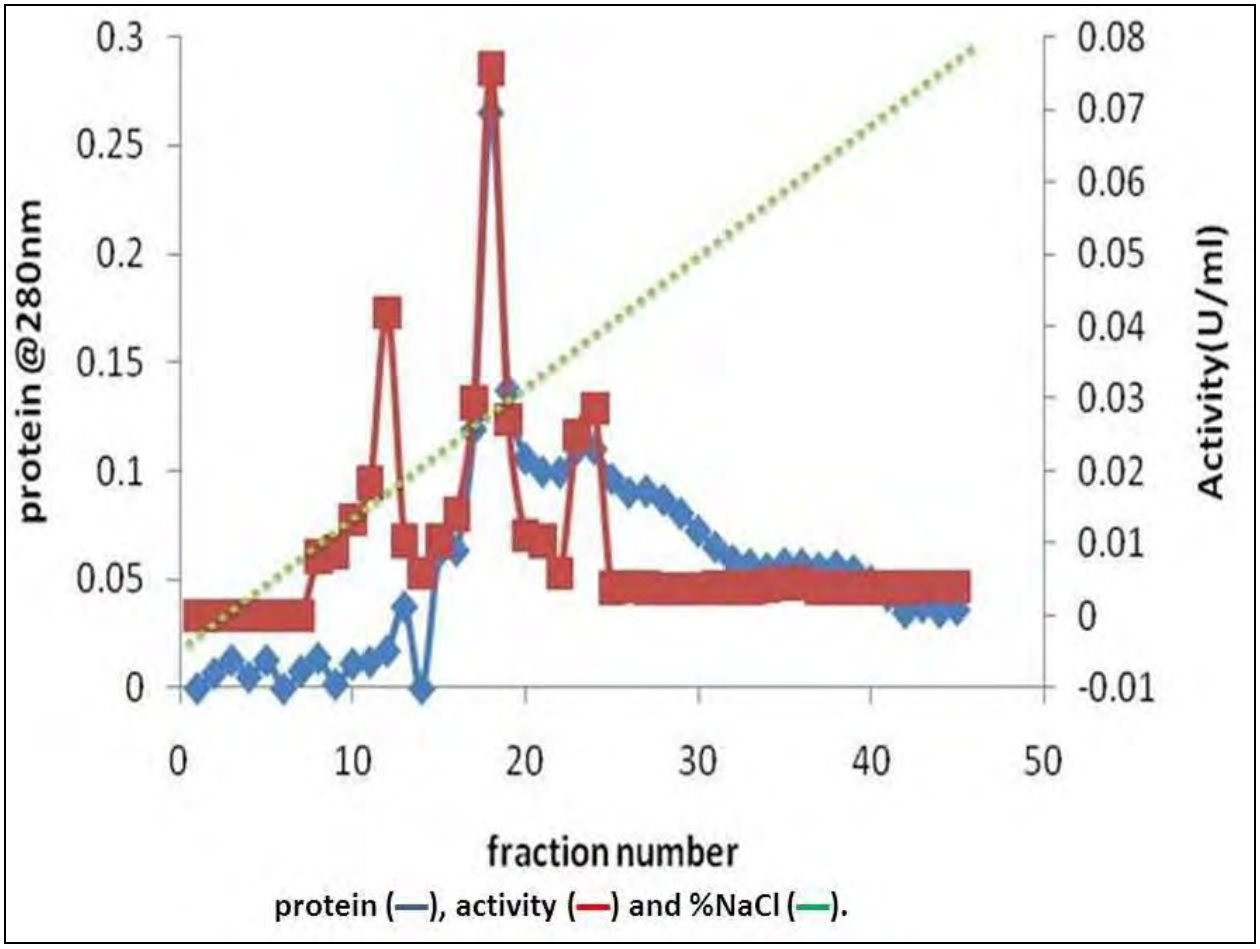

Figure 3.7: DEAE-Sephacel ion exchange chromatography profile showing the proteins eluted with linear NaCl gradient (0-1 M) in Tris-HCl buffer protein and activity of nNOS; values represent the mean (± S.E.M) of three trials

According to Table 3.1 above, a fold purity of 6.6 came for the Sephacryl (S-300HR) Gel filtration chromatography (see Figure 3.8 below). The specific activity of the dialyzed pooled fractions from this step increased (1.4 U/mg) and thus produced a decrease in yield of 3%, (see Table 3.1 above), indicating a more successful purification step. The sample was then used for further purification such SDS and native page.

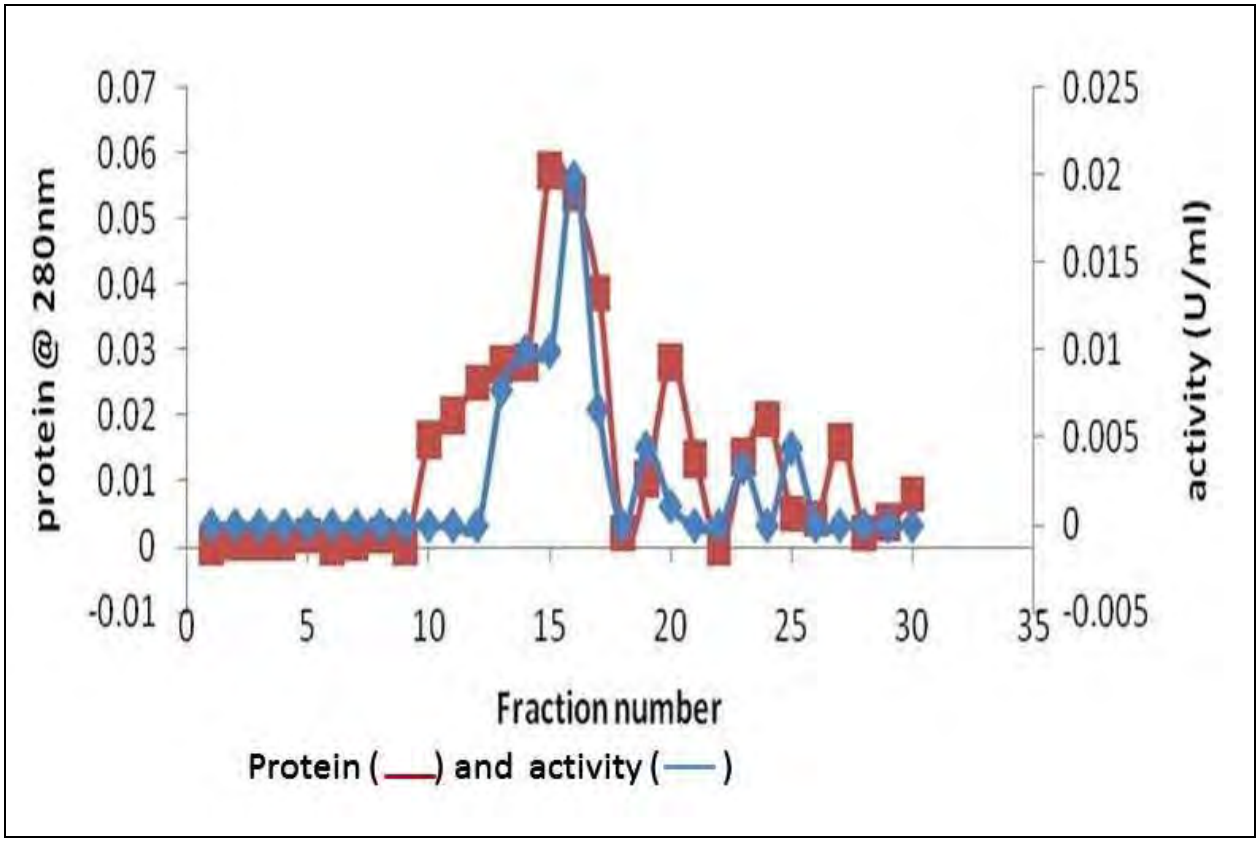

Figure 3.8: Gel filtration chromatography Sephacryl (S-300HR) profile showing the proteins eluted and activity of nNOS; values represent the mean (± S.E.M) of three trials

A pure protein should give a single band on an SDS-polyacrylamide gel, unless the molecule is made up of two or more subunits of different molecular mass. The partial purification steps for nNOS (see Figure 3.9 below) showed that nNOS appeared to be a dimer (as indicated by the arrow in lane 4) of approximately 75 kDa and 72 kDa, indicating a homodimer with an overall molecular weight of the total enzyme may be 150 kDa. These findings were similar to values reported by Packer, 1994.

Native-PAGE revealed a single subunit at 150 kDa although there were some proteins that were purified from the purification due to the use of non-denaturing conditions (see Figure 3.10 below). This single protein band was estimated at a molecular weight of 150 kDa as confirmed using the commercial enzyme as a control and from the results from SDS-PAGE.

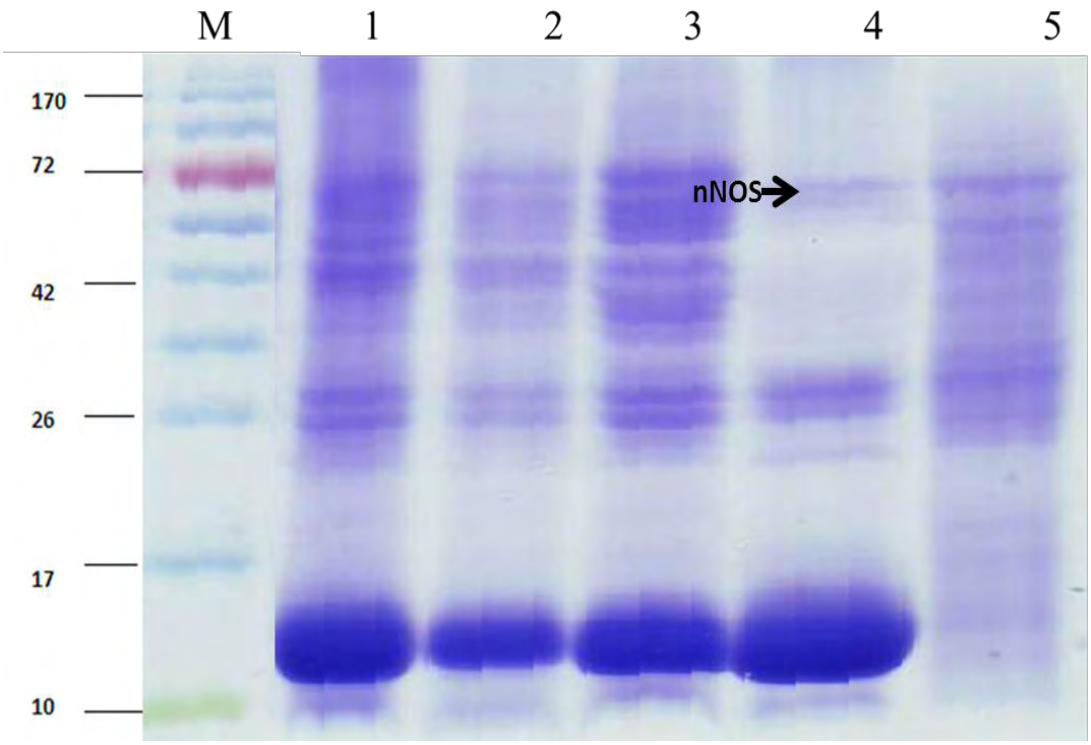

Figure 3.9: 12% SDS gel M: peq Gold protein marker, lane 1 Crude; lane 2 40% $(NH_4)_2SO_4$; lane 3 PEG; lane 4 IEX (DEAE-Sephacel); lane 5 Gel (DEAE-Sephacryl SHR-300)

A western blot analysis was conducted based on the observations from the SDS. Cow brain was selected for this study because of its homology with the human brain, and a western blot was conducted understands the semi-quantitative measurement of the protein. Based on the findings (Table 3.1; Figure 3.9), the purification of nNOS from cow brain was not a success. The rabbit anti-nNOS antibody did not cross-reacted with cellular proteins, and it was not specific as indicated in Figure 3.10 below. This may be because of using anti rabbit instead of anti-bovine antibody.

The temperature, thermal stability and pH optimum of purified nNOS was determined at various ranges under the conditions described in 3.4.2 and 3.4.3_above. The results in Figure 3.12 show that 100% activity remained at pH 7.5, but decreased substantially to 60% at pH 8, while at pH 6.5 there was only 60% activity which decreased to 40% at pH 4.5. These values were well within those reported in the literature with optimum pH ranging between pH 9 and pH 7. Thus, the optimum pH for nNOS was found to be pH 7.5 (see Figure. 3.12 below).

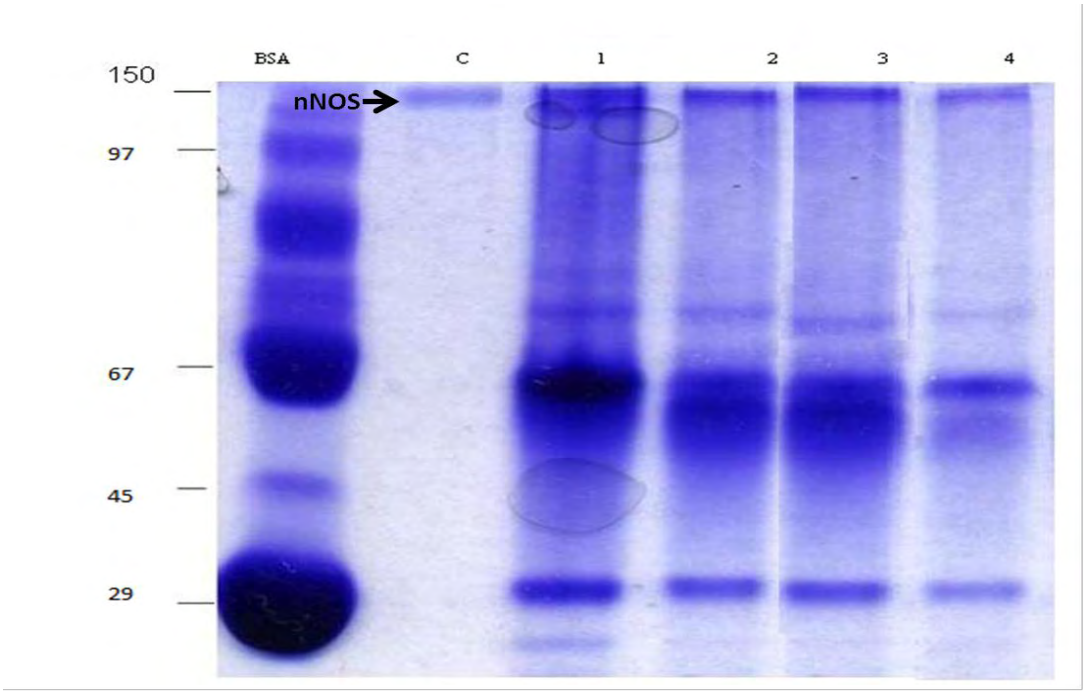

Figure 3.10: 8% Native gel. BSA: Bovine serum albumin, C: Control, 1: Crude extract, 2: 40% $(NH_4)_2SO_4$, 3: PEG, 4: IEX

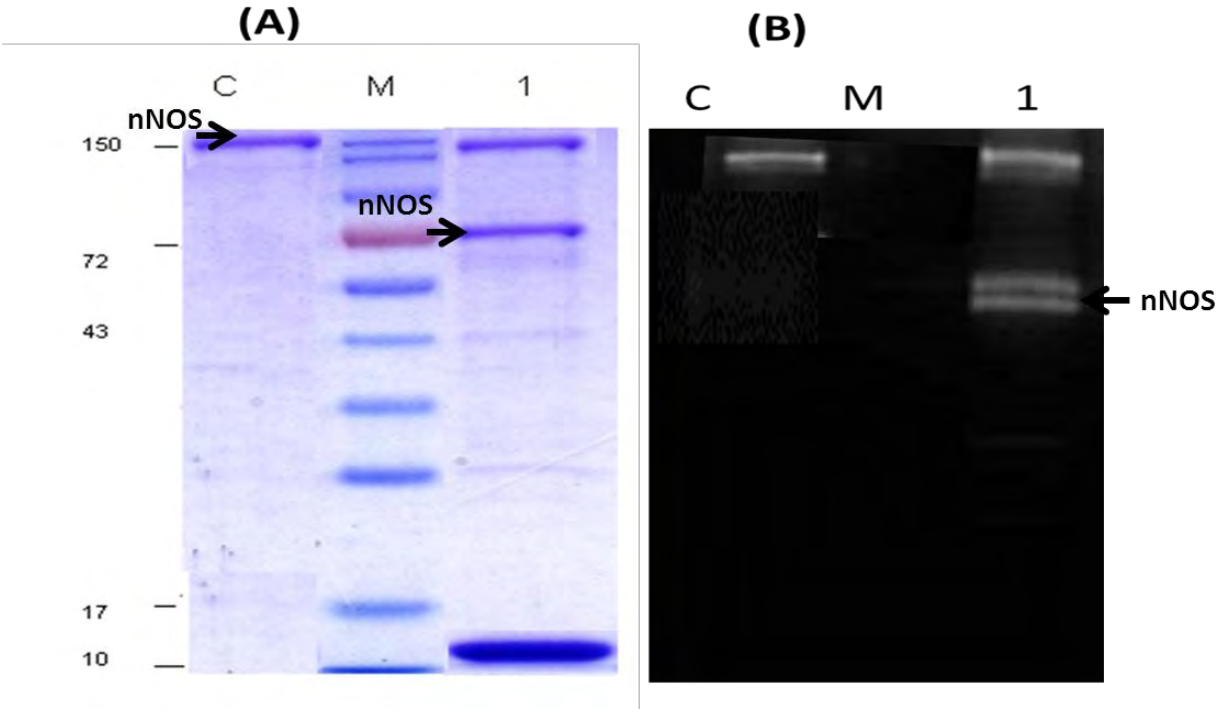

Figure 3.11: Western Blot: C: control (commercial nNOS), M: peq Gold protein marker, lane 1A IEX purified. 1B. 12% SDS gel C: control (commercial nNOS), M: peq Gold protein maker, lane 1 IEX purified

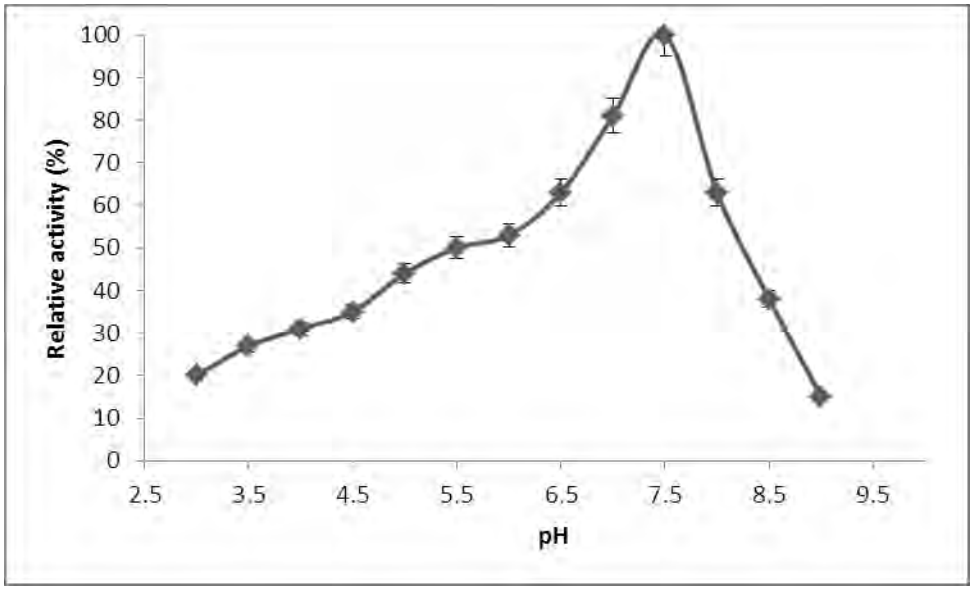

Figure 3.12: pH profile of the purified nNOS from bovine brain, 100% relative activity = 0.08U/ml ; values represent the mean (± S.E.M) of three trials

Based on the temperature profile (see Figure. 3.13 below), the enzyme showed 40% decrease in activity between 100 °C and 40 °C and 50 °C - 65 °C, but rapidly lost its activity beyond these temperature ranges. Thus, nNOS showed an optimum of 100% activity at 50 °C with a half-life of approximately 1hour 40min (see Figure 3.14 below). This optimum temperature was considerably different to that reported by Hiki *et al*. (1992). They reported a value of 37 °C for nNOS.

The kinetic study of the enzyme is useful in measuring the concentration of the enzyme, its purity and catalytic efficiency. The parameters K_m and V_{max} were calculated from the intercept and slope of the straight line of the Hanes-Woolf plot (see Figure. 3.15 below). The results showed that for benzoyl arginine hydrolysis, the V_{max} and K_m were 0.0865 µmol.min^{-1} and 1.8 µM, respectively. The turnover number (k_{cat}) and the catalytic efficiency (k_{cat} / K_m), calculated using equations 3 and 4 and were found to be 0.095 min^{-1} and 0.05 min^{-1}µM^{-1}, respectively, and the total amount of enzyme [Et] was 1.8 µmol where K_m is the Michealis constant.

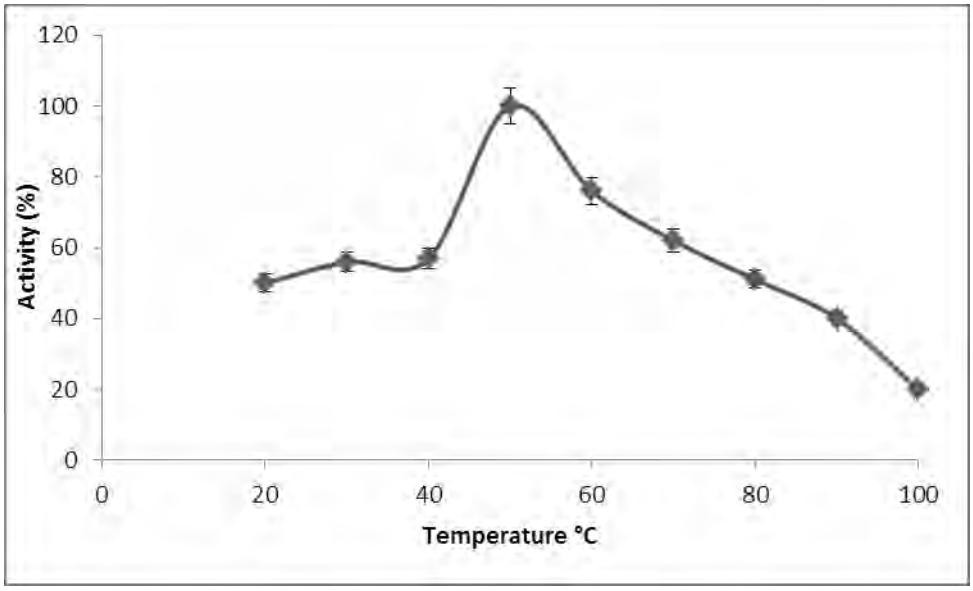

Figure 3.13: Temperature profile of the purified nNOS from bovine brain, 100% relative activity = 0.08U/ml; values represent the mean (± S.E.M) of three trials

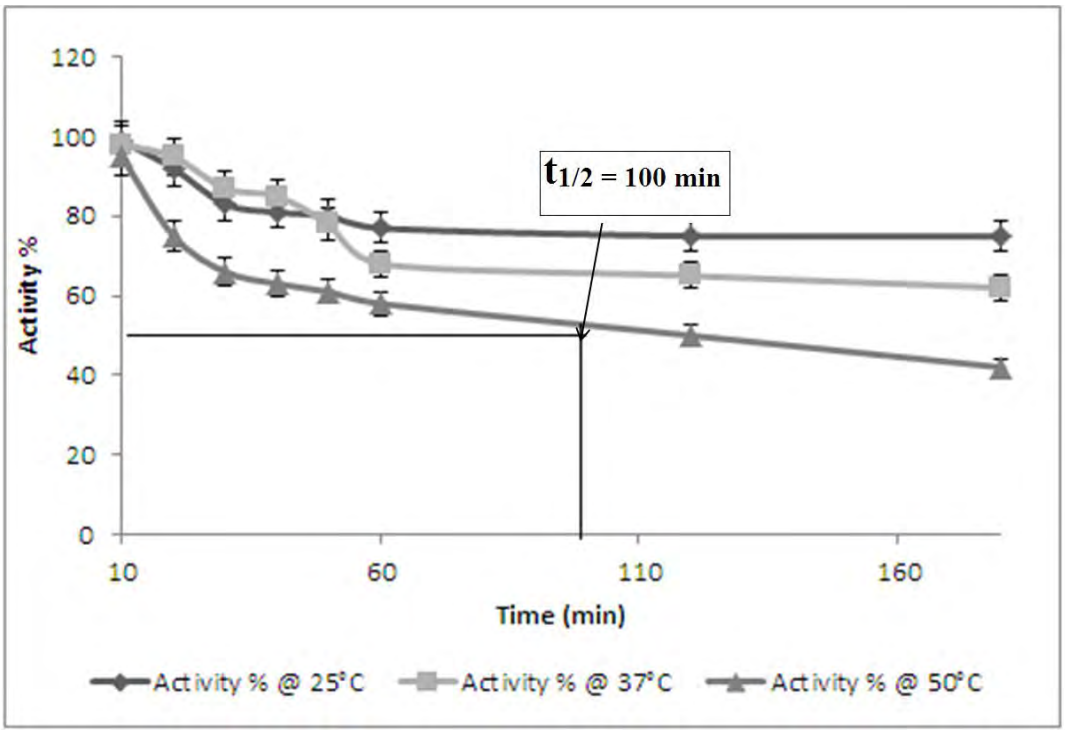

Figure 3.14: Temperature stability of the purified nNOS from bovine brain, 100% relative activity = 0.08U/ml; values represent the mean (± S.E.M) of three trials

Interestingly, the kinetic constant Km (1.8 µM) indicated a higher affinity for benzoyl arginine, closely related to the results found in other nNOS studies (Riveros-Moreno et al., 1995; Bredt and Snyder, 1990; Giraldez and Zweier, 1998; Hiki *et al*., 1992). This finding also shows that the degree of purity was relatively the same to those reported Km values in the literature although they were from a highly purified form of nNOS. The Vmax of the partially purified nNOS was found to be 0.0865 µmol.min^{-1}, which was lower than that of 1 µmol.min^{-1} reported by Bredt and Snyder (1990).

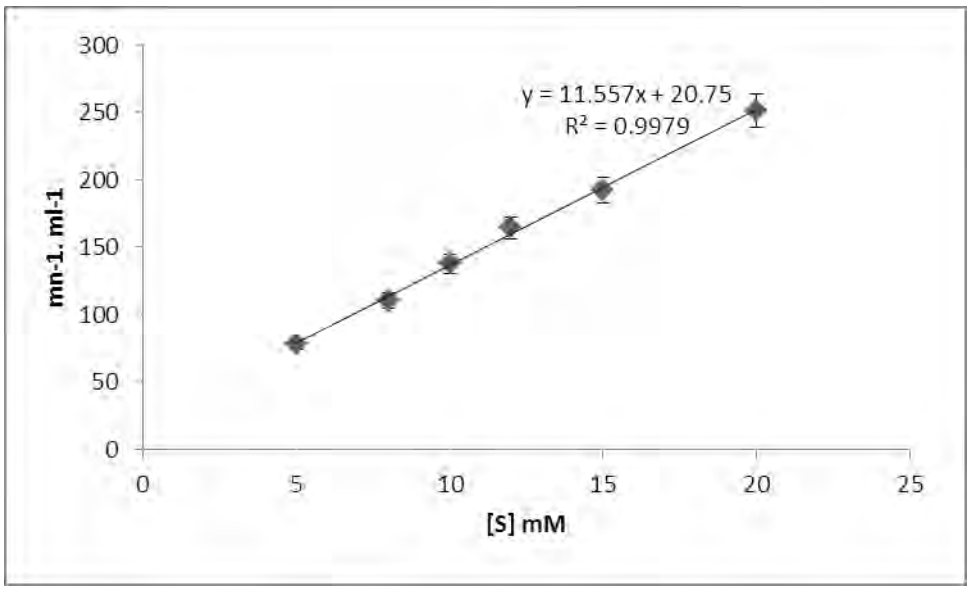

Figure 3.15: Hanes-Woolf plot for the determination of kinetic parameters (V_{max} and K_m) ; values represent the mean (± S.E.M) of three trials

3.6. Conclusions

Purification results proved that it was very difficult to purify nNOS as indicated from in Table 3.1. As shown in the characterisation results, the enzyme had a half-life of 1h 40min (Figure. 3.1) and optimum temperature of 50 ºC indicated that the enzyme was relatively stable, yet lost its stability at each purification step. The purification techniques namely $(NH_4)_2SO_4$ and PEG 20 000 precipitation were attempted but were unsuccessful in concentrating the enzyme. The time involved in stirring, centrifugation and dialysis for these techniques was longer than the half-life of 1h40min. For example, dialysis involved a 24 h period which could have resulted in loss of activity. In addition to anion exchange on DEAE Sephacel (see Figure. 3.7 above), the first 45 fractions were eluted at a flow rate of 2 ml/min indicating that the enzyme was still bound to the column and possibly lost 50 % of its activity in the first 100 min according to the thermal stability profile of nNOS (see Figure 3.14 above)

and thus lowering the specific activity of the enzyme considerably. Gel filtration chromatography was successful in producing a very high specific activity (1.4 U/mg) compared to Ion exchange chromatography (0.09 U/mg). Native-PAGE revealed a single subunit at although there were some proteins purified for the purification due to the use of non-denaturing conditions. A Western blot analysis showed that the antibody was not specific for the protein of interest as indicated in Figure 3.11 above, this maybe caused by primary antibody had low affinity to the protein of interest and cross reacted with other protein in the cell lysate. As shown in Figure 3.15 above, the enzyme kinetic data and the catalytic behaviour of the purified nNOS obeyed Michealis-Menten kinetics, with V_{max} and K_m values estimated from the Hanes-Woolf plot of 0.0865 μmol.min.^{1} and 1.8 μM, respectively. The enzyme retained > 80% optimal activity between pH 7.5 at an optimal temperature of 50 °C. The relative stability of nNOS and its high catalytic activity made it a suitable biocatalyst for benzoyl-L-arginine ethyl ester under controlled reaction conditions.

CHAPTER 4: SYNTHESIS AND CHARACTERISATION OF NANOPARTICLES

4.1. Introduction

Metal nanoparticles have been the subject of common research over the past two decades. In recent years noble metals have been the focus of numerous studies involving synthesis, characterisation, and applications (Wang *et al*., 2005, He *et al*., 2002). Different ways to prepare these nanostructures have been demonstrated, and among the different techniques, chemical synthesis of metallic nanoparticles has been suggested as a simple and economical synthetic route which can be applied on a large scale (Bonsaki *et al*., 2010). Nanoparticles can be produced using two techniques, (1) the top-down approach or (2) the bottom-up approach. The top-down approach is the breakdown of larger structures by use of ultra fine grinders, lasers and vaporisation followed by cooling. The bottom-up approach allows for the rearrangement of these molecules to form complex structures with new and useful properties. The bottom up approach has an advantage to obtain nanostructures with fewer errors and with more homogeneous chemical composition, whereas top down approach main challenge is the creation of increasingly small structures with sufficient accuracy (Whiteley *et al*., 2011). This chapter explains and implements the synthesis of metallic nanoparticles using a bottom-up approach. The advantage of using the bottom-up approach is that it synthesises nanoparticles between 8 and 100 nm that are more stable nanoparticles (Cao, 2004) compared to nanoparticles produced the top-down approach. Because of its high surface to volume ratio the top down approach cause a lot of imperfection of the surface structure which is significant on physical properties of the nanoparticles. It is well recognized that properties of metal nanoparticles depend largely on the size, shape, composition, structure, and crystallinity. Therefore, various approaches have been developed to attempt to satisfy the parameters distinguishing metal nanoparticles and, hence, meet the requirements for various applications (Sau and Rogach, 2010). It is critical that a nanoparticle be stable, as this feature is important especially when examining and exploiting their properties. This chapter explains the synthesis and characterization of gold and silver nanoparticles which was carried out with the following aims.

- To chemically synthesize silver and gold nanoparticles using sodium borohydride.
- To chemically synthesize silver and gold nanoparticles using sodium citrate.
- To characterise silver and gold nanoparticles by UV-Visible spectroscopy (UV-Vis).

- To characterise silver and gold nanoparticles by Transmission electron microscopy (TEM).

4.2. Principles of techniques applied

4.2.1. Chemical synthesis of silver and gold nanoparticles

Chemical synthesis of nanoparticles in solution requires the use of methods allowing a precise control over the size and the shape of the nanoparticles to yield a set of monodisperse nanoparticles displaying a specific property (Zhang *et al*., 2003). In general, the synthesis of metal nanoparticles in solution involves the use of the following components: a metal precursor; a reducing agent and a stabilizing agent (Andreescu *et al*., 2007). The chemical reduction methods being used to produce nanoparticles depend on the choice of the metal precursor, the reducing agent and their relative quantities and concentrations, the temperature, the mixing rate the duration of reaction. The shape and size of the nanoparticle are largely determined by the reagents and conditions used during the synthesis process (Krutyakov *et al*., 2008). Sodium borohydride and sodium citrate are the most commonly used reducing reagents (Mozghan, 2008) with the former reagent the most widely used particularly in the preparation of silver nanoparticles as it has a higher reactivity than sodium citrate (Solomon *et al*., 2007). In most studies the reduction of silver nitrate by borohydride, produces colloidal silver which is described as bright yellowish, with a plasmon absorbance peak at 400 nm and with particle diameters ranging from 5-15 nm with varying size distributions (Mozghan, 2008; Solomon *et al*., 2007). Based on the success and the wide use of the two reducing reagents, this current study was conducted using both of them in the method outlined (i) and (ii):

(i). Borohydride Reduction: The reduction by borohydride has been in existence for a number of years (Turkevich *et al*., 1951), and involves the hydrolysis of the borohydride accompanied by the evolution of hydrogen, as shown in equation 6 below (Solomon *et al*., 2007).

$$AgNO_3 + NaBH_4 \rightarrow Ag + \frac{1}{2}H_2 + \frac{1}{2}B_2H_6 + NaNO_3 \quad \text{.....equation 6}$$

Various metal nanocrystals such as copper (Yee *et al*., 1999), silver and gold (Selvakannan *et al*., 2002) have been synthesized via the borohydride reduction. The disadvantage of this

method includes irreproducibility, especially in the aqueous medium and the incorporation of boron in the product (Chen *et al*., 2005).

(ii). Citrate Reduction This is the most common method for synthesizing gold nanoparticles (Turkevich *et al.*1951; Silekaite *et al*., 2009). It has a disadvantage in that the particles are difficult to isolate from solution and to store them in the solid state (Silekaite *et al*., 2006).

4.2.2. Nanoparticle characterisation

Nanoparticles are synthesized to achieve unique physicochemical properties and functionalities, and are finding applicability in many commercial products (The Royal Society 2004). Characterisation is the significancy factor in nanoparticle synthesis in establishing average core diameter and shape of the synthesized material (Khan, 2008). Transmission electron microscopy (TEM) and UV-Visible spectroscopy (UV-Vis) are often used to determine the size, shape and the distribution of the nanoparticle (Pigozzi, 2006).

4.2.2.1. UV-Vis spectroscopy

A spectrophotometer is a device used to measure the light intensity as a function of the wavelength of the light. Figure 4.1 below illustrates the standard spectrophotometry setup. The change in absorbance can show difference of the quantity of absorbing species, that is, silver nanoparticles or gold nanoparticles in the liquid. When white light passes through the substance, the wavelength of maximum absorbance is removed by absorption and the remaining wavelengths are transmitted to determine the color of the substance observed. When a beam of monochromatic radiation (see Figure 4.1 below) passes through any solution, the intensity of the beam reduces to some amount and the amount of light intensity absorbed by the sample is directly proportional to the concentration and the thickness of the absorption material equation 7 (Chen *et al*,. 2006; Silekaite *et al*., 2006).The width and the position of the peak can be used to determine particle size distribution (Silekaite *et al*., 2006).

$$A = E.\ c.\ l \qquad \text{.....Equation 7}$$

Where
A = absorbance
E = molar extinction co efficient
c = concentration of the molar solution
l = length of the light path

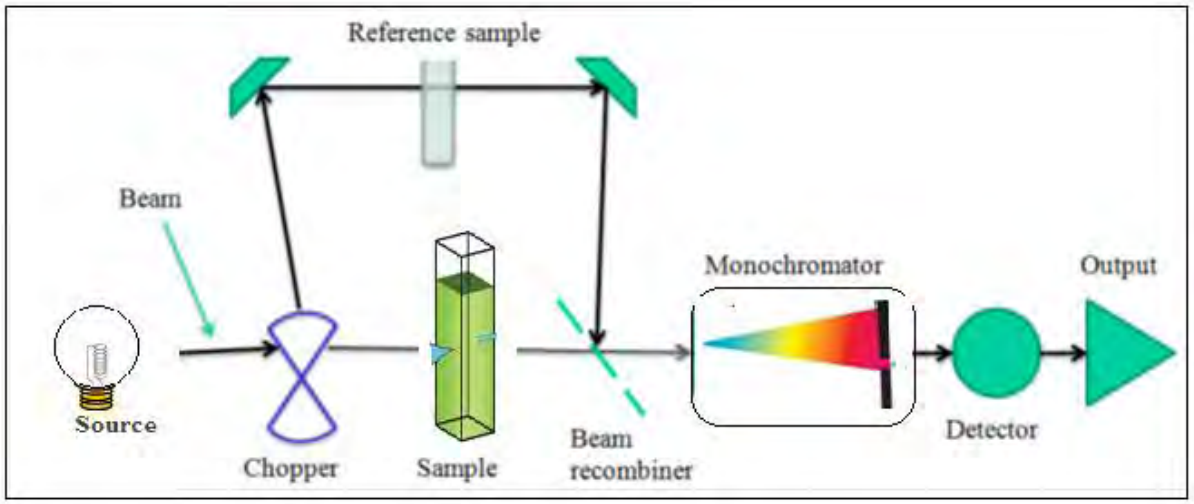

Figure 4.1: Schematic of a standard spectrophotometry setup (Bonsaki, 2010)

4.2.2.2. Transmission electron microscopy

Transmission electron microscopy (TEM) is a useful technique for characterisation of the nanoparticles because it can provide an information on the atomic scale and local chemical information at resolution of 1 nm or less and structural information through electron diffraction (Figure 4.2 below illustrates the basic principles of TEM) (Andreescu *et al*., 2007). In transmission electron microscopy, a beam of electrons is transmitted through an ultra thin sample, constructing an image based on the interaction of the electrons with the specimen (Gunnaes, 2010).

The image is then magnified and focused onto an imaging device such as a fluorescent screen or phosphor screen (Figure. 4.2) The darker areas of the image represent those areas of the sample that fewer electrons were transmitted through (they are thicker or denser). The lighter areas of the image represent those areas of the sample that more electrons were transmitted through (they are thinner or less dense).

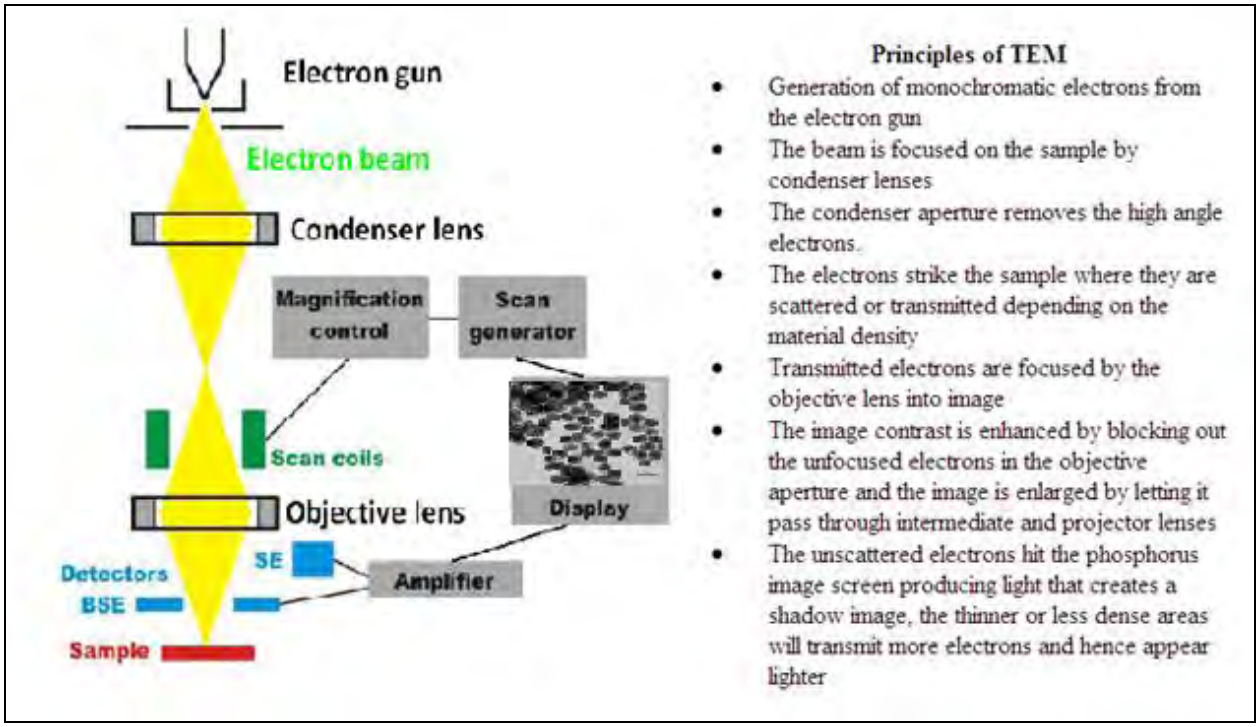

Figure 4.2: Principle schematic of the components and a basic description of the workings of a transmission electron microscope (TEM) adapted from (Gunnaes, 2010)

4.3. Reagents and materials

Silver nitrate ($AgNO_3$), trisodium citrate ($Na_3C_6H_5O_7$), sodium borohydride ($NaBH_4$), potassium carbonate (K_2CO_3) and polyvinylpyrrolidone (PVP, Polyvinyl Difluoride (PVDF) were purchased from Merck Chemicals (South Africa). Gold (III) chloride trihydrate ($HAuCl_4.3H_2O$) were bought from Sigma Aldrich chemicals (South Africa). All the solutions and the buffer were prepared with deionized water obtained from a Milli-Q system. UV spectrophotometer (Spectroquant Pharo300 Merck) to evaluate the plasmon bands associated with the metal nanoparticles, TEM microscopy (Jeol JEM 200X), and copper grids.

4.4. Methods

4.4.1. Nanoparticle synthesis

4.4.1.1. Synthesis of silver nanoparticles using sodium borohydride

20 mM solution of freshly prepared sodium borohydride (100ml) was stirred for 30 minutes in ice. Sodium borohydride (20 mM, 29ml) was stirred (30 min, 4ºC), then treated drop wise with silver nitrate (10 mM, 1ml). The solution immediately turned yellow confirming that silver nanoparticles were formed. The solution was stirred for another 2 hours in order to

allow the nanoparticles to consolidate. A drop of polyvinylpyrrolidon (PVP) was then added to stabilize the nanoparticles. This was filtered using polyvinyl difluoride (PVDF) syringe filters 0.45µm and stored until required (see Appendix B).

4.4.1.2. Synthesis of silver nanoparticles using sodium citrate

The silver nanoparticles were prepared according to Ivana and Blanka (2001) with modification. Typical silver nitrate (1 mM, 10 ml) was heated to boil while the solution was mixed vigorously and trisodium citrate (1 %, 50µl) was added dropwise. The reaction was allowed to stand for 10 minutes with heating until the color change to pale yellow, indicative of the presence of silver nanoparticles. Then it was cooled to room temperature and the pH was adjusted to pH 9 with K_2CO_3. This was filtered using the polyvinyl difluoride (PVDF) syringe filters (0.45µm) (Appendix B).

4.4.1.3. Synthesis of gold nanoparticles using sodium borohydride

PVP (400mg) in distilled water (25ml) was treated dropwise with an aqueous solution of $HAuCl_4$ (2.5mM, 5 ml) and left to stand for 5 minutes while stirring, then reduced with sodium borohydride (10 mM, 600µl) for 10 minutes. A drop of polyvinylpyrrolidon (PVP) was added to stabilize the nanoparticles and then filtered using the polyvinyl difluoride (PVDF) syringe filters (0.45µm) (Appendix B).

4.4.1.4. Synthesis of gold nanoparticles using sodium citrate

The gold nanoparticles were also prepared according to Ivana and Blanka, 2001 with modification. Typically, $HAuCl_4$ (1 mM, 10 ml) was heated to boil while the solution was mixed vigorously and trisodium citrate (1 %, 50µl) was added dropwise. The reaction was allowed to stand for 10 minutes with heating until the color changed to wine red, indicative of the presence of gold nanoparticle. Then it was cooled to room temperature and the pH was adjusted to pH 9 with K_2CO_3. This was filtered using the polyvinyl difluoride (PVDF) syringe filters (0.45µm) (Appendix B).

4.4.2. Characterisation of silver and gold nanoparticles

4.4.2.1. UV-Vis Spectroscopy

Both silver and gold nanoparticles were analyzed using a UV-Vis spectrophotometer (Elechiguerra *et al.,* 2005). Prior to any spectrophotometric measurements, the UV-Vis cuvette was filled with distilled water and used as a blank. The nanoparticle solution (2ml)

was each introduced to standard quartz cuvettes with 1 cm path before measuring the optical absorption. For silver nanoparticles the absorbance was scanned between 250 to 700 nm ranges, which include the maximum absorbance peak of the silver nanoparticles centered at 400 nm (García-Barrasa *et al.*, 2011). For gold nanoparticles the absorbance was also scanned between 250 to 700 nm ranges, which include the maximum absorbance peak of the gold nanoparticles centered at 520 nm (Eustis and EI-Sayed, 2005).

4.4.2.2. Transmission Electron Microscopy

The particle size of the freshly synthesized nanoparticles was monitored using a transmission electron microscope model (Jeol JEM 200X) (Dass *et al*., 2005). For the sample preparation a drop of the nanoparticle solution was placed on the grid, blotted dry with filter paper, left to dry overnight at room temperature in a desiccator and viewed the following day.

4.5. Results and discussion

Silver nanoparticles

The prepared (borohydride) silver nanoparticle yellow solution was yellow (see Figure 4.3A below) and characterised by a strong absorbance of 400 nm as shown by the UV-Vis spectrum (see Figure 4.3B below) (Dass *et al*., 2005). The transmission electron microscope (TEM) micrograph (see Figure 4.3C below) was used to confirm the size and shape of the nanoparticles. The particles appear to have a spherical shape with an average diameter of 7 nm.

The colour of the prepared (citrate) silver nanoparticles is light yellow (see Figure 4.4 A below). The colour of the chemically synthesized nanoparticles normally depends on the particle size, dielectric medium and chemical surroundings. Small spherical nanoparticles: < 20 nm exhibit a single surface plasmon band of 400 nm as shown in Figure 4.4B below) (Solomon *et al*., 2007). The particles appear spherical and consequently, the same in shape and size as those prepared by borohydride method. The average diameter of 4.5 nm (see Figure 4.4C below) and the use of PVP as capping agent ensure the stability for nanoparticles.

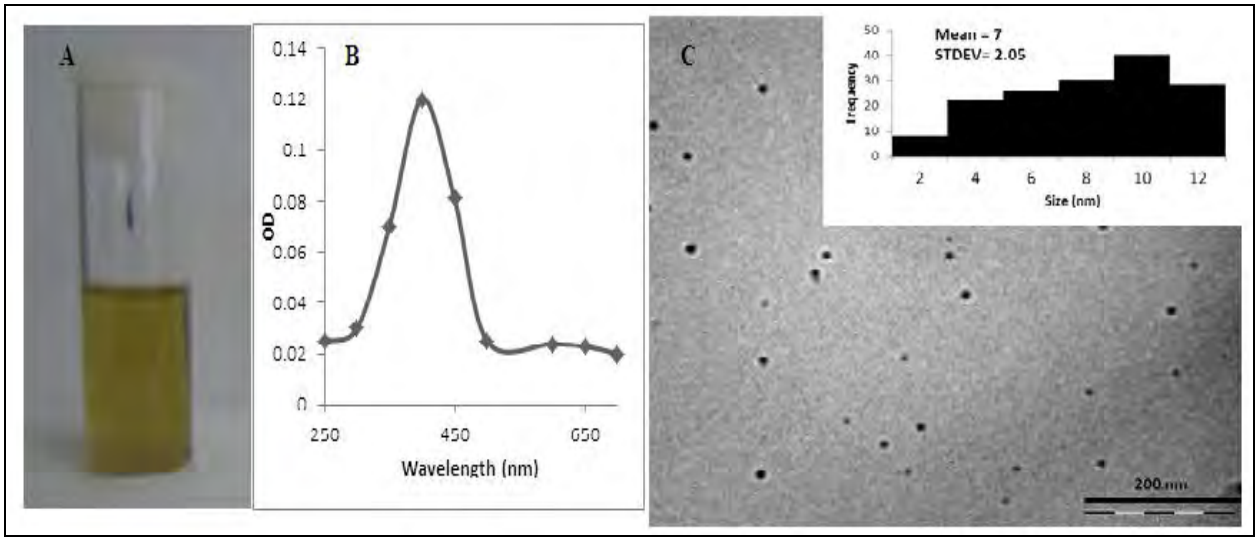

Figure 4.3: (A) Colour of the chemical synthesized silver (Ag) nanoparticles using sodium borohydride (B) the UV/Vis absorbance spectra of Ag nanoparticles (C) TEM image of Ag nanoparticles

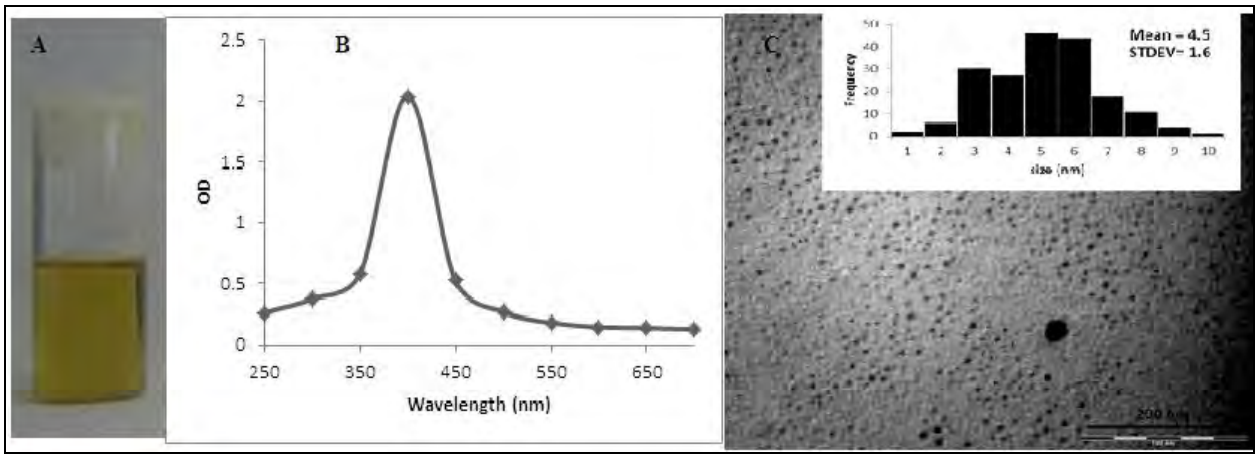

Figure 4.4: (A) Colour of the chemical synthesized (Ag) nanoparticles using sodium citrate (B) The UV/Vis absorbance spectra of Ag nanoparticles (C) TEM image of Ag nanoparticles

Gold nanoparticles

The colour of the borohydride prepared gold nanoparticles was wine red (see Figure 4.5A below) and characterised by a strong absorbance of 520 nm (see Figure 4.5 B below) as an indicative of gold nanoparticles at nanometer scale (Silekaite *et al*., 2006). Transmission electron microscopy (TEM) was used for quantitative determination of the gold nanoparticles including direct visualization of the metallic core and to confirm their size and shape

(Silekaite *et al*., 2006). As shown in Figure 4.5 C below, the particles appear to have a spherical shape with an average diameter of ± 10 nm. Gold nanoparticles prepared with sodium citrate produced a deeper wine red colour (see Figure 4.6 A below) than those prepared using borohydride. Both methods of preparation yielded the same maximum absorbance at 520 nm (see Figure 4.6 B below). The TEM images in Figure 4.5 C and Figure 4.6 C below show that the particles mostly are spherical in shape with the average diameter of ± 10 nm borohydride ± 3 nm citrate.

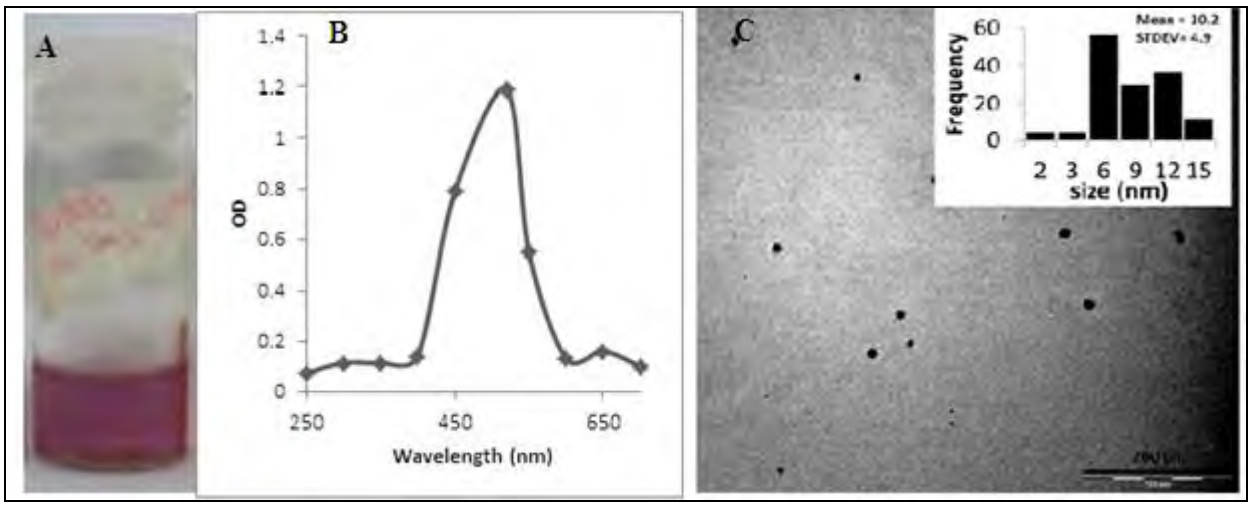

Figure 4.5: (A) Colour of the chemical synthesized silver (Au) nanoparticles using sodium borohydride (B) the UV/Vis absorbance spectra of Au nanoparticles (C) TEM image of Au nanoparticle

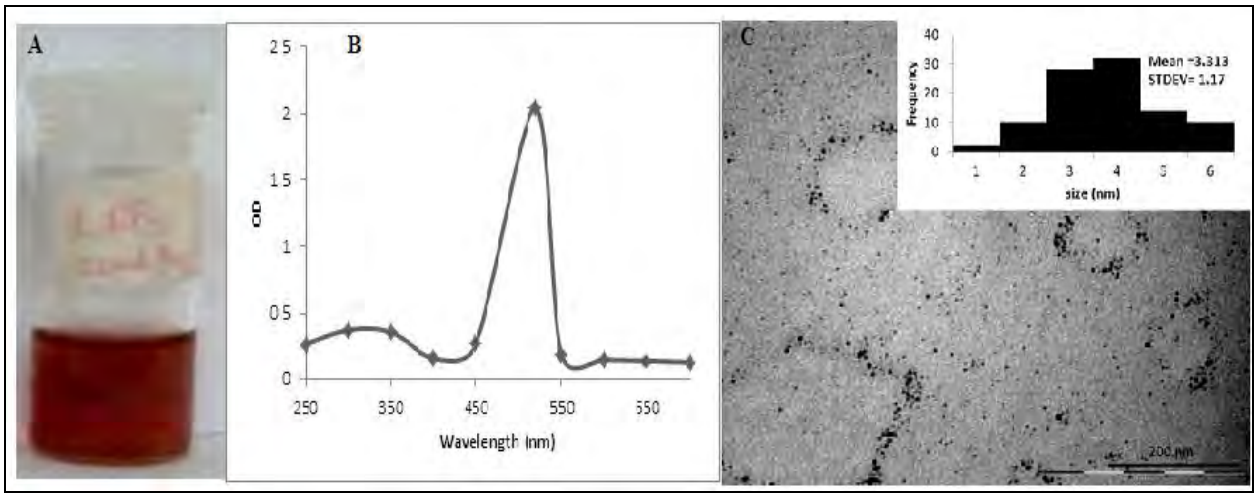

Figure 4.6: (A) Colour of the chemical synthesized (Au) nanoparticles using sodium citrate (B) The UV/Vis absorbance spectra of Au nanoparticles (C) TEM image of Au nanoparticles.

4.6. Conclusion

The experimental work of this chapter has involved primarily two objectives: (i) the chemical synthesis of silver and gold nanoparticles, and (ii) the characterisation of the nanoparticles. By employing different reducing agents and varying synthetic conditions it was possible to obtain particles of different average size. When synthesizing nanoparticles it is very important to control not only the particle size, but also the particle shape and morphology as well. The silver nanoparticles exhibited an intense and narrow absorption peak at a wavelength of 400 nm and gold nanoparticles had wavelength of around 520 nm. The reduction with aqueous sodium citrate resulted in the formation of mostly spherical and smaller nanoparticles for both silver and gold nanoparticles (i.e. ± 5 nm and ± 3 nm, respectively) as compared to the reduction by sodium borohydride (i.e. ± 7 nm and ± 4 nm, respectively).

CHAPTER 5: INTERACTION OF SILVER AND GOLD NANOPARTICLES WITH NEURONAL NITRIC OXIDE SYNTHASE

5.1. Introduction

Recently there have been developments with regards to the studies of nanoparticles and their effect on cellular and metabolic pathways. A keen interest has been taken in the biological effect of nanoparticles especially their interactions with proteins (Sanfins, 2011). Although nanoparticles can pass through the blood brain barrier it is still a challenge to have new nanoparticulate systems that would be useful in the choice of the polymer core to enable controlled degradation, entrapment and release of a variety of bioactive materials. This may also contain a hydrophilic corona that would allow easy coupling of ligands at controlled surface densities, without degrading either the ligand or the nanoparticles (Chopra *et al*., 2008). Enzyme inhibitors are substances which decrease the rate of an enzyme-catalyzed reaction when combined directly to the enzyme. If the velocity of an enzymatic reaction is decreased or inhibited, the kinetics of the reaction are disturbed. Inhibition may be of two types, reversible and irreversible. Reversible inhibitory mechanisms usually have high activity when the concentration of the inhibitor is low and low activity when the concentration of the inhibitor is high. Irreversible inhibition usually results from a covalent and permanent modification of a functional group which may result inactivity of an enzyme (Cornish-Bowden, 2004).

The use of nanoparticles is on the increase in research of some non-communicable diseases such as Alzheimer‟s disease. They have been used to slow down and possibly disrupt the aggregation of amyloid beta peptides in Alzheimer‟s disease (AD) after using techniques such as: capillary electrophoresis, surface plasmon resonance, confocal microscopy studies and Thioflavin T assays (Brambilla *et al*., 2010). A study (Cantoni *et al*, 2002) showed the effect of nanoparticles on beta amyloid peptides resulting in an understanding of certain biological injuries such as changes in protein fibrillation, exposure of new antigenic epitopes, and loss of function such as enzymatic activity impairment. Neuronal nitric oxide synthase has the two cysteine residues per monomer, which form a disulphide bridge between the monomers which are 3 nm apart. Since nanoparticles of silver and gold have a strong affinity towards sulphur (Monteiro *et al*., 2009), and nNOS neuronal nitric oxide synthase was an enzyme involved in the etiology of AD, it was reasonably feasible that the interaction of these nanoparticles with nNOS could be a tool to investigate the treatment of AD. In this chapter

fluorimetric and kinetic analysis were carried out in order to investigate this interaction. The following objectives were carried out:

- Determine the effect of inhibition of nNOS by metallic nanoparticles relative to both substrate concentration and time dependent factors.
- Use fluorescence quenching technique to calculate Ksv (Stern Volmer constant) and Θ (fraction of tryptophan residues near or on the surface of the enzyme) in order to measure the degree of quenching from and the ease of accessibility to the nNOS molecules.
- Use transmission electron microscopy (TEM) to visually examine the morphology (shape and size) of nanoparticles towards nNOS over a given time.

5.2. Principles of techniques applied

5.2.1. Kinetics

This chapter looks at a simple model for the catalytic behavior of an enzyme and the kinetic model that arises from its reaction with metallic nanoparticles by determining K_m and V_{max} (Somero, 1978). The mechanism of enzyme catalyzed reactions is often studied by making kinetic measurements on enzyme-substrate reaction systems. This involves measuring rates of the enzyme-catalyzed reactions at different substrate and enzyme concentrations. Enzymes function by sterically binding to a substrate. So, if a molecule interferes with that binding, it would be more likely to inhibit the activity of the enzyme that can be calculated using equation 8 (Palmer, 1991). There are two main types of inhibitors: competitive and non-competitive. In the former, the inhibitor molecule binds to the same active site as the substrate. Non-competitive inhibitors on the contrary, do not bind to the enzyme‟s active site but rather binds to other inhibitory sites on the enzyme molecule itself (Palmer, 1991). Most reactions catalyzed by enzymes can be described by the Hanes-Woolf (refer to equation 2 in Chapter 3) (English *et al*., 2006). The determination of these constants involves the performance of kinetic enzymatic activity measurements. For every reaction, the enzyme has its physical characteristics with regard to substrate specificity and reaction velocity (Palmer, 1991).

$$K_i = \frac{np.\ V_{max}^{app}}{V_{max} - V_{max}^{app}}$$

np = concentration of nanoparticle

V_{max}^{app} = apparent maximum velocity in the presence of nanoparticle.

V_{max} =enzyme activity without nanoparticles

...equation 8

5.2.2. Fluorimetric analysis

The fluorescence (FL) method is used for the analysis of many compounds and has advantages over the absorbance spectroscopy because it is a relatively simple instrument. It has also a low detection limit and a large linear dynamic range of samples can be analysed (Karim *et al*., 2006). The FL method uses high intensity light beam which is passed through a monochromator for the selection of an excitation wavelength (a wavelength efficiently absorbed by the fluor). The exciting light beam then passes through a cell containing the sample. Fluorescence is emitted in all directions by the sample. But, most systems look at only that emitted at 90° with respect to the exciting light (Tsien, 1994). The fluorescence then passes through a monochromator for wavelength analysis and finally falls on a photosensitive detector (usually a photomultiplier tube) (Freifelder, 1976). Figure 5.1 illustrates the the principle of spectrofluorometry. Fluorescence is short-lived created by electromagnetic excitation and it is generated by a substance that absorbs light energy at a short wavelength and re-emits it at a longer wavelength (Mark *et al*., 2011). Proteins are complex and involve many internal motions. The amplitude and time scale of internal protein motion may be deciphered from the rates at which agents of varying molecular can reach tryptophan side chains and quench their fluorescence (Calhoun, *et al.,* 1986). Metallic nanoparticles (NPs) do not fluoresce but they can enhance the emission of fluorophores through local field effects and consequently fluorescence emission of molecules can be modified through interaction with these particles (Chiu and Huang, 2009).

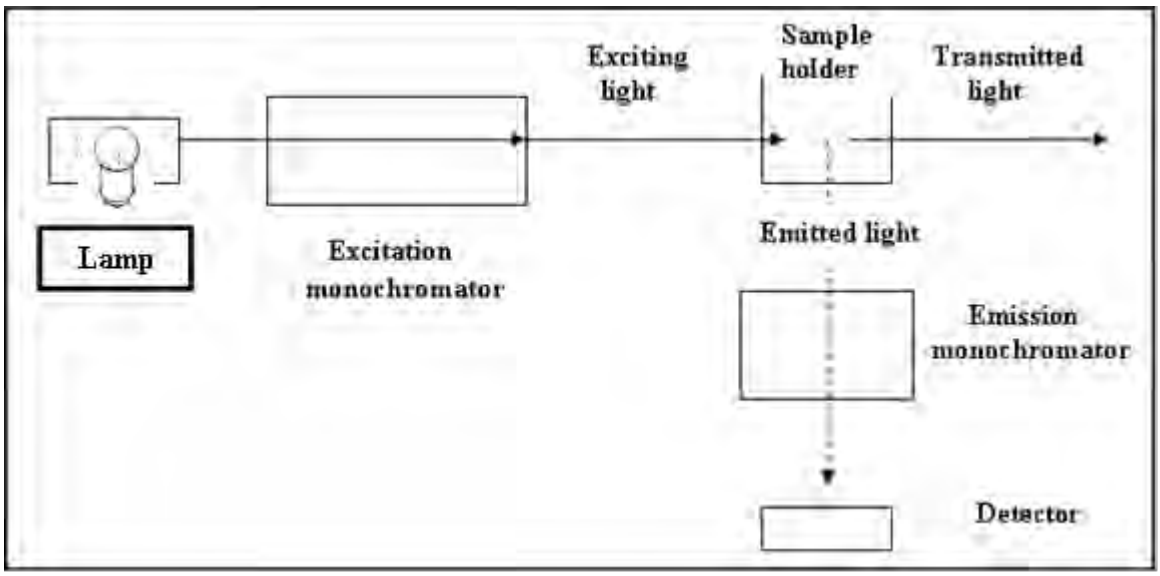

Figure 5.1: Spectrofluorometer used in fluorescence analysis (Freifelder, 1976)

The molecules involved in fluorescence are known as fluors. There are two types of fluors used in fluorescence analysis of proteins namely: intrinsic fluors (usually aromatic rings within the protein itself) and extrinsic fluors (added to the protein, e.g. the quencher molecule fluorescein) (Freifelder, 1976). For proteins, there are only three intrinsic fluors, namely tryptophan, tyrosine and phenylalanine. However, phenylalanine has a very low quantum yield and tyrosine fluorescence is frequently very weak due to quenching (Freifelder, 1976). Thus, in this chapter, it is only the fluorescence of the tryptophan amino acids that will be considered as it is this fluorescence that is quenched with a subsequent estimation of the Stern Volmer constant (K_{SV}). This constant is dependent on the fluorescence intensity, the concentration of a quencher and the degree of quenching.

The classical Stern-Volmer plot (see Figure. 5.2 below) and the corresponding Stern-Volmer equation (see Equation 9 below) were used in the estimation of K_{sv} and θ. In addition, the second parameter (Θ) was a reflection of the fraction of tryptophans near or on the surface of the enzyme. Θ may be determined from equation 9, where Fo represents F = fluorescence in the absence and presence of amyloid peptide respectively; Q = concentration of amyloid peptide; Ksv = Stern-Volmer constant; ΔF = Fo – F; Θ = fraction of accessible tryptophan residues.

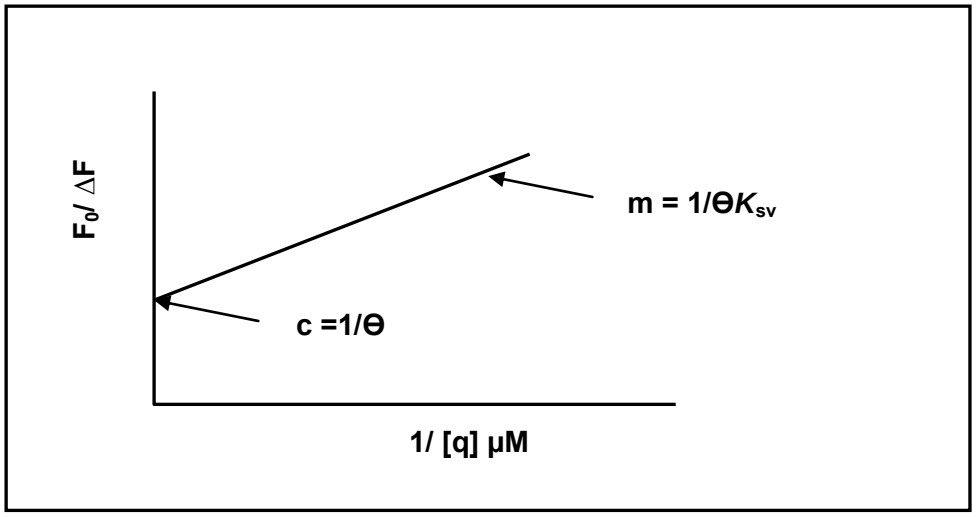

Figure 5.2: Classical Stern-Volmer plot. KSV is calculated from the slope of the plot while θ is estimated from the intercept

$$\frac{Fo}{\Delta F} = \frac{1}{\theta Ksv[q]} + \frac{1}{\theta}$$

.....equation 9

The concentration of binding sites (n) on the purified enzyme, that were available for nanoparticles, and the dissociation constants (Kd) were estimated, respectively, from the slope of the linear regressions and the intercept on the log [(F-Fo)/(Fmax-F)] equation 10.

$$\frac{\log[(F\text{-}Fo)}{F} = \log Kd + n\log[q]$$

n = the concentration of binding site on the purified enzyme
Kd = dissociation constants

.....equation 10

5.2.3. Transmission electron microscopy (TEM)

The technique of transmission electron microscopy (TEM) (refer to 4.2.2 in Chapter 4) for the background information regarding this technique) was employed to determine the morphology of nanoparticles. TEM will be used to observed and analyse the changes in the nanoparticles (size and shape) at different time intervals.

5.3 Reagents and materials

Neuronal nitric oxide synthase was isolated, purified and characterised according to details mentioned in Chapter 3. Fluorescence was measured using a Hitachi fluorimeter (model F-2500, 230 V, 1.8 A, 50/60 Hz). Uranyl acetate, Nα-benzoyl-L-arginine ethyl ester hydrochloride (BAEE) and Tri ethanolamine buffer pH 7.4 were obtained from Sigma-Aldrich (South Africa). Silver and gold nanoparticles were synthesized (refer to Chapter 4, section 4.4.1.). Sodium chloride (NaCl), sodium hydroxide (NaOH) and hydrochloric acid (HCl) were obtained from Merck Chemicals (South Africa). UV analyses were performed on a PowerWaveX^{TM} microplate reader which was purchased from Bio-Tek Instruments (Vermont, USA).

5.4 Methods

5.4.1. Interaction based on variable substrate concentration

Partially purified nNOS (5 µl) in Tris HCl buffer (50 mM, pH 7.6, 76 µl) was treated with nanoparticles (0 µM, 5 µM, 15 µM, 25 µM, 50µM (5 µl)) in the presence of varying amounts of the substrate benzoyl arginine ethyl ester (5-25 mM (80 µl)) and in the presence of chromogenic reagent (200 µl) to investigate the effect of substrate dependent inhibition on nNOS. This was monitored by determining the kinetic properties of Hanes-Woolf plot constant (Km) and the maximal enzyme velocity (Vmax).

5.4.2. Interaction based on variable time

The interaction of nNOS, both with silver and gold nanoparticles was monitored. The interaction of the enzyme with nanoparticles was monitored for up to 3 hours, at fixed substrate and different time intervals. Nanoparticle concentrations 5µM, 15 µM, 25 µM, 50 µM were used in interactions with partially purified enzyme. Varying times of incubation for nanoparticle-enzyme interactions at intervals of 10, 20, 30, 40, 60, 120 and 180 minutes were applied, using 10 µl aliquots of the reaction mixture. The value of K_i (inhibitor constant) for nanoparticles was calculated using equation 8.

5.4.3. Estimation of K_{sv} and Θ parameters by fluorescence quenching

Fluorescence quenching was performed using the graphical method of the Stern-Volmer and Θ plot as described above in 5.2.2 (Lakos *et al*., 1995; Matyus *et al*., 2006) with modifications. The spectrofluorimetry was used to determine structural changes induced in

nNOS by interaction of nanoparticles with the purified enzyme with the excitation and emission wavelength (i.e. 295, 482). The change in fluorescence of a solution was monitored as increasing concentration of nanoparticles (0-50µM) was added to a reaction mixture of nNOS (5µl) Triethanolamine buffer pH 7.4 (200µl). The K_{SV}, Θ and other binding constants were obtained from equations 9 and 10 (see Appendix C).

5.4.4. Transmission electron microscopy (TEM)

A 10 µl sample of either gold or silver nanoparticles as a negative control or those that had been challenged with nNOS was placed onto a carbon-coated copper grid. Excess liquid was removed by carefully blotting with filter paper. The sample was then negatively stained with uranyl acetate (2%, 30 sec) and left to dry overnight at room temperature in a desicator. The samples were viewed using a JEOL JEM-1210 TEM at an acceleration voltage of 100 kV.

5.5 Results and discussion

5.5.1. Kinetic analysis

The main purpose of the study was to investigate the effect of metal nanoparticles on nNOS. For substrate dependence, it was shown that all the nanoparticles competitively inhibited nNOS at all of the concentrations of nanoparticles (see Figure 5.3A and B).

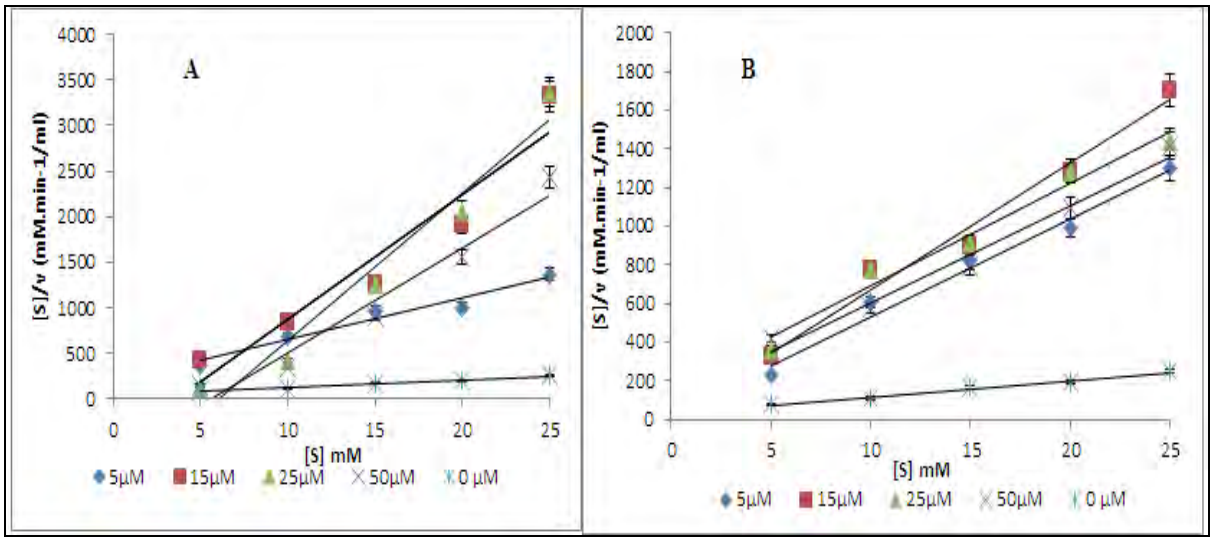

Figure 5.3: Hanes-Woolf plot showing influence of silver nanoparticles prepared by A: borohydride, B: citrate method on nNOS purified from bovine brain

Table 5.1(a): Kinetic parameters determined from the interaction of nNOS with Ag nanoparticles (borohydride method) using different substrate concentrations

Parameter	**Enzyme only**	**5µM**	**15µM**	**25µM**	**50µM**
Vmax (µmol.min^{-1})	0.0865	0.022	0.007	0.006	0.009
Km (µM)	1.8	3.9	3.57	5.9	5.96
Kcat (min^{-1})	0.95	0.024	0.008	0.007	0.0098

Table 5.1(b): Kinetic parameters determined from the interaction of nNOS with Ag nanoparticles (citrate method) using different substrate concentrations

Parameter	Enzyme only	5µM	15µM	25µM	50µM
Vmax (µmol.min^{-1})	0.0865	0.0198	0.0152	0.019	0.02
Km (µM)	1.8	0.59	0.242	3.045	2.11
Kcat (min^{-1})	0.95	0.02	0.017	0.021	0.022

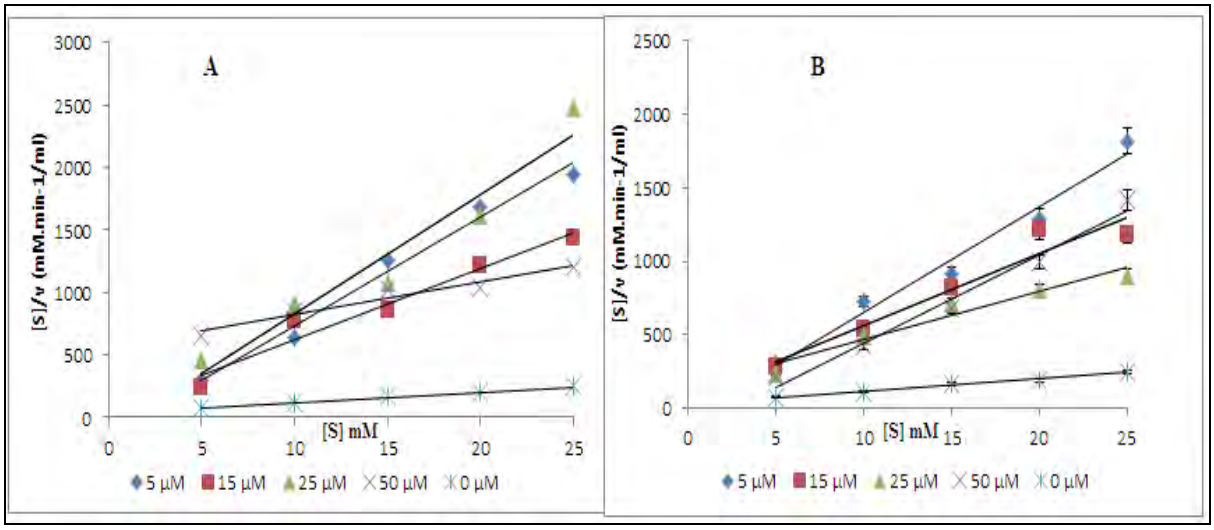

Figure 5.4: Hanes-Woolf plot showing influence of gold nanoparticles prepared by A: borohydride, B: citrate method on nNOS purified from bovine brain

Table 5.2(a): Kinetic parameters determined from the interaction of nNOS with Au nanoparticles (borohydride method) using different substrate concentrations

Parameter	Enzyme only	5µM	15µM	25µM	50µM
Vmax (µmol.min^{-1})	0.0865	0.011	0.0176	0.01	0.038
Km (µM)	1.8	1.6	0.99	1.2	2.2
Kcat (min^{-1})	0.95	0.012	0.0193	0.01	0.41

Table 5.2(b): Kinetic parameters determined from the interaction of nNOS with Au nanoparticles (citrate method) using different substrate concentrations

Parameter	Enzyme only	5µM	15µM	25µM	50µM
Vmax (µmol.min^{-1})	0.0865	0.0203	0.014	0.0304	0.017
Km (µM)	1.8	1.43	0.96	4.2	2.62
Kcat (min^{-1})	0.95	0.022	0.015	0.0334	0.019

Table 5.3: Table reflecting relative K_i values for nanoparticles

Parameter	**Ag nanoparticles (borohydride)**	**Ag nanoparticles (citrate)**	**Au nanoparticles(borohydride)**	**Au nanoparticles (citrate)**
K_i (µM)	9	1.4	5.7	0.2

Those particles prepared by borohydride afforded K_i values of 9 µM and 5.7 µM for silver and gold, respectively (see Table 5.3 above). This can also be realized by the fact that the K_m value decreases in the presence of nanoparticles (see Table 5.1; 5.2 above). The difference, with respect to the inhibitor constant K_i was size of the particles since citrate nanoparticles (Ag 4.5nm, Au 3nm) had more effect than borohydride nanoparticles (Ag 7nm, Au 10nm).

5.5.2. Time dependence

For time dependence it was notable that there was an increase in inhibition during the first 50 to 60 min. Furthermore, as expected, there was an increase in inhibition as well as an increase in concentration of the particles. There was no real significant difference in the inhibitory trend observed between gold and silver nanoparticles that were prepared by the borohydride method. However, it may be argued that gold nanoparticles had slightly higher inhibition towards the enzyme. Comparing the nanoparticles prepared by the citrate method, the results showed the highest inhibition see Figure 5.5(c) and 5.5(d) with gold nanoparticles. The decrease in enzyme activity was an indication of the inhibition of nNOS by the nanoparticles which correlates with the finding that citrate nanoparticles, specifically, gold nanoparticles had the tightest binding affinity to the enzyme as earlier shown in Table 5.3 above. Interestingly, enzyme activity was restored to nearly that value of the control after the enzyme was incubated with the nanoparticles for longer than 90 minutes. This was particularly noted with the silver particles that were prepared by borohydride.

Though these experiments were not done in the present study, it could be argued that enzyme activity could have been restored to 100% with the other particles prepared by either method and incubated for longer than 120 min. It does point to a probability that with time, the nanoparticles aggregate and dissociate from the enzyme, restoring its complete activity back.

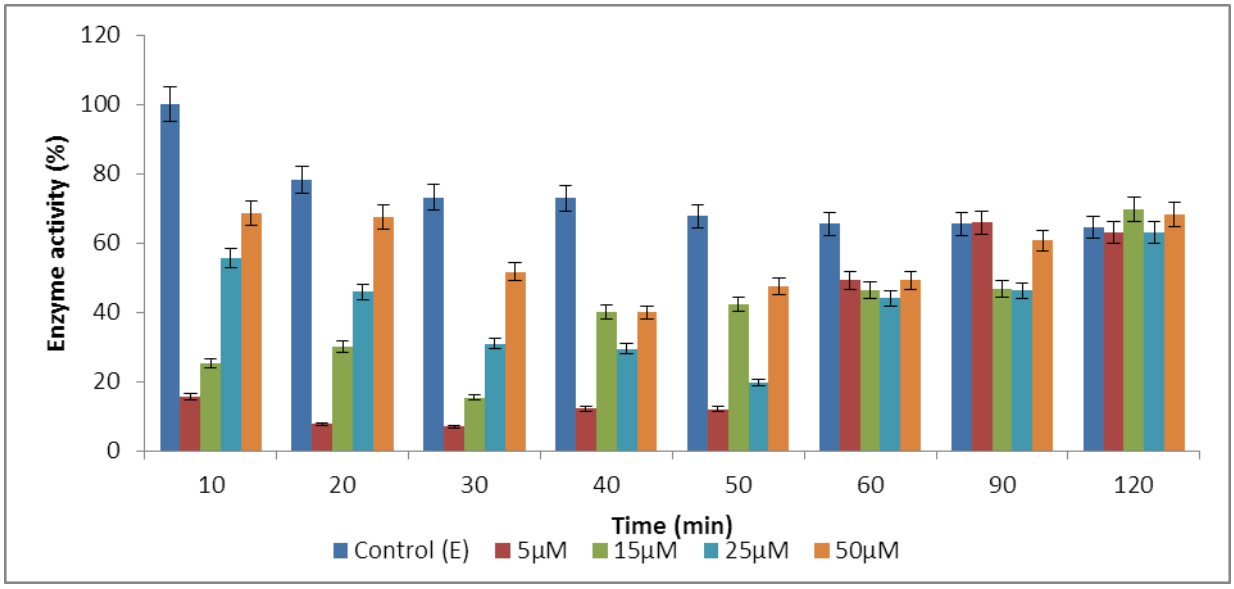

Figure 5.5(a): The nNOS inhibitory effect of silver nanoparticles (borohydride method)

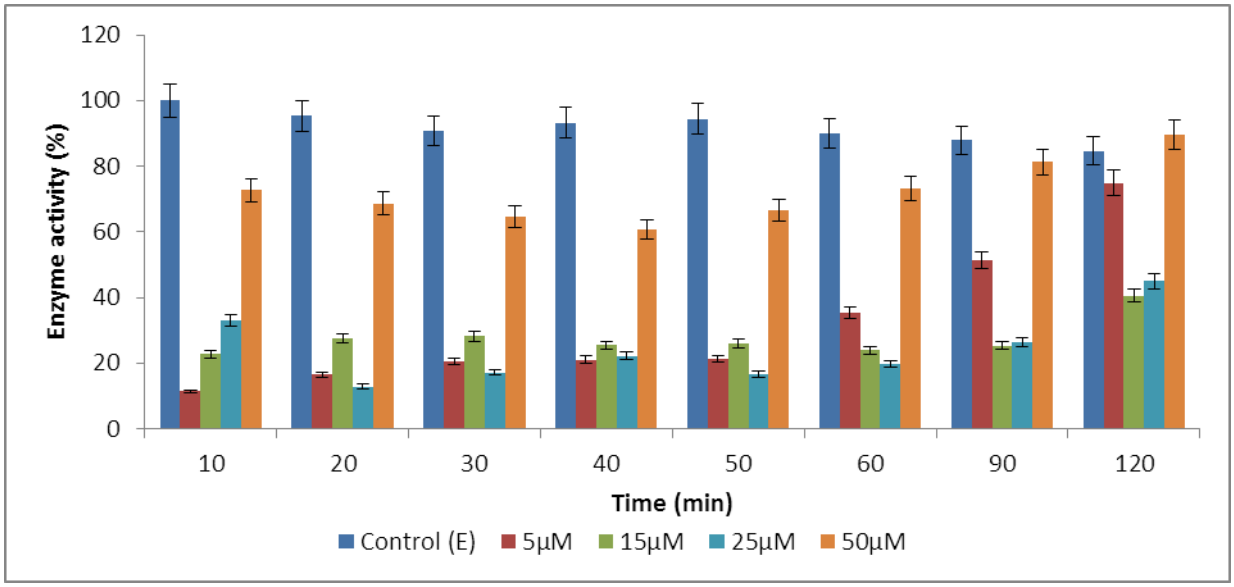

Figure 5.5(b): The nNOS inhibitory effect of gold nanoparticles (borohydride method)

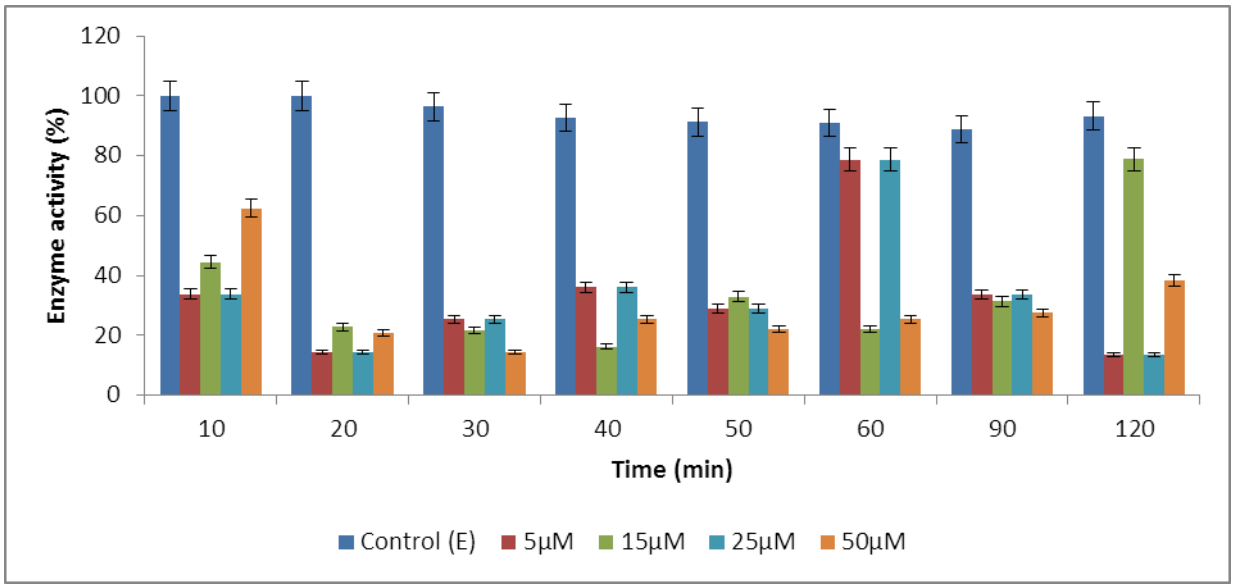

Figure 5.5(c): The nNOS inhibitory effect of silver nanoparticles (citrate method)

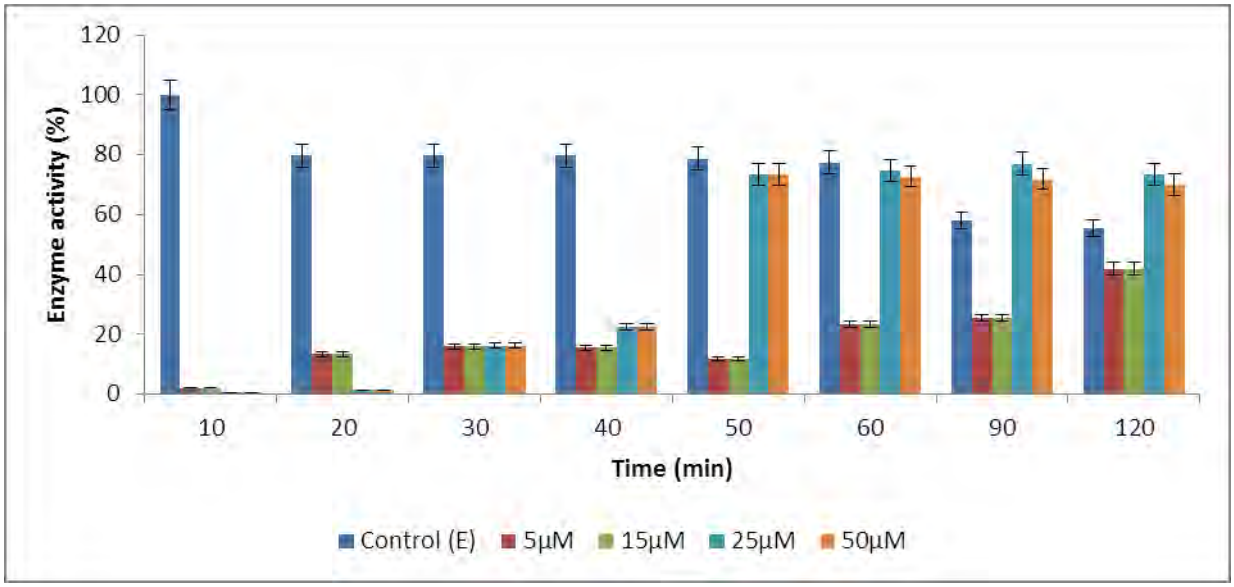

Figure 5.5(d): The inhibition of nNOS by gold nanoparticles (citrate method)

Moreover, the characteristic inhibition observed was due to the association of both nanoparticle enzyme complexes. As the nanoparticle became bound to nNOS, it inhibited the activity of the enzyme and the fluctuations in the activity of nNOS over time were due to the possible association between nanoparticle and enzyme which resulted in inhibition and dissociation which resulted in decreased inhibition.

5.5.3. Fluorimetric analysis

Generally, a greater K_{SV} means the greater quenching and ease of accessibility to fluor molecules (Nguyen, 2003). It was observed that the K_{SV} determined from the plots by the interaction of the purified nNOS with gold and silver nanoparticles (see Figure 5.6(a) and Figure 5.6(b) was almost the same (see Table 5.4 below). Thus, the highest K_{SV} value of 0.01092 µM from the estimated gold nanoparticles indicated that these nanoparticles had the greatest quenching ability and were easily accessible to the fluor molecules (see Figure 5.6(a) below).

Calculations of Θ were limited to gold nanoparticles as shown in Table 5.4 below. The fraction of tryptophans (TRP) near the enzyme surface (Θ) was determined as the reciprocal of the y-intercept (see Figure 5.6(a) and Figure 5.6(b) below). The parameter Θ is generally dependent on the polarity of the solvent. Thus, the nanoparticles induced a conformational change in nNOS, bringing a TRP residue to the surface of the enzyme (Θ = 1.5) for gold nanoparticles (see Table 5.4 below) as opposed to the binding of nanoparticles to the enzyme

where approximately five tryptophan residues were exposed on the enzyme surface (Θ ≈ 5), and respective values for Kd were (108.3 µM; 108.3 µM).

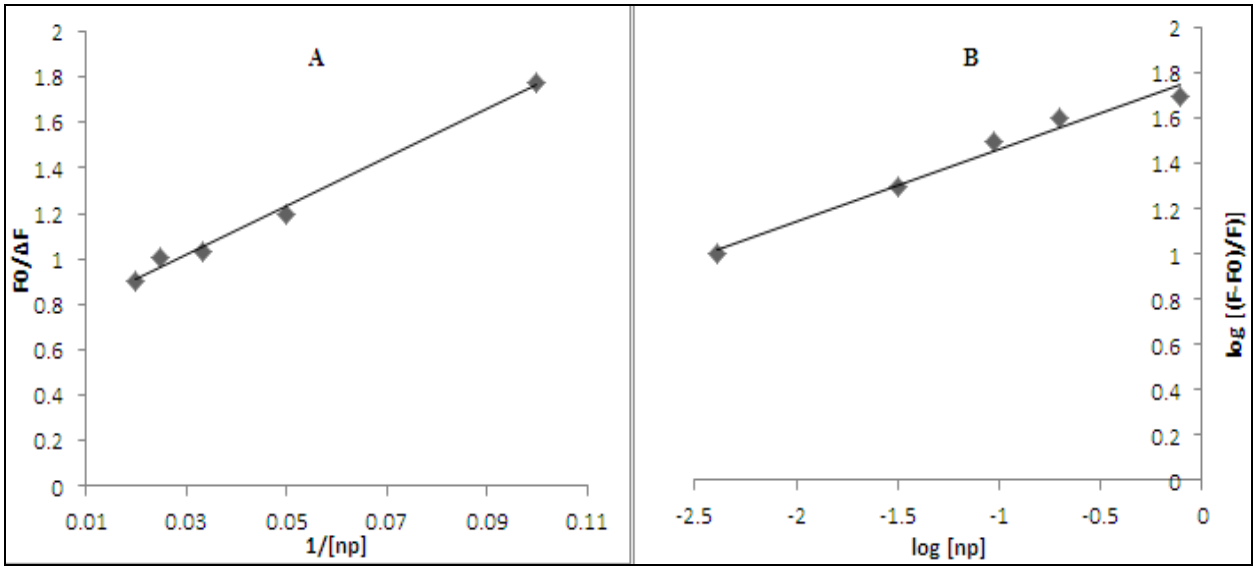

Figure 5.6(a): Spectrofluorimetric plots to determine fluorescence quenching constants of nNOS treated with silver nanoparticles (citrate method, A: Stern Volmer plot, B: Hill plot

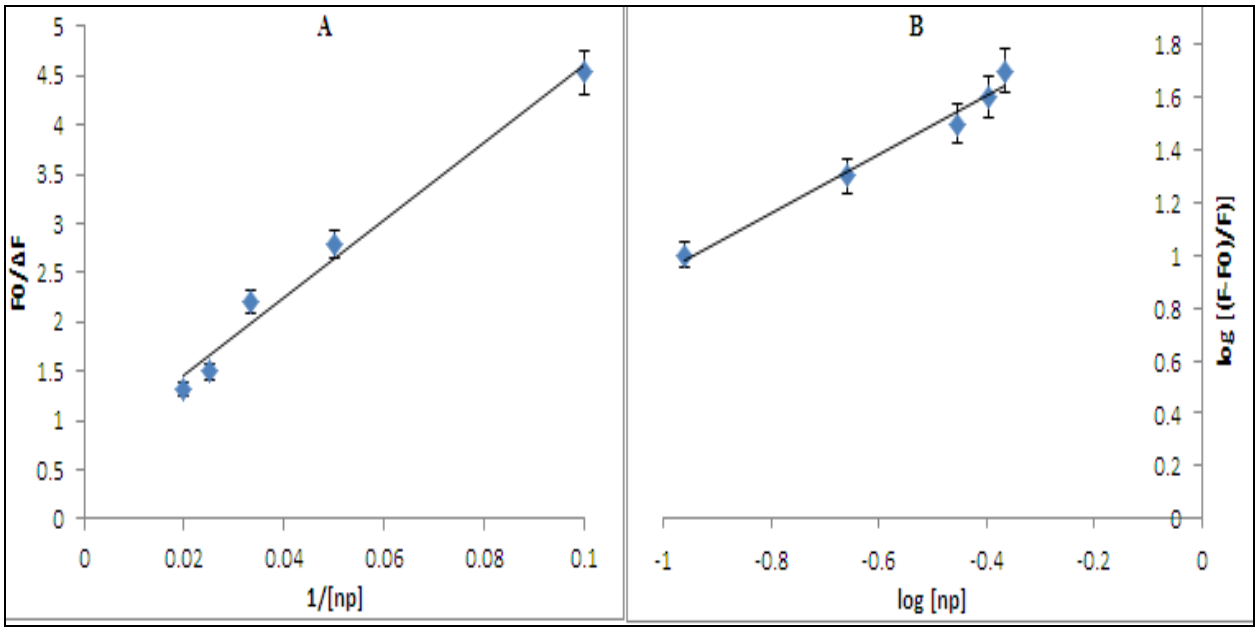

Figure 5.6(b): Spectrofluorimetric plots to determine fluorescence quenching constants of nNOS treated with gold nanoparticles (citrate method), A: Stern Volmer plot, B: Hill plot

Table 5.4: Constants from the interaction nNOS with metallic nanoparticles calculated from Hill plot and Stern –Volmer plot.

Parameter	Ag nanoparticles (citrate)	Au nanoparticles (citrate)
n	1	1
Ka($\mu M)^{-1}$	0.0092	0.009
Kd(μM)	108.3	108.3
Ksv($\mu M)$	0.0084	0.01092
θ	5.38	1.5

5.5.4. TEM analysis

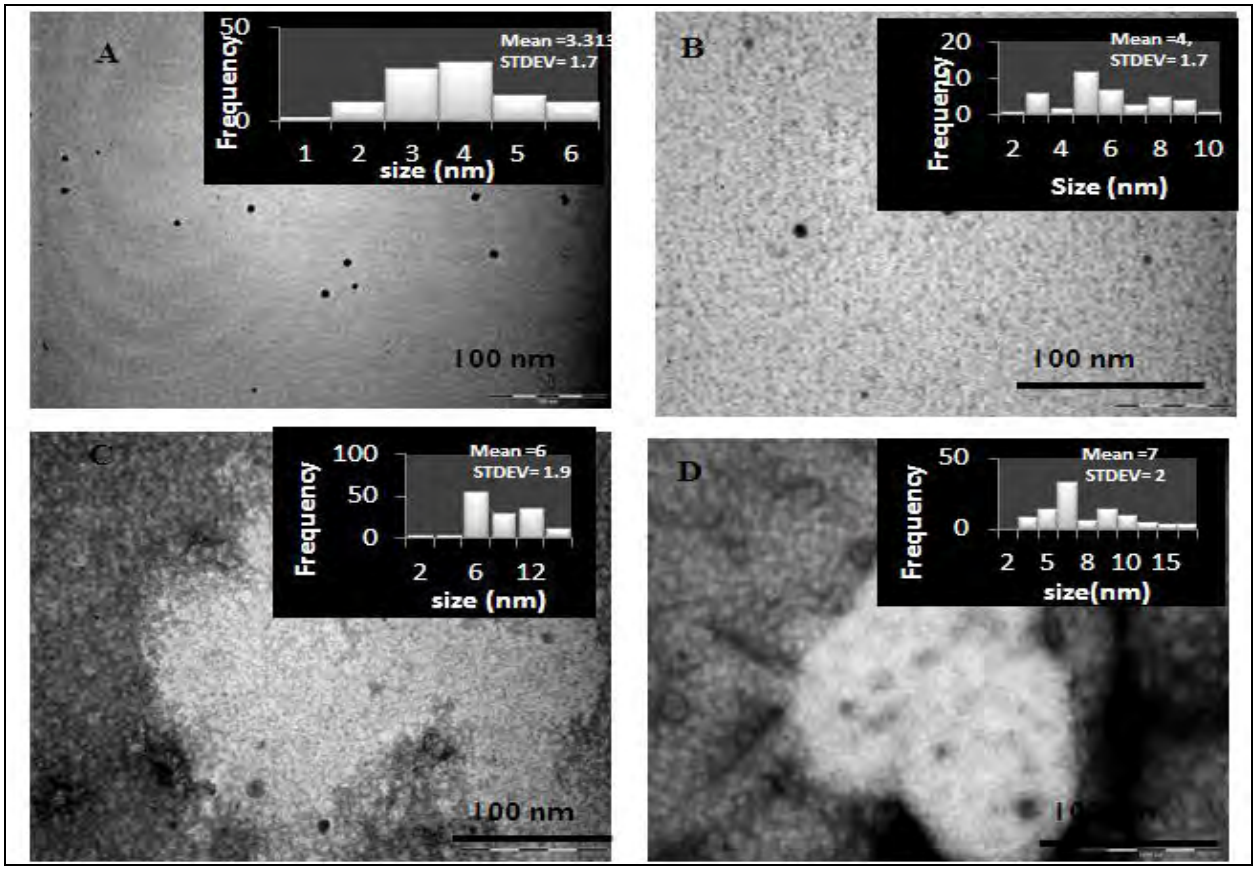

Figure 5.7: Transmission electron microscopy views of: (A) gold nanoparticles alone (B) nNOS with gold nanoparticles [30min incubation] (C) nNOS with gold nanoparticles [60 min incubation] (D) nNOS with gold nanoparticles [120 min incubation]

At time zero before any incubation of enzyme with nanoparticles, the TEM images showed nanoparticles alone with an average size of 3 nm (see Figure 5.7A above). Within the first 30 minutes of incubation with the enzyme the nanoparticles appeared to increase in size (see Figure 5.7 (B.C, D above), and even more so with time. These observations also substantiate earlier results that showed nNOS was inhibited at a nanoparticle concentration as low as 5 μM (see Figure 5.5(a-d) above).

5.6. Conclusion

It was shown both silver and gold nanoparticles competitive inhibited nNOS. The degree of inhibition was measured by the parameter K_i. Results showed that nanoparticles prepared by the citrate method inhibited nNOS to a greater degree as reflected by low K_i value of 1.7 μM (silver) and 0.2 μM (gold) compared to the higher K_i values of borohydride 9 μM (silver) and 5.7 μM (gold). The characteristic inhibitions observed initially were due to the association of the respective nanoparticle with the enzyme. With time, however, it was assumed that the nanoparticles aggregated and dissociated from the enzyme, allowing the original activity of the enzyme to be restored. This suggests that the nanoparticles were in no longer able to bind to the enzyme. Fluorescence results, on the other hand, indicated the K_{SV} of silver nanoparticles were similar gold nanoparticles (0.0084 μM and 0.01092 μM) and that nanoparticles had a substantial quenching ability. This indicates that fluorescence was only due to internal quenching rather than the interplay of other fluors in solution which may result in external quenching.

CHAPTER 6: GENERAL SUMMARY, CONCLUSION AND FUTURE PESPECTIVES

6.1. General summary

Neuronal nitric oxide synthase (nNOS) catalyzes the oxidation of L-arginine to form L-citrulline and nitric oxide. Depending on the catalytic mechanism and on the levels of arginine in the brain, nNOS could be an effective diagnostic marker in the onset of AD (Packer, 1994). In this study, the neuronal isoform of nitric oxide synthase (NOS) was purified and biochemically characterised. Bovine brain was an excellent and convenient source of the enzyme as the neuronal isoform of the enzyme is widely distributed in general tissue cells. However, high concentrations and corresponding high activity is normally found in the cerebella regions of bovine brain. The study used the bovine brain since it was homologous to the human brain based on the 90% amino acids sequence identity between the two sequences. However, nNOS has also been characterised in 28 regions of human, bovine and rat brain according to previous literature (Blum-Degan *et al*., 1999). These regions include the cortical and subcortical areas, basal ganglia, the limbic system, thalamus and brainstem. It was however difficult to estimate the exact region of localization of nNOS within the brain. Consequently, the entire brain was homogenized for the present study.

With regard to characterisation and application of the enzyme, the purification was unsuccessful using ammonium sulphate $(NH_4)_2SO_4$ precipitation method. There was fold 0.6 reduction in purity. However, poly ethylene glycol (PEG) 20 000 managed to increase the fold to 0.8. Eventually, a single purification step was performed, anion exchange chromatography on DEAE- Sephacel. However, it was only after dialysis of the pooled fractions that 10 % yield and 0.43 fold purification was produced with the specific activity of 0.09 U/mg. This has clearly indicated that purification of nNOS was not successfully compared to the previous study by Padayachee *et al*., 2011 where the nNOS was purified using DEAE-Sepharose anion-exchange with a 38% yield and 3-fold recovery. The purified nNOS was shown to be a dimeric protein consisting of two subunits approximately (75 kDa, respectively). The optimum pH and temperature of nNOS from bovine brain were determined to be 7.5 and 50 °C, respectively, with a half-life of 100 min under these conditions.

AD is characterised by intracellular appearance of neurofibrilary tangles, and synaptic and neuronal loss; and extracellular accumulation of amyloid-β (Aβ) peptide in senile plaques

(De Felice *et al*., 2004). Senile plaques are surrounded by astrocytes, which also function to store reserve arginine in brain tissue. This brings a potential connection between brain arginine content and the increase of nitric oxide (Haas *et al.*, 2002). It was significant that nanoparticles bind to nNOS and inhibit the enzyme to varying degrees with their respective K_i values between silver 1.4 μM and gold 0.2 μM. The smaller size (± 4nm) nanoparticles appeared to inhibit the enzyme the most at 5 μM and 15 μM. Moreover, the interaction of the various size nanoparticles with nNOS further showed an association–dissociation, suggesting that the enzyme behaved as a catalyst and converted the nanoparticle into a form which could no longer bind. However, the nanoparticles became dissociated from the enzyme allowing the original activity of the enzyme to be restored. This suggested that the nanoparticles were no longer able to bind to the enzyme and perhaps, the particles had aggregated, thereby changing their shape. To our knowledge, there are no studies in literature showing the inhibition of nNOS with nanoparticles.

Transmission electron microscopy (TEM), on the other hand, described the morphology of nanoparticles. It revealed that different nanoparticles are produced in different sizes over a given time because of this association–dissociation described above. Fluorescence quenching showed that nanoparticles had a similar degree of quenching and they were easily accessible to fluor molecules with gold K_{SV} value of 0.01092 μM and silver d K_{SV} value of 0.0084 μM , respectively.

6.2. Conclusions

In this study, a procedure was developed for the successful isolation and purification of neuronal nitric oxide synthase from crude bovine brain extract. The results show that nNOS is capable of metabolizing the substrate arginine. However, it is evident that there is a need for further study that will look into the regulation of nNOS with specific focus on arginine and citrulline levels in the brain. Such study would be of great significance as it will contribute to our understanding of why high levels of arginine and low levels of citrulline were found in the cerebrospinal fluid of Alzheimer‟s patients. The results also confirmed that smaller sized nanoparticles have greater impact compared to the big sized nanoparticles. Both silver and gold nanoparticles inhibited the activity of nNOS extensively because they bound strongly to the inhibitor site on the enzyme and they were more in contact with fluorophores on the enzyme, which were involved in energy transfer and conformational change. It is therefore hoped that a broader classification of amyloid fibrils will emerge and the traditional

techniques will give way to novel techniques and new discoveries in the field of nanoparticles.

6.3. Future perspectives

Current treatment of Alzheimer‟s is largely symptomatic with different pharmacological drugs designed to temporarily suppress these debilitating symptoms. Therefore, it is vital to identify suitable enzyme biomarkers like nNOS, for the concentration level of the enzyme relative to its substrate concentration level may allow for a less invasive and more accurate diagnosis, as well as serve as a predictor of future Alzheimer disease progression and treatment response. There is a need for another study that will investigate the mechanism of binding of nanoparticles to nNOS by the use of site-directed mutagenesis to remove specific cysteine residues which are thought to be the inhibiting site for nanoparticles; to evaluate whether protein will be inhibited after incubation with nanoparticles if there are no cysteine residues. Atomic force microscopy (AFM) which is a novel technique could also be employed to study nanoparticle binding. The assumed inhibition and binding by these proposed techniques could be elaborated using molecular modelling programmes such nanoscale molecular dynamics (NAMD) and fluorescence resonance energy transfer (FRET) to confirm results.

REFERENCES

Alderton, W.K., Cooper C.E. and Knowles R.G. (2001). Nitric oxide synthases: structure, function and inhibition. *Biochemistry Journal.,* **357**:593-615.

Andreescu D., Eastman C., Balantrapu K., Goia D.V. (2007). A simple route for manufacturing highly dispersed silver nanoparticles. *Journal of Materials Resources.*, **22**:2488–2496.

Andreescu S, Sadik O.A, McGee D.W. (2005). Effect of natural and synthetic estrogens on A549 lung cancer cells: correlation of chemical structures with cytotoxic effects. *Chemical Research Toxicology.*, **18**:466-74.

Andrew P.J. and Mayer B. (1999). Enzymatic function of nitric oxide synthases. *Cardiovascular Research.,* **43**: 521–531.

Archibald R.M. (1944). Determination of citrulline and allantoin and demonstration of citrulline in blood plasma. *Journal of Biological Chemistry.*, **156**: 121-142.

Barbu D., Mert I., Kruger M., Bahado-Singh R.O. (2009) Evidence of fetal central nervous system injury in isolated congenital heart defect: microcephaly at birth. *American Journal of Obstetrics & Gynecology.*, **201** (1):118-119.

Bazylinski A.B. and Frankel B.R. (2004). Magnetosome formation in Procayotes, *Nature Reviews Microbiology*,. **2**: 213-230.

Banerjee J. and Ghosh S. (2004). Bax increases the pore size of rat brain mitochondrial voltage-dependent anion channel in the presence of Bid 2. *Biochemical and Biophysical Research Communications.*, **323**:310-314.

Behan N., Birkinshaw C., Clarke N. (2001). Poly n-butyl cyanoacrylate nanoparticles: a mechanistic study of polymerization and particle formation. *Biomaterials.*, **22**: 1335– 1344.

Billecke S. S., Draganov D. I., Morishima Y., Murphy P. J., Dunbar A. Y., Pratt W. B. and Osawa Y. (2004). The role of hsp90 in heme dependent activation of apo-neuronal nitric-oxide synthase. *Journal of Biological Chemistry.,* **279**: 30252–30258.

Blum-Degan D., Heinemann T., Lan J., Pedersen V., Leblhuber W.P., Riederer P. and Gerlach M. (1999). Characterisation and regional distribution of nitric oxide synthase in the human brain during normal ageing. *Brain Research.*, **834**: 128-135.

Boissel J.P, Schwarz P.M. and Forstermann U. (1998). Neuronal-type NO synthase: transcript diversity and expressional regulation. *Nitric Oxide***, 2**:337–349.

Bondy C.S. (2011). Nanoparticles and Colloids as Contributing Factors in Neurodegenerative Disease. *International Journal of Environmental Research and Public Health.*, **8**(6):2200-2211.

Bonifacino J. S. (2004). The GGA proteins: adaptors on the move. *Nature Reviews Molecular Cell Biology.*, **5**:23-32.

Bonnerjera J., Oh S., Hoare M. and Dunhill P. (1986). The right step at the right time. *Biotechnology.*, **4:** 954-958.

Bonsak J. (2010). Chemical synthesis of silver nanoparticles for light trapping applications in silicon solar cells. Maters Thesis, Faculty of Mathematics and Natural Sciences University of Oslo, Norway. 55-65.

Bradford, M. (1976). A Rapid and Sensitive Method for the Quantitation of Microgram Quantities of Protein Utilizing the Principle of Protein-Dye Binding. *Analytical Biochemistry*., **72**:248-254.

Brambilla C., Fieve F., Jeanmart M., de Fraipont F., Lantuejoul,S., Frappat V., Ferretti G., Bricho, P.Y. and Moro-Sibilot D. (2003). Early detection of lung cancer: role of biomarkers. *European Respiratory Journal.,* **21**:36s-44s.

Brambilla D., Nicolas J., Le Droumaguet B., Andrieux K., Marsaud V., Couraud P.O. and Couvreur P. (2010). Design of fluorescently tagged poly(alkyl cyanoacrylate) nanoparticles for human brain endothelial cell imaging. *Chemical Communications.*, **46**:2602–2604.

Bredt D.S., (1999). Endogenous nitric oxide synthesis: Biological functions and pathophysiology. *Free Radical Research*., **31**: 577-596.

Bredt D.S, Snyder S.H. (1990). Isolation of nitric oxide synthetase, a calmodulin-requiring enzyme. *Proceedings of the National Academy of Sciences of the United States of America,* **87**:682– 685.

Brucki S.M.D. (2009). Does prevention for Alzheimer's disease exist? *Dementia and Neuropsychologia*., **3**(3):209-213.

Bronich T.K., Bontha S., Shlyakhtenko L.S., Bromberg L., Hatton T.A. and Kabanov A.V. (2006). Template-assisted synthesis of nanogels from pluronic-modified poly (-acrylic acid). *Journal of Drug Targeting.,* **14**: 357–366.

Burnette W.N. (1981). Western blotting': electrophoretic transfer of proteins from sodium dodecyl sulfatepolyacrylamide gels to unmodified nitrocellulose and radiographic detection with antibody and radioiodinated protein A. *Analytical Biochemistry.,* **112**:195-203.

Calabrese V., Mancuso C., Calvani M., Rizzarelli E., Butterfield D.A, Stella A.M. (2007). Nitric oxide in the central nervous system: neuroprotection versus neurotoxicity. *Nature Reviews Neuroscience.,* **8**:766–775.

Calvo P., RemunanLopez C., VilaJato J.L. and Alonso M.J. (1997). Novel hydrophilic chitosan-polyethylene oxide nanoparticles as protein carriers, *Journal of Applied Polymer Science.*, **63**:125–32.

Cantoni O., Palomba L., Musci G., Ascenzi P., Fioravanti E., Persichini T., Colasanti M. and Venturini G. (2002). β–amyloid inhibits NOS activity by subtracting NADPH availability. *FASEB Journal.*, **10**: 1096.

Cao G. (2004). Nanostructures and Nanomaterials. *Imperials College Press*, World Scientific Publishing Co. Pte. Ltd.

Carpenter J.F., Pikal M.J., Chang B.S. and Randolph T.W. (1997). Rational design of stable lyophilized protein formulations: some practical advice. *Pharmaceutical Research.,* **14**: 969-975.

Castellani R.J., Shah R.S., Lee H.G., Xiongwei Z., Perry G., Smith M.A. (2008). Current approaches in the treatment of Alzheimer‟s disease. *Biomedical and Pharmacology Journal.,* **62**: 199-207.

Chamow S. and Ashkenazi A. (1999). Antibody Fusion Proteins (eds.*), John Wiley and Sons Inc. Publisher*, New York: 53-110.

Chekhonin V.P., Zhirkov Y.A., Gurina O.I. Dmitrieva T.B., Shepeleva I.I., Ryabukhin and I.A., Babich GN. (2005). Pegylated immunoliposomes directed against brain astrocytes. *Drug delivery.*, **12**: 1–6.

Cheon J. and Horace G. (2009). Inorganic nanoparticles for biological sensing, imaging and therapeutics. *Journal of Materials Chemistry.*, 1**9**:6249- 6250.

Che Y.H., Tamatani M. and Tohyama M. (2000). Changes in mRNA for post-synaptic density-95 (PSD-95) and carboxy-terminal PDZ ligand of neuronal nitric oxide synthase following facial nerve transection. *Molecular Brain Research.*, **76**: 325–335.

Chen J., Saeki F., Wiley BJ. Cang H., Cobb M.J., Li Z.Y., Au L., Zhang H., Kimmey M.B., Li X.D and Xia Y. (2005). Gold nanocages: bioconjugation and their potential use as optical imaging contrast agents. *Nano Letters.*, **5**:473–7.

Chen M.P., Kuroishi K. and Kitamoto Y., (2005). Magnetic properties and microstructure of isolated Fe-Pt nanoparticle-monolayer assembly by protective coating. *IEEE Transactions on Magnetics*, **41**:3376–3378.

Chiu T.C., Tu W.C. and Chang H.T. (2008). *Electrophoresis.,*. **29**:433-440.

Chopra N., Gavalas V.G., Hinds B.J. and Bachas L.G. (2007a) Functional one-dimensional nanomaterials: applications in nanoscale biosensors. *Analytical Letters.*, **40**:2067–2096.

Chun-Xia L., Dong-Ya Z., (2011). Research progress on neurobiology of neuronal nitric oxide synthase. *Neuroscience Bulletin*., **27**(1): 23-35.

Citron M. (2002). Alzheimer"s disease: treatments in discovery and development. *Nature Neuroscience Supplement.*, **5**: 1055-1057.

Cornish-Bowden A., Ca´rdenas M.L. (2000). From genome to cellular phenotype – a

role for metabolic flux analysis. *Nature Biotechnology.,* **18**:267 – 268.

Cornish-Bowden A. (2004). Fundamentals of enzyme kinetics. London, UK: *Portland Press*.

Cummings J.L. (2003). The neuropsychiatry of Alzheimer‟s disease and related dementias. Taylor and Francis. London and New York.

Craig-Schapiro R., Fagan A.M. and Holtzman D.M. (2009). Biomarkers of Alzheimers disease. *Neurobiology of Disease.,* **35**: 128-140.

Cras P., Kawai M., Lowery D., Gonzalez-DeWhitt P., Greenberg B. and Perry G. (1991). Senile plaque neurites in Alzheimer disease accumulate amyloid precursor protein. *Proceedings of the National Academy of Sciences of the United States of America*., **88**:7552–7556.

Das M., Saxena N. and Dwivedi P.D. and Autier C. (2009). Emerging trends of nanoparticles application in food technology: Safety paradigms. *Nanotoxicology.*, **3**:10-18.

Denis A., Brambati N., Dessauvages B., Guedj S., Ridoux C. and Meffre N. (2008).

Molecular weight determination of hydrolyzed collagens. *Food Hydrocolloids.*, **22**: 989–994.

Deutscher M.P. (1990). Methods in Enzymology-Guide to Protein Purification. Academic Press Inc. San Diego, California. **182**: 38-49.

De Felice F.G. and Ferreira S.T. (2002). Beta-amyloid production, aggregation, and clearance as targets for therapy in Alzheimer‟s disease. Cell. *Molecular Neurobiology*., **22**: 545-563.

De Felice F.G., Vieira M.N.N., Saraiva L. M., Figueroa-V. J. D., Garcia-Abreu J., Liu Y., Chang L., Klein W. L. and Ferreira S.T. (2004) Targeting the neurotoxic species in Alzheimer‟s disease: inhibitors of Aß oligomerization. *The Journal of the Federation of American Societies for Experimental Biology.,* 1**8**: 1366 – 1372.

Deutscher M.P. (1990). Methods in Enzymology-Guide to Protein Purification. *Academic Press New York.*, **182**:38-49.

De Meyer G.R.Y., Martinet W., Van De Parre T.J.L., Herman A.G., Bult H., Kockx M.M. and Jans D.M. (2006). Processing of amyloid precursor protein as a biochemical link between Atherosclerosis and Alzheimer disease. *Cardiovascular & Haematological Disorders-Drug Target*s., **6**: 21-34.

Dugan L.L., Turetsky D.M., Du C., Lobner D., Wheeler M., Almli C.R., Shen C.K., Luh T.Y., Choi DW., Lin T.S. (1997). Carboxyfullerenes as neuroprotective agents. *Proceedings of the National Academy of Sciences of the United States of America.,* **94**:9434 –9439.

Elechiguerra J.L., Burt J.L., Morones J.R., Bragado A.C., Gao X., Lara H.L. and Yacaman, M.J. (2005). Interaction of silver nanoparticles with HIV-I. *Journal of Nanobiotechnology,* **3**: 6- 16.

English B., Min W., van Oijen A.M., Lee K.T., Luo G., Sun H., Cherayil B.J., Kou S.C. and Xie X.S. (2006). Ever-Fluctuating Single Enzyme Molecules: Michaelis–Menten Equation Revisited. *Nature Chemical Biology.,* **2**:87–94.

Eustis S and El-Sayed M.A. (2006). Why gold nanoparticles are more precious than pretty gold: Noble metal surface plasmon resonance and its enhancement of the radiative and nonradiative properties of nanocrystals of different shapes. *Chemical Society Reviews.*, 3**5**:209–217.

Ehehalt R., Michel B., Pietri, D.D., Zacchetti D., Kai Simons K. and Kellera P. (2002), Splice variants of the b-site APP-cleaving enzyme BACE1 in human brain and pancreas. *Biochemistry and Biophysics Research Communications.*, **203**:30-37.

Eugenin E.A., King J.E., Nath A., Calderon T.M., Zukin R.S., Bennett M.V.L. and Berman J.W. (2007). HIV-tat induces formation of an LRPPSD- 95-NMDAR-nNOS complex that promotes apoptosis in neurons and astrocytes. *Proceedings of the National Academy of Sciences of the United States of America*., **104**:3438–3443.

Fawole O.A.; Amoo S.O., Ndhlala A.R., Light M.E., Finnie J.F., Van Staden J. (2010). Antiinflammatory anticholinesterase, antioxidant and phytochemical properties of medicinal plants used for pain-related ailments in South Africa. *Journal of Ethnopharmacology*., **127**: 235-241.

Fazil M., Baboota S.S., Sahni J.K. and Ali J. (2012). Nanotherapeutics for Alzheimer"s disease (AD): Past, present and future. *Journal of Drug Targeting,* **20** (2): 97-113.

Firestein B.L., and Bredt D.S. (1999). Interaction of neuronal nitric-oxide synthase and phosphofructokinase-M. *Journal of Biological Chemistry*., **274**:10545-10550.

Foy M.R., Xu J., Xie X., Brinton R.D., Thompson R.F. and Berger T.W. (1999) 17ß-estradiol enhances NMDA receptor-mediated EPSPs and long-term potentiation. *Journal. Neurophysics*., **81**:925–928

Friedrich I., Reichl S. and Muller-Goymann C.C. (2005). Drug release and permeation studies of nanosuspensions based on solidified reverse micellar solutions (SRMS). *International Journal of Pharmacy.,* **305**: 167–175.

Freifelder D. (1976). Physical Biochemistry: applications to Biochemistry and Molecular biology. *W.H. Freeman and Company*, United States of America.

Frost D., Meechoovet B., Wang T., Gately S., Giorgetti M., Shcherbakova I. and Dunckley T. (2011). β-Carboline Compounds, Including Harmine, Inhibit DYRK1A and Tau Phosphorylation at Multiple Alzheimer's Disease-Related Sites. *PLoS One*, **6**:6 (5):e19264.

Giorgio A., Santelli L., Tomassini V, Bosnell R, Smith S., Stefano D. and Johansen-Berg. H. (2010). Age-related changes in grey and white matter structure throughout adulthood. *Neuroimage*. **51**(2-3): 943–951.

García-Barrasa J., López-de-Luzuriaga J.M. and Monge M (2011).Silver nanoparticles: synthesis through chemical methods in solution and biomedical applications. *Central European Journal of Chemistry*, **9**(1):7-19.

Giraldez R.R., Zweier J.L. (1998). An improved assay for measurement of nitric oxide synthase activity in biological tissues. *Analytical Biochemistry,* **261** :29–35.

Goedert M, Spillantini MG (2006). A century of Alzheimer's disease. *Science.,* **314**(5800):777-81

Ghosh P.S, Kim C.K., Han G., Forbes N.S. and Rotello V.M. (2008). Efficient gene delivery vectors by tuning the surface charge density of amino acid-functionalized gold nanoparticles. *ACS Nano*, **2**:2213–2218.

Guzmán M.G., Dille J. and Godet S. (2008). Synthesis of Silver Nanoparticles by chemical Reduction Method and their antibacterial activity. *World Academy of Science: Engineering and Technology*., **43**: 357-364.

Haag M.D., Hofman A., Koudstaal P.J., Stricker B.H. and Breteler M.M. (2009) Statins are associated with a reduced risk of Alzheimer disease regardless of lipophilicity. The Rotterdam Study. *Journal* of *Neurology*, *Neurosurgery and Psychiatry.,* **80**: 13–17.

Hafiz A. (2005). Preparation of Buffer for Protein Extraction in Principles and Reaction of Protein Extraction, Purification and Characterisation. *CRC Press USA*., 1-33.

Harlow E. and Lane D. (1988). Ammonium sulfate precipitation in Antibodies: A Laboratory Manual. *Cold Spring Harbor Laboratory; New York*., 298-299.

Haas J., Storch-Hagenlocher B., Biessmann A. and Wildemann B. (2002). Inducible nitric oxide synthase and argininosuccinate synthetase: co-induction in brain tissue of patients with Alzheimer‟s dementia and following stimulation with b-amyloid 1–42 in vitro. *Neuroscience Letters.,* **322**:121–125.

Hiki K., Hattori R., Kawai C. and Yui Y. (1992). Purification of insoluble nitric oxide synthase from rat cerebellum. *Journal of Biochemitry.*, **11**:556-558.

He C., Yu Y., Hu X. and Larbot, A. (2002). Influence of silver doping on photocatalytic activity of titania films. *Applied Surface Science.*, **200**:239-247.

Humberto H.L., Nilda V. A., Carmen L., Turrent I. and Rodríguez C. (2010). Bactericidal effect of silver nanoparticles against multidrug-resistant bacteria . *World Journal of Microbiology and Biotechnology.,* **26**:615–621.

Hyuk I.M.S., Jeong U. and Xia Y. (2005). Polymer hollow particles with controllable holes in their surfaces. *Nature Materials.,* **4**: 671–675.

Iriti M., Castorina G., Vitalini G., Mignani I., Soave C., Fico G. and Faoro F. (2010) Chitosan-induced ethylene-independent resistance does not reduce crop yield in bean plants. *Biological Control.*, **54**: 241–247.

Ivana S. and Blanka V. (2001).Two-dimensional Assembling of Au Nanoparticles Mediated by Tetrapyridylporphine Molecules. *Nano Letters*., **2**: 2.

Iwanaga K., Wakabayashi K., Yoshimoto M., Tomita I., Satoh H., Takashima H., Satoh A., Seto M., Tsujihata M. and Takahashi H. (1999). Lewy body-type degeneration in cardiac plexus in Parkinson‟s and incidental Lewy body diseases. *Neurology.,* **52**: 1269-1271.

Jaffrey S.R., Snowman A.M., Eliasson M.J., Cohen N.A. and Snyder S.H. (1998). CAPON: a protein associated with neuronal nitric oxide synthase that regulates its interactions with PSD95. *Neuron.,* **20**:115- 124.

Jhala S. and Hazell A.S. (2011). Modeling neurodegenerative disease pathophysiology in thiamine deficiency; consequences of impaired oxidative metabolism. *Neurochemistry International*, **58** :248-260.

Jing Yi., Laura L., Horky., Avi L., Friedlich, Ying Shi, Jack T. Rogers and Xudong Huang (2009). L-Arginine and Alzheimer's Disease. *International Journal of Experimental Pathology.*, **2**(3): 211-238.

Jomova K., Vondrakova D., Lawson M., Valko M. (2010). Metals, oxidative stress and neurodegenerative disorders. *Molecular and Cellular Biochemistry.*, **345**: 91-104.

Kabanov A.V. and Gendelman H.E. (2007). Nanomedicine in the diagnosis and therapy of neurodegenerative disorders. *Progress in Polymer Science*., **32** (8–9): 1054–1082.

Karim M.M., Lee H.S., Kim Y.S., Bae H.S. and Lee S.H. (2006). Analysis of salicylic acid based on the fluorescence enhancement of the arsenic (III)-salicylic acid system. *Analytica Chimica Acta.*, **576**(1):136–139

Kajava A., Squire J.M. and Parry D.A.D. (2006). Fibrous proteins: amyloids, prions and beta proteins. *Advances in Protein Chemistry.*, **73**: 1-320.

Kemp W.M. and Boynton W.R. (1980). Influences of biological and physical processes on dissolved oxygen dynamics in an estuarine system: implications for measurement of community metabolism. *Estuarine and Coastal Marine Science.,* **11**:407–431.

Khan A. (2008). Preparation and characterisation of magnetic nanoparticles embedded in microgels. *Materials Letters.,* **62**:898-902.

Kowshik M., Deshmukh N., Vogel W., Urban J., Kulkarni S.K. and Paknikar K.M. (2002). Microbial synthesis of semiconductor CdS nanoparticles, their characterisation and their use in the fabrication of an ideal diode. *Biotechnology and Bioengineering.,* **78** :583- 588.

Krutyakov Y.A., Kudrinskiy Y.A., Olenin A.Y., Lisichkin, G.V. (2008). Synthesis and properties of silver nanoparticles: advances and prospects. *Russian Chemical Reviews.*, **77** (3):233-257.

Lakos Z., Szarka A., Koszorfis L and Somogyi B. (1995). Quenching-resolved emission anisotropy: a steady state fluorescence method to study protein dynamics. *Journal of Photochemistry and Photobiology.,* **27**:55-60.

Laemmli U.K. (1970). Cleavage of structural proteins during the assembly of the head of bacteriophage T4. *Nature*, **227**: 680-685.

Layne E. (1957). Methods in Enzymology *Journal of Biological Chemistry.,* **167**:447-454

Li H., Flinspach M.L., Igarashi J., Jama J., Yang W., Gomez-Vidal J.A., Litzinger E.A., Huang H., Erdal E.P., Silverman R.B. and Poulos T.L. (2005). Exploring the binding conformations of bulkier dipeptide amide inhibitors in constitutive nitric oxide synthases. *Biochemistry.*, **44**:15222–15229.

Luo X., Zhu D. (2011). Research progress on neurobiology of neuronal nitric oxide synthase. *Neuroscience bulletin.*, **27**(1):23-35.

Louzada, P.R., Paula Lima A.C., Mendonca-Silva D.L., Noel F., De Mello F.G. and Ferreira S.T., 2004. Aurine prevents the neurotoxicity of β-amyloid and glutamate receptor agonists: activation of GABA receptors and possible implications for Alzheimer`s disease and other neurological disorders. *FASEB Journal*., **18**: 511-518.

Moncada S. and Higgs.A. (1993). The L-Arginine-Nitric Oxide Pathway. *The New England Journal of Medicine.*, **329**: 2002-2012

Modi A., Feld J., Park Y., Kleiner D., Everhart J., Liang J., and Hoofnagle J. (2010). Increased caffeine consumption is associated with reduced hepatic fibrosis. *Hepatology*., **51**(1): 201–209.

Mora M., Sagrista M.L., Trombetta D., Bonina F.P., De Pasquale A. and Saija A. (2002). Design and characterisation of liposomes containing long-chain N-acylpes for brain delivery: penetration of liposomes incorporating GM1 into the rat brain. *Pharmaceutical Research.*, **19**: 1430–1438.

Morris J.C. (2006). Mild cognitive impairment is early-stage Alzheimer disease: Time to revise diagnostic criteria. *Archives of Neurology.*, **63**(1):15-16.

Morris M.C., Evans D.A., Bienias J.L., Tangney C.C., Bennett D.A., Wilson R.S., Aggarwal N. and Schneider J. (2003). Consumption of fish and n-3 fatty acids and risk of incident Alzheimer disease. *Archives of Neurology.,* **60**(7): 940-946.

Mukherjee P., Ahmad A., Mandal D., Senapati., S., Sainkar S.R., Khan., M.I., Ramani R., Parischa R., Kumar P.A.V., Alam M., Sastry M. and Kumar R. (2001). Bioreduction of AuCl by the fungus, Verticillium sp. and surface trapping of the gold nanoparticles formed. *Angewandte Chemie International Edition.*, **40**:3585- 3588.

Mackenzie J. D. and Bescher E. P. (2007). Chemical routes in the synthesis of nanomaterials using the sol-gel process. *Accounts of Chemical Research.*, **40** (9):810–818.

Mark S.J., Couto E.G., Abdo M. and Lehmann J. (2011). Fluorescence index as an indicator of dissolved organic carbon quality in hydrologic flow paths of forested tropical watersheds .*Biogeochemitry*, **105**:149–157.

Matyus L., Szo J. and Jenei A. (2006). Steady-state fluorescence quenching applications for studying protein structure and dynamics. *Journal of Photochemistry and Photobiology.,* Biology, **83**: 223-236.

Martinez-Ruiz A., Villanueva L., Gonzalez de Orduna C., Lopez-Ferrer D., Higueras M. A., Tarin C., Rodriguez-Crespo I., Vazquez J. and Lamas S. (2005). S-nitrosylation of Hsp90 promotes the inhibition of its ATPase and endothelial nitric oxide synthase regulatory activities. *Proceedings of the National Academy of Sciences USA*., 102:8525–8530.

Medina C., Santos-Martinez M.J., Radomski A., Corrigan O.I. and Radomski M.W. (2007). Nanoparticles: pharmacological and toxicological significance. *British Journal of Pharmacology.*, **150**: 552–558.

Menezes A.G., Menezes P.S. and Menezes C. (2011). Nanoscience in diagnostics: A short review Internet *Journal of Medicine.,* **6**(1):16-23.

Monteiro D.R., Gorup L.F., Takamiya A.S., Ruvollo-Filho A.C., de Camargo E.R. and Barbosa D.B. (2009). The growing importance of materials that prevent microbial

adhesion: antimicrobial effect of medical devices containing silver. *International Journal of Antimicrobial Agents.*, **34** (2):103-110.

Mozhgan B (2008). Synthesis of Noble Metal Nanoparticles (PhD Thesis). Drexel University Philadelphia, USA. 147-149.Mungrue I.N., Bredt D.S., (2004). nNOS at a glance: implications for brain and brawn. *Journal of Cell Science.*, **117**:2627–2629.

Neugroschl, J. and Sano M. (2010). Current treatment and recent clinical research in Alzheimer‟s disease. *Mount Sinai Journal of Medicine*., **77**: 3-16.

Nazema A. and Mansoorib G.A. (2008). Nanotechnology Solutions for Alzheimer ‟s disease: Advances in Research Tools, Diagnostic Methods and Therapeutic Agents. *Journal of Alzheimer's Disease.,* **13**:199–223.

Neuwelt E., Hamilton B., Varallyay C., Rooney W., Edelman R., Jacobs P. and Watnick, S. (2009). Ultrasmall superparamagnetic iron oxides (USPIOs): A future alternative magnetic resonance (MR) contrast agent for patients at risk for nephrogenic systemic fibrosis (NSF). *Kidney International.*, **75**(5):465-474.

Ochekpe N.A., Olorunfemi, P.O. and Ngwuluka N.C. (2009). Nanotechnology and drug delivery Part 2: Nanostructures for drug delivery. *Journal of Pharmaceutical Research.*, **8**(3): 275– 287.

Oishi M., Hayashi H., Iijim M. and Nagasaki, Y. (2007). Endosomal release and intracellular delivery of anticancer drugs using pH-sensitive pegylated nanogels. *Journal of Materials Chemistry.,* **17**: 3720–3725.

Padayachee ER, Ngqwala N.P and Whiteley C.G (2011). Association of β-amyloid peptide fragments with neuronal nitric oxide synthase: Implications in the etiology of Alzheimer‟s disease. *Journal of Enzyme Inhibition and Medicinal Chemistry.,* 1-9.

Palmer T. (1991). Enzyme inhibition. In: Understanding enzymes. 3rd ed. Ellis Horwood Series in Biochemistry and Biotechnology.

Packer L. (1994). Oxygen radicals in biological systems (Part C): Methods in Enzymology. *Academic Press Inc*. *USA*, **233**:357-363.

Pathan S.H., Iqbal Z., Zaidi S.M.A., Vohra S.T.D., Jain G.K, Azeem A., Jain N., Lalani J.R., Khar R.K. and Ahmad F.J. (2009). CNS Drug Delivery Systems: Novel Approaches. *Recent Patents on Drug Delivery & Formulation.*, **3**:71-89.

Pardridge W.M. and Boado R.J. (2009). Pharmacokinetics and safety in rhesus monkeys of a monoclonal antibody-GDNF fusion protein for targeted blood-brain barrier delivery. *Pharmaceutical Research*., **26**: 2227–2236.

Pardridge W.M. (2007). Blood–brain barrier delivery. *Drug Discovery.,* **12**: 54–61.

Parihar M.S. and Hemnani T. (2004). Alzheimer‟s disease pathogenesis and therapeutic interventions. *Journal of Clinical Neuroscience.*, **11:** 456-467.

Penelope J. Andrew, Bernd Mayer. (1999). Enzymatic function of nitric oxide synthases. *Cardiovascular Research*., **43**:521–531.

Perry G., Moreira P.I., Oliveira C.R., Santos M.S., Nunomura A., Honda K., Zhu X. and Smith M.A. (2005). A second look in to the oxidant mechanisms in Alzheimer‟s disease. *Current Neurovascular Research.*, **2**:179-184.

Pigozzi P., Mukherji D., Gilles R., Barbier B. and Kostorz G. (2006) "Ni3Si(Al)/a-SiOx core/shell nanoparticles: characterization, shell formation and stability". *Nanotechnology.*, **17**: 4195.

Plassman B.L., Langa K.M., Fisherd G.G., Heeringad S.G., Weird D.R., Ofstedald M.B., Burkeb J.R., Hurdf M.D., Pottera G.G., Rodgersd W.L., Steffensa D.C., Willis R.J., Wallace R.B. (2007). Prevalence of dementia in the United States: The aging, demographics, and memory study. *Neuroepidemiology.,* **29**:125-132.

Poulos T.L., Li H., Shimizu H., Flinspach M., Jamal J., Yang W., Xian M., Cai T., Zhong W.E., Jia Q. and Wang P.G. (2002). The novel binding mode of N-Alkyl-N‟-hydroxyguanidine to neuronal nitric oxide synthase provides mechanistic insights into NO biosynthesis. *Biochemistry.*, **41**:13868-13875.

Plourde G., Lavoie J.P., Rousseau-Migneron S. and Nadeau A. (1991). Validation of the polyethylene glycol precipitation techniques for the characterisation of rat ventricular beta-adrenoceptors. *Analytical .Biochemistry.*, **192**: 426-428.

Rai A, Singh A., Ahmad A. and Sastry M. (2006). Role of halide ions and temperature on the morphology of biologically synthesized gold nanotriangles, *Langmuir.*, **22**:736–741.

Reif A., Jacob C.P., Rujescu D., Herterich S., Lang S., Gutknecht L., Baehne C.G., Strobel A., Freitag C.M., Giegling I., Romanos M., Hartmann A., Ro¨sler M., Renner T.J., Fallgatter A.J., Retz W., Ehlis A.C., Lesch K.P. (2009). Influence of functional variant of neuronal nitric oxide synthase on impulsive behaviors in humans. *Arch Gen Psychiatry.,* **66**:41–50

Reddy P.H. and Beal F.M. (2010). Amyloid beta, mitochondrial dysfunction and synaptic damage: implications for cognitive decline in aging and Alzheimer‟s disease. *Trends in Molecular Medicine*., **14**:2.

Reymond J.L. and Sicard R. (2006). Enzyme assays: High–throughput screening, genetic selection and fingerprinting. *Wiley-VCH Verlag GmbH & Co*. KGaA., Weinheim.

Reisberg B., Doody R., Stöffler A., Schmitt F., Ferris S., Möbius H.J. (2003). Memantine Study Group. Memantine in moderate-to-severe Alzheimer‟s disease. *The New England Journal of Medicine.*, **348**:1333–1341.

Richier L., Williton K., Clattenburg L., Colwill K., O‟Brien M. and Tsang C. (2010). NOS1AP associates with Scribble and regulates dendritic spine development. *Journal of Neuroscience.,* **30**:4796–4805.

Reisberg B., Doody R., Stoffler A., Schmitt F., Ferris S., and Mobius HJ (2003). Memantine in moderate-to-severe Alzheimer's disease. *The New England Journal of Medicin*., **348**: 1333–1341.

Riveros-Moreno V., Heffernan B., Torres B., Chubb A., Charles I. and Moncada S. (1995). Purification to homogeneity and characterisation of rat brain recombinant nitric oxide synthase. *European Journal of Biochemistry*., **230**:52-57.

Riviere S. Birlouez-Aragon I., Nourhashemi F. and Vellas, B.1998). Low plasma vitamin C in Alzheimer patients despite an adequate diet. *International Journal of Geriatric.*, 1**3**:749-754.

Sagami I., Daff S., Shimizu T. (2001). Intra-subunit and inter-subunit electrontransfer in neuronal nitric-oxide synthase. *The Journal of Biological Chemistry.,* **27**6(32):30036 –30042.

Salomon S. D., Bahadory M., Jeyarajasingam A. V., Rutkowsky S. A. , Boritz C. and Mulfinger L. (2007). Synthesis and Study of Silver Nanoparticles. *The Journal of Chemical Education.*, **84**(2): 322-325.

Sakakibara Y. and Yanagisawa H. (2003). Agmatine deiminase from cucumber seedlings is a mono-specific enzyme: purification and characteristics. *Protein Expression and Purification*., **30**: 88-93.

Sanfins E., Dairou J., Rodrigues-Lima F. and Dupre J. (2011). Nanoparticle-protein interactions: from crucial plasma proteins to key enzymes. *Journal of Physics., Conference Series*., **304** (1):012039.

Sau T.K., Rogach A.L. Thomas J.A. Klar. and Feldmann J. (2010). Properties and Applications of Colloidal Nonspherical Noble Metal Nanoparticles. *Advanced Materials.*, **22**:1805–1825.

Schägger H. (2003). Blue native electrophoresis. in Membrane Protein Purification and Crystallization. A Practical Guide 2nd edn. Academic, San Diego, California. 105–5.130.

Scheuner D., Eckman C., Jensen M., Song X., Citron M., Suzuki N., Bird T.D., Hardy J., Hutton M., Kukull W. (1996). Secreted amyloid beta-protein similar to that in the senile plaques of Alzheimer‟s disease is increased in vivo by the presenilin 1 and 2 and APP mutations linked to familial Alzheimer‟s disease. *Nature Medicine.*, **2**: 864–870.

Schmidt, J., Metselaar, J.M., Wauben, M.H.M., Toyka, K.V., Storm, G., Gold, R. (2003). Drug targeting by long-circulating liposomal glucocorticosteroids increases therapeutic efficacy in a model of multiple sclerosis. *Brain.,* **126**: 1895–1904.

Scheuner D., Eckman C., Jensen M., Song X., Citron M., Suzuki N., Bird T.D., Hardy J., Hutton M., Kukull W. (1996). Secreted amyloid beta-protein similar to that in the senile plaques of Alzheimer‟s disease is increased in vivo by the presenilin 1 and

2 and APP mutations linked to familial Alzheimer"s disease. *Nature Medicine*., **2**: 864–870.

Selvakannan P. R., Mandal S., Pasricha R. and Sastry M. (2004). Hydrophobic, organically dispersible gold nanoparticles of variable shape produced by the spontaneous reduction of aqueous chloroaurate ions by hexadecylaniline molecules. Journal of Colloid and Interface Science., **279**:1.

Shea T.B., Ortiz D., Nicolosi R.J., Kumar R. and Watterson A.C. (2005). Nanosphere-mediated delivery of vitamin E increases its efficacy against oxidative stress resulting from exposure to Amyloid β. *Journal of Alzheimer's disease*., 7(4): 297–301

Silekaite A., Prosycevas I., Puiso J., Juraitis A. and Guobiene A. (2006). Analysis of silver nanoparticles produced by chemical reduction of silver salt solution, *Materials Science (Medziagotyra)*., **12**:287–291.

Sagami I., Daff S., Shimizu T. (2001). Intra-subunit and inter-subunit electrontransfer in neuronal nitric-oxide synthase. *The Journal of Biological Chemistry.,* **27**6(32):30036 –30042.

Shankar S.S., Ahmad A. and Sastry M. (2003). Geranium leaf assisted biosynthesis of silver nanoparticles. *Biotechnology Progress.,* **19**:1627- 1631.

Singh M., Sinha I., Premkumar M., Singh A.K., Mandal R.K. (2010). Structural and surface plasmon behavior of Cu nanoparticles using different stabilizers. *Colloids and Surfaces A-Physicochemical and Engineering Aspects*., **359**:88–94.

Singh M., Sinha I., Mandal R.K. (2009). Role of pH in the green synthesis of silver nanoparticles. *Materials Letters*., **63**:425–427.

Singh M., Singh S., Prasada S., Gambhir S. (2008). nanotechnology in medicine and antibacterial effect of silver nanoparticles. *Digest Journal of Nanomaterials and Biostructures*., **3**(3): 15 – 122.

Singh N., Cohen C.A. and Rzigalinski B.A. (2007). Treatment of Neurodegenerative Disorders with Radical Nanomedicine. *Neuroprotective Agents: Eighth International Neuroprotection Society Meeting*. **1122**: 219 – 230.

Somero G. (2004). Adaptation of enzymes to temperature: searching for basic “strate-

gies". *Comparative Biochemistry and Physiology B-Biochemistry & Molecular Biology*., **139**:321–333.

Somero G. (1978). Temperature adaptation of enzymes- biological optimization through structure-function compromises. *Annual Review of Ecology and Systematics*., **9**:1–29.

Song Q., Young K.B., Chu G., Gulick J., Gerst M., Grupp I.L, Robbins J. and Kranias EG (2004). Overexpression of phospholamban in slow-twitch skeletal muscle is associated with depressed contractile function and muscle remodelling. *FASEB J,* **18**: 974–976.

Sonneville-Auburn O., Simonnet J.T. and L"Alloret F. (2004). Nanoemulsions: a new vehicle for skin care products. *Adv. Colloid. Interface Sci*. 108–109, 145–149.

Swiatek G. and Ward W.W. (2009). Protein purification. *Current Analytical Chemistry*. 5: 85-105.

Stoscheck C.M. (1990). Quantitation of Protein. *Methods in Enzymology*, **182**: 50-69.

Takada Y, Yonezawa A, Kume T, Katsuki H, Kaneko S, Sugimoto H, and Akaike A. (2003). Nicotinic acetylcholine receptor-mediated neuroprotection by donepezil against glutamate neurotoxicity in rat cortical neurons. *Journal of Pharmacology and Experimental Therapeutics.,* **306**:772–777.

Thrash S.L., Otto J.C. Jnr. and Deits T.L. (1991). Effect of divalent ions on protein precipitation and polyethylene glycol: mechanism of action and applications. *Protein Expression and Purification*., **2**: 83-89.

The Royal Society. (2004). Nanoscience and nanotechnologies: Opportunities and uncertainties. RS Policy document 19/04.

Tsien R.Y. (1994). Fluorescence imaging creates a window on the cell. *Chemical news, chemical.,***72**:34-36.

Turkevich J, Stevenson P.C, Hillier J.A. (1951). Study of the nucleation and growth processes in the synthesis of colloidal gold. *Discuss Faraday Soceity*., **11**:55–75.

Vinogradov S.V., Zeman A.D., Batrakova E.V. and Kabanov, A.V. (2005). Polyplex nanogel formulations for drug delivery of cytotoxic nucleoside analogs. *Journal of Controlled Release.*, **107**: 143–157.

Wang D., Qian L., Xiong H., Liu J., Neckameyer W.S., Oldham S., Xia K., Wang J., Bodmer R. and Zhang Z. (2006). Antioxidants protect PINK1-dependent dopaminergic neurons in Drosophila. *Proceedings of the National Academy of Sciences of the United States of America*., **103** (36): 13520--13525.

Wang C.B., Gau G.Y., Gau S.J., Tang C.W. and Bi J.L. (2005). Preparation and characterisation of nanosized nickel oxide. *Catalysis Letters.,* 101: 241.

Werner R., Höche T. and Mayer S.G. (2011). Synthesis of shape, size and structure controlled nanocrystals by pre-seeded inert gas condensation. *CrystEngCommunity.,* **13** :3046-3050.

Whiteley C, Govender Y., Riddin T. and Rai M. (2011). Enzymatic Synthesis of Platinum Nanoparticles: Prokaryote and Eukaryote Systems. Chapter 5, Springer-Verlag Berlin Heidelberg.

Wittig I. and Schägger H. (2008). Features and applications of blue-native and clear-native electrophoresis. *Proteomics*., **8**:3974-90.

Wu J., Liu W., Xue C., Zhou S., Lan F., Bi L., Xu H., Yang Z. and Zeng F.D. (2009). Toxicity and penetration of TiO2 nanoparticles in hairless mice and porcine skin after subchronic dermal exposure. *Toxicology Letters.*, **191**: 1–8.

Wu G. and Morris S.M. (1998). Arginine metabolism: nitric oxide and beyond. *Biochemical Journal.*, **336**: 1-17.

Xu Z.C., Shen C.M., Xiao C.W., Yang T.Z., Chen S.T., Li H.L., Gao H.J. (2006). Fabrication of gold nanorod self-assemblies from rod and sphere mixtures via shape self-selective behavior. *Chemical Physics Letters.*, **432**:222–5.

Yarin A.L., Koombhongse S. and Reneker D.H. (2001). Bending instability in electrospinning of nanofibers. *Journal of Appied Physics.*, **89**(5):3018e26.

Yee C., Kataby G., Ulman A., Prozorov T., White H., King A., Rafailovich M., Sokolov J. and Gedanken A. (1999). Self assembly monolayers of alkanesulfonic and phosphonic acids on amorphous iron oxide nanoparticles. *Langmuir*., **15** (21):7111–7115.

Zhang J. and Snyder S.H. (1995). Nitric oxide in the nervous system. *Annuual Reveiw of Pharmacology and Toxicology.*, **35**: 213-233.

Zhang Q. and Gao L. (2003). Preparation of oxide nanocrystals with tunable morphologies by the moderate hydrothermal method: insights from rutile TiO2. *Langmuir.,* **19**:967-971.

Zweier J.L. and Giraldez R.R. (1998). An improved assay for the measurement of nitric oxide synthase activity in biological tissues. *Analytical Biochemistry.*, **261**: 29-35.

Zündorf G., Reiser G. (2011). The phosphorylation status of extracellular-regulated kinase 1/2 in astrocytes and neurons from rat hippocampus determines the thrombin-induced calcium release and ROS generation. *Journal of Neurochemistry.,* **119**(6):1194-204.

APPENDICES

APPENDIX A

A.1: Protein was quantified by the Bradford method, using bovine serum albumin (BSA) as a standard. Stock solution of BSA = 2 mg/ml

Table A.1A: Standards containing a range of 0.1mg to 1.2 mg of BSA

Con (mg/ml)	Conc. Of stock (mg/ml)	Amount of distilled water (µl)	Final volume water (µl)
0	0	1000	1000
0.1	50	950	1000
0.2	100	900	1000
0.4	200	800	1000
0.8	400	600	1000
1.2	600	400	1000

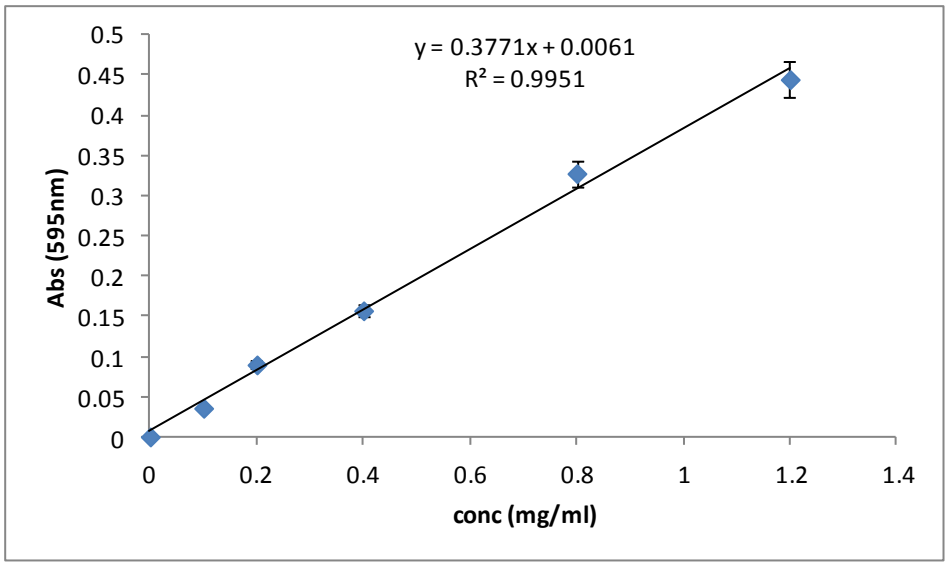

Figure A.1: Bradford standard curve. The standard curve was produced in order to determine the protein content of the enzyme

A.2. nNOS assay

Buffers and reagents used for nNOS assay

50 mM Tris-HCl buffer at pH 7.6 (500ml)	**50 mM Tris-HCl buffer at pH 7.6 (200ml)**	**5Mm NADPH (5ml)**
3.0285g Tris base in 300ml dH2O The pH was adjusted with HCL to 7.6	0.342.84g benzoyl-L-arginine ethyl ester (5 mM) 0.0147g CaCl2 0.0617 dithiothreitol	0.021g NADPH in 5ml dH_2O
Ferric chloride solution (1L)	**Chromogenic reagent**	**5M perchloric acid (50 ml)**
125 mg FeCl3 205 ml sulfuric acid and 200 ml orthophosphoric acid add up to 1L with distilled water	1.375mg thiosemicarbazide 2.3 butanedione monoxime solution (50 mg in 20 ml distilled water) and 10ml ferric chloride solution	7.5 ml perchloric acid 42.5 ml of distilled water

A.3. The activity was measured by nNOS (Citrulline) assay, using citrulline as a standard. Stock solution of Citrulline = 1 mg/ml

Table A.1.C: Standards containing a range of 5 µM to 75 µM of citrulline

Stock (µM)	0	5	10	15	20	25	50	75
Citrulline (µl)	0	5	10	15	20	25	50	75
Buffer (µl)	100	95	90	85	80	75	50	25
Chromogenic reagent (µl)	900	900	900	900	900	900	900	900

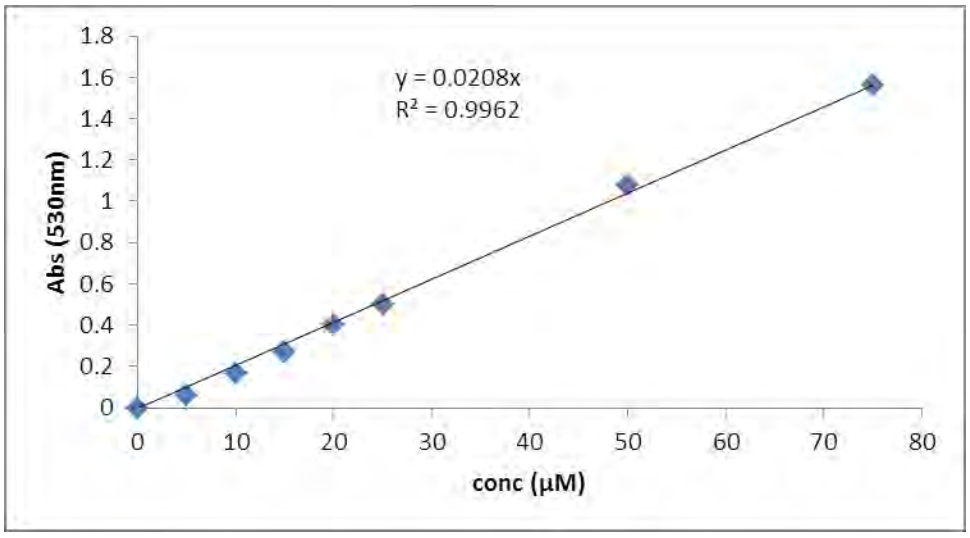

Figure A.2: Citrulline standard curve. The standard curve was produced in order to determine the activity of the enzyme.

A.4. 10 mM Tris-HCl buffer at pH 7.6 (500ml)

0.61g of Tris base in 300ml distilled water (dH2O)

The pH was adjusted with HCL to 7.6

Volume of the sample = 2% of the bed volume

A.5. Anion- exchange on DEAE-Sephacel and Size-exclusion chromatography

Slurry of the respective resin or beads was made in the equilibration buffer by filling the glass column with the equilibration buffer and allowed the material to settle till the required level. The column was washed thoroughly with 2 to 3 column volumes of equilibration buffer before loading the sample onto the column.

A.5. (a) 1mM NaCl (500 ml)

m = c.v.Mr

29.22g of NaCl then topped up to 500ml with distilled water.

A.5(b). The bed volume was calculated using the following formula

Anion- exchange on DEAE-Sephacel.	**Size-exclusion chromatography Sephacryl SH300R**
$V = \pi r^2 . h$ 3.142* (0.81 x 44 cm) = 57 ml	V=πr^2.h 3.142* (1 x44 cm)

The effectiveness of the purification process was determined by SDS-PAGE on samples exhibiting nNOS activity.

A.5(c). Buffers and reagents used for SDS and NATIVE-PAGE

1.5 MTris buffer (200 ml)	**1MTris (100 ml)**	**10% SDS (50ml)**
36.34 g Tris	12.11g Tris	5 g of SDS
150 ml o distilled water	60 ml distilled water	50 ml water
Adjust the pH to 8.9 with HCl, and then bring the volume to 200 ml	Adjust the pH to 6.8 with HCl. Bring the volume to 100 ml	

10% Ammonium persulphate (APS)

0.1 g of Ammonium persulphate in 1 ml of water

Running Buffer (1litre)

3.03 g Tris

14.04 g Glycine and

1 g of SDS in water and bring the volume to 1 litre

4X sample buffer (10 ml)

4mg of Bromophenol Blue

0.6ml of 1M Tris pH6.8

2.5 ml of 100% Glycerol

3ml of 10% SDS and

1.4ml of distilled water. Aliquot 375µl in fresh eppendorf tube. Store at −20◦C. Add 125µl of 2-Mercaptoethanol before using.

Staining Solution (1L)

0.25 g Coomassie Brilliant blue R250

125 ml methanol

25 ml acetic acid and

100 ml of distilled water

Distaining Solution (1L)

400 ml Methanol and

70 ml of acetic acid

bringing the volume to 1 litre with water

Table A.1 (a): Components of SDS-PAGE

Components	**12% separating gel (10ml)**	**5% stacking gel(3ml)**
Water	3.3	2.1
30% ACYRLAMIDE	4	0.5
1.5M Tris pH 8.8 (1M Tris pH 6.8)	2.5	0.38
10% SDS	0.1	0.03
10% APS	0.1	0.03
TEMED	0.004	0.003

Table A.1 (b): Components of NATIVE-PAGE

Components	**8% separating gel (10ml)**	**5% stacking gel(3ml)**
Water	4.83	2.3
30% ACYRLAMIDE	2.67	0.67
1.5M Tris pH 8.8 (1M Tris pH 6.8)	2.5	1
10% APS	0.05	0.03
TEMED	0.005	0.005

A.6. Buffers and reagents used for Western blot analysis

Transfer buffer (1L)

5.82 g of Tris base

2.93 g of Glycine

3.75 ml of 10% SDS in 800 ml water

200 ml of Methanol

blocking solution

5 g of fat free milk in 100 ml of TBST

Ponceau stain (0.1 %)

0.1g Ponceau stain

1ml acetic acid

TBS-Tween (TBST)

TBS containing

2 % Tween-20

Tris buffered saline (TBS)

8.8 g of Tris base

1.2 g of Sodium Chloride and

500µl of Tween 20 in 750 ml of water. Adjust the pH of the solution to 7.5 and finally bring the volume to 1 litre

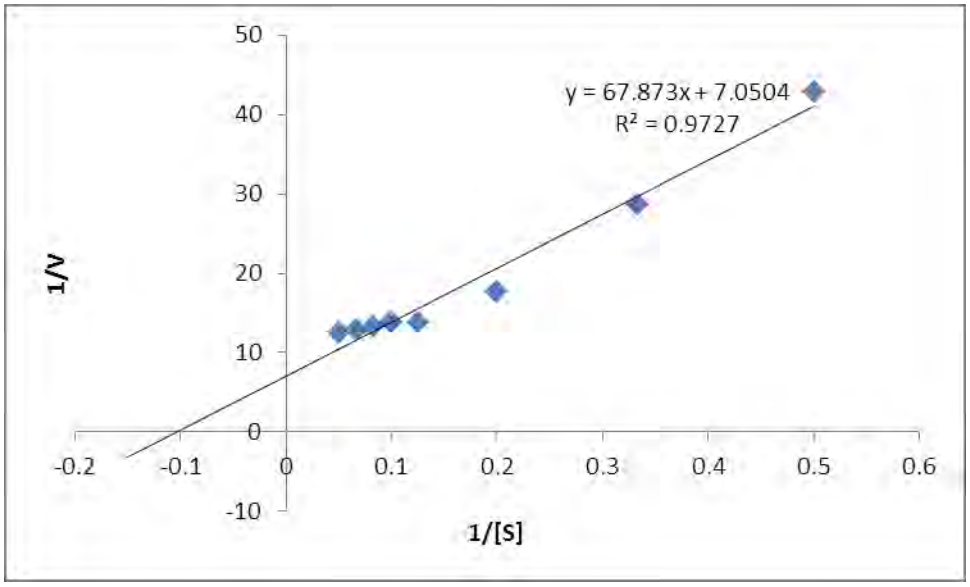

Figure A.3: Lineweaverback plot. This plot was produced in order to determine Hanes-Woolf plot

APPENDIX B

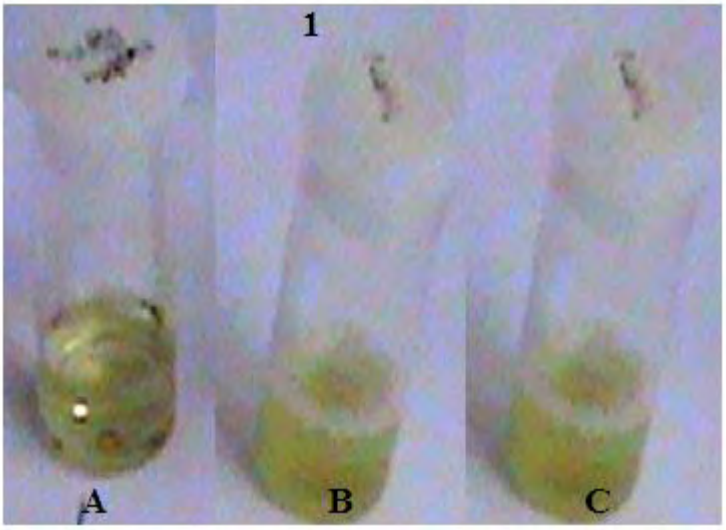

Figure B.1: The colour of silver nanoparticles synthesized using sodium citrate method on different concentrations of citrate A: 50 µl, B: 100 µl, C: 200 µl. This was carried out to show that the higher the concentration of citrate the larger the size of the nanoparticles.

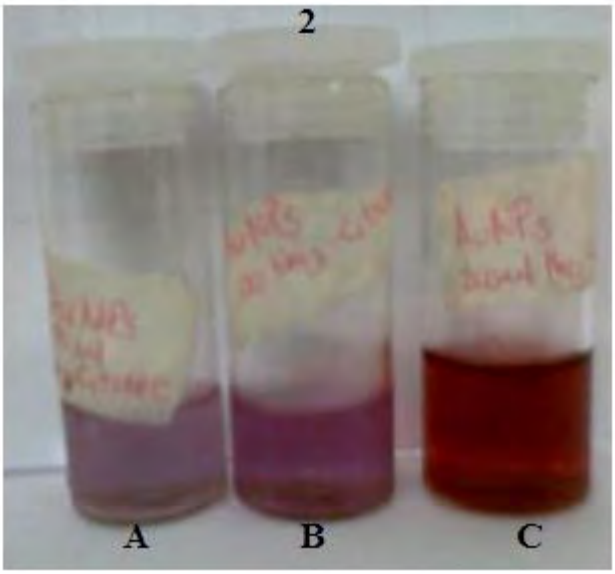

Figure .B.2: The colour of gold nanoparticles synthesized using sodium citrate method on different concentrations of citrate A: 50 µl, B: 100 µl, C: 200 µl. This was carried out to show that the higher the concentration of citrate the larger the size of the nanoparticles.

B.2. reagents used for synthesis of nanoparticles

silver nitrate ($AgNO_3$) (1 mM**)**

0.01g silver nitrate topped up with 10 ml dH_2O

tetrachloroauric acid ($HAuCl_4$) (1 Mm)

0.01g HAuCl4 topped up with 10 ml dH_2O

K_2CO_3 (potassium carbonate) (1M)

13.821g

100 ml dH_2O

then filtered with 0.22 µM filter

Trisodium citrate ($C_6H_5Na_3O_7$) (1%)

0.5g Sodium citrate

50ml dH_2O then filtered with 0.22 µM filter

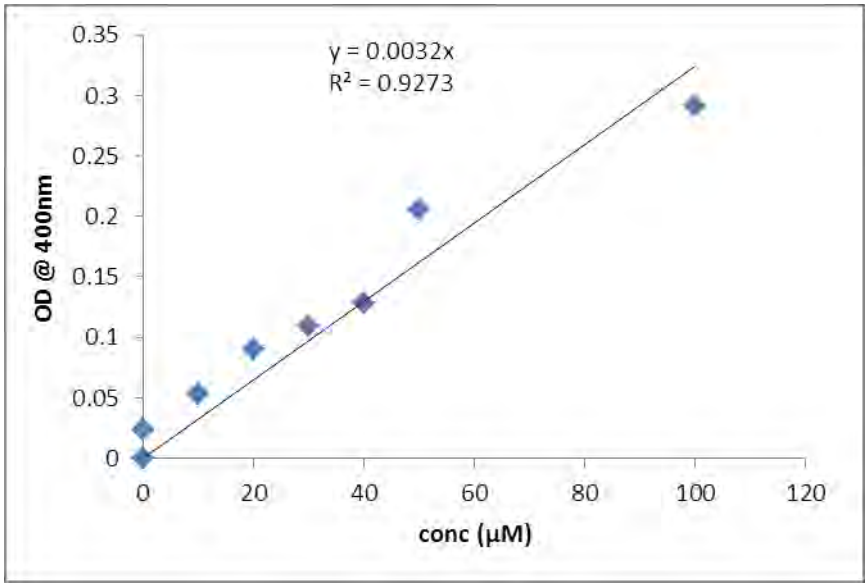

Figure B.3: Silver nanoparticle standard curve. The standard curve was produced in order to determine the effect of the nanoparticles on the enzyme.

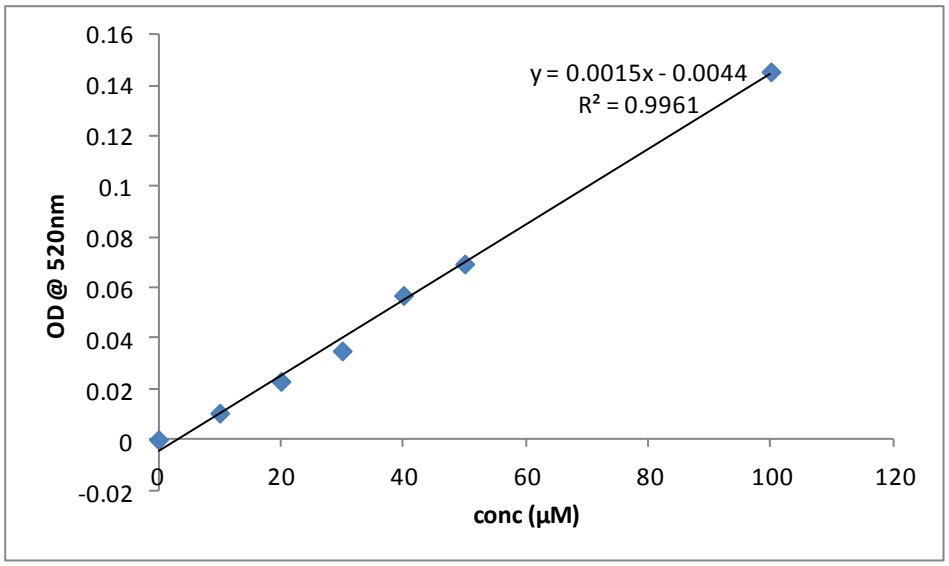

Figure B.4: Gold nanoparticle standard curve. The standard curve was produced in order to determine the effect of the nanoparticles on the enzyme

APPENDIX C

C.1. fluorimetric analysis was used to identify the actual binding pocket for the nanoparticles peptides in the nNOS. Any insight into molecular recognition of the binding of the nanoparticles with nNOS involves an investigation of hydrogen bonds, van der Waals forces as well as electrostatic and hydrophobic interactions.

C.2. Triethanolamine buffer pH 7.4 (200ml)

0.317g Triethanolamine, 1.17g NaCl Adjust the pH with NaOH

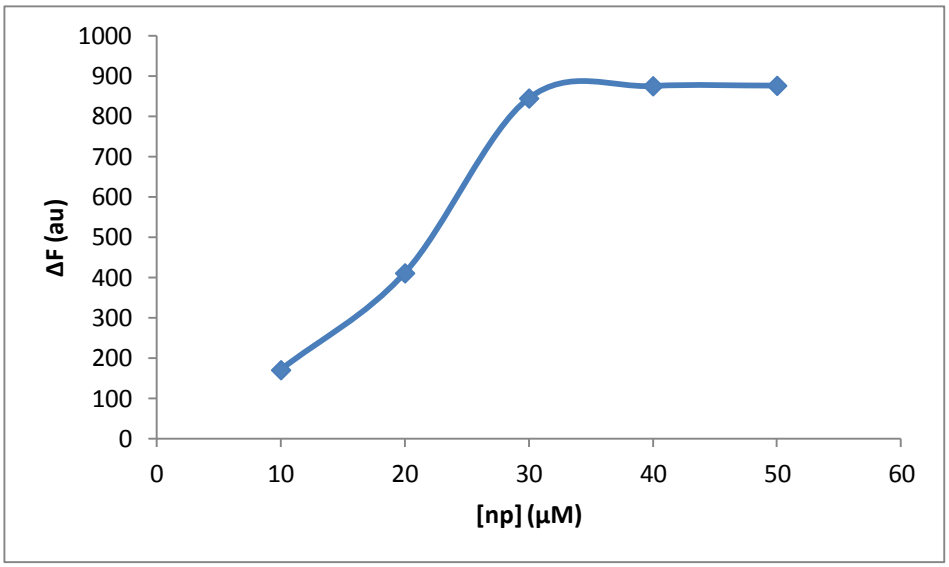

Figure C.1: The titration of nNOS with the silver nanoparticles at various concentrations showed typical hyperbolic relationship. The concentration of binding sites (n) on the purified enzyme, that were available for nanoparticles, and the dissociation constants (Kd) were estimated

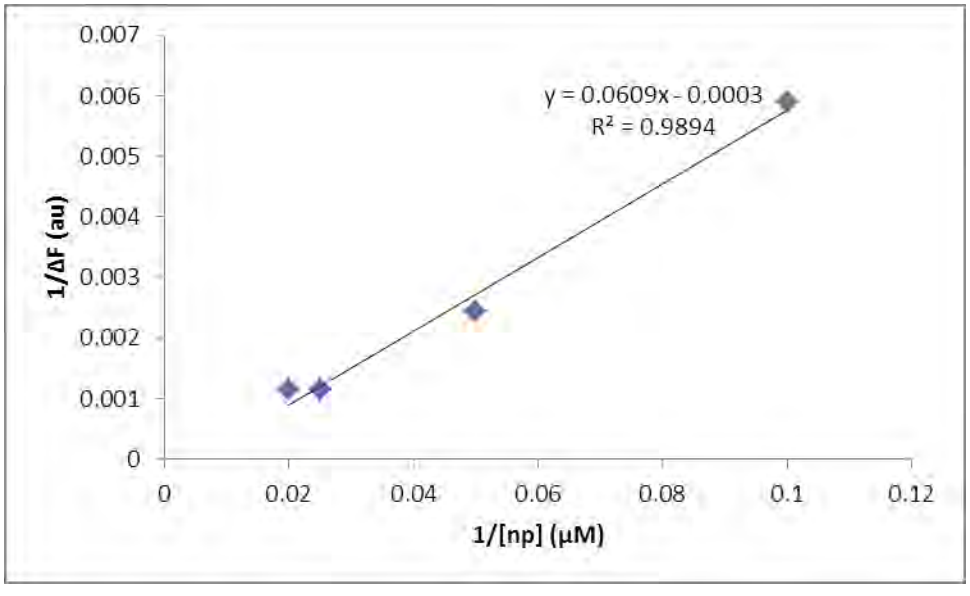

Figure C.2: The concentration of binding sites (n) on the purified enzyme, that were available for silver nanoparticles, and the dissociation constants (Kd) were estimated respectively from the slope of the linear regressions and the intercept.

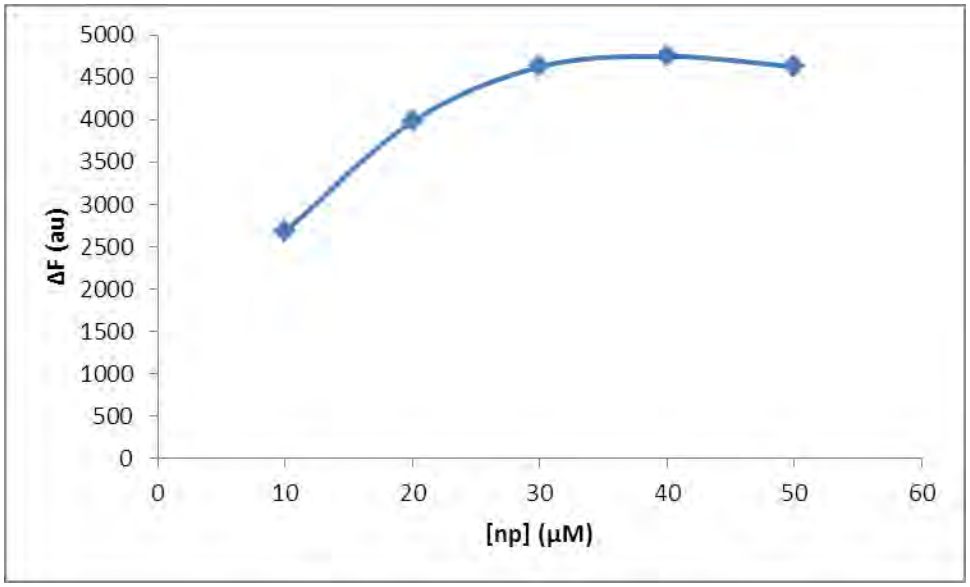

Figure C.3: The titration of nNOS with the gold nanoparticles at various concentrations showed typical hyperbolic relationship. The concentration of binding sites (n) on the purified enzyme, that were available for nanoparticles, and the dissociation constants (Kd) were estimated

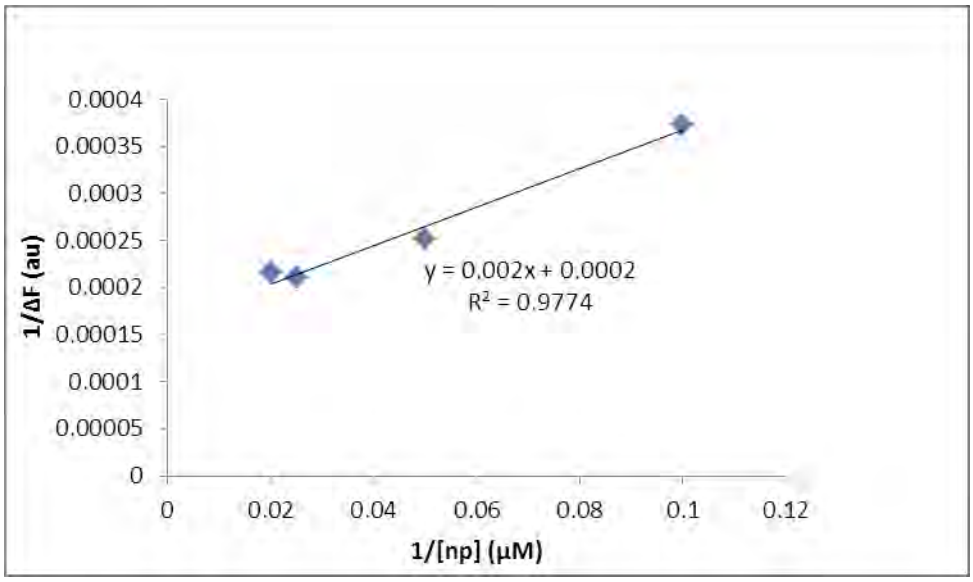

Figure C.4: The concentration of binding sites (n) on the purified enzyme, that were available for gold nanoparticles, and the dissociation constants (Kd) were estimated respectively from the slope of the linear regressions and the intercept

APPENDIX D (Internet references)

Internet 1: **http://scinewsblog.blogspot.com/2011_10_01_archive.html**

Internet 2: **http://www.ucl.ac.uk/~ucbcdab/enzpur/amso4.htm**

Internet 3: **http://www.waters.com/waters/nav.htm?cid=10083845&locale=en_GB**

Internet 4:
http://chemwiki.ucdavis.edu/Analytical_Chemistry/Instrumental_Analysis/Chromatography/Liquid_Chromatography/Ion_Exchange_Chromatography

Internet 5: **http://www.files.chem.vt.edu/chem-ed/sep/lc/size-exc.html**